COOL ROOFS FOR IMPROVING THERMAL PERFORMANCE OF EXISTING EU OFFICE BUILDINGS

BY

VINCENZO COSTANZO

A thesis submitted to the University of Catania in fulfilment of the requirements for the degree of *Doctor of Philosophy in Energetics (XXVIII Cycle)*

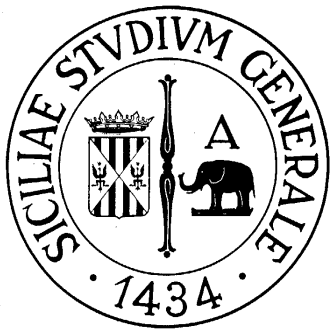

University of Catania

Academic year 2015-2016

Supervisor & Course Coordinator: Prof. Luigi Marletta

Abstract

Cool materials are characterized by having a high solar reflectance *r* – which is able to reduce heat gains during daytime - and a high thermal emissivity *ε* that enables them to dissipate the heat absorbed throughout the day during night.

Despite the concept of *cool roofs* - i.e. the application of cool materials to roof surfaces - is well known in US since 1990s, many studies focused on their performance in both residential and commercial sectors under various climatic conditions for US countries, while only a few case studies are analyzed in EU countries.

The present thesis work aims at analyzing the thermal benefits due to their application to existing office buildings located in EU countries. Indeed, due to their weight in the existing buildings stock, as well as the very low rate of new buildings construction, the retrofit of office buildings is a topic of great concern worldwide.

After an in-depth characterization of the existing buildings stock in the EU, the thesis gives an insight into roof energy balance due to different technological solutions, showing in which cases and to what extent cool roofs are preferable.

A detailed description of the physical properties of cool materials and their availability on the market provides a solid background for the parametric analysis carried out by means of detailed numerical models that aims at evaluating cool roofs performance for various climates and office buildings configurations.

With the help of dynamic simulations, the thermal behavior of representative office buildings of the existing EU buildings stock is assessed in terms of thermal comfort and energy needs for air conditioning. The results, which consider several variations of building features that may affect the resulting energy balance, show how cool roofs are an effective strategy for reducing overheating occurrences and thus improving thermal comfort in any climate. On the other hand, potential heating penalties due to a reduction in the heat fluxes passing through the roof are taken into account, as well as the aging process of cool materials.

Finally, an economic analysis of the best performing models shows the boundaries for their economic convenience.

Keywords: cool roofs, office buildings, thermal analysis, building simulations, building energy efficiency

TABLE OF CONTENTS

NOMENCLATURE

Variables

A	solar absorptance
COP	Coefficient Of Performance
EER	Energy Efficiency Ratio
G	solar spectral distribution /W m^{-2} nm^{-1})
h_c	convective heat transfer coefficient (W m^{-2} K^{-1})
H	heat flux (W)
I	global horizontal solar irradiance (W m^{-2})
ITD	Intensity of Thermal Discomfort Index (°C h)
K	thermal conductivity (W m^{-1} K^{-1})
PE	Primary Energy (MWh)
PER	Primary Energy Ratio
q	specific heat flux (W m^{-2})
Q	energy needs (Wh)
r	solar reflectance
R	thermal resistance (m^2 K W^{-1})
RWR	Roof to Walls Ratio
SRI	Solar Reflectance Index
T	temperature (°C)
U	thermal transmittance (W m^{-2} K^{-1})

Greek letters

α	thermal diffusivity (m^2 s^{-1})
ε	thermal emissivity
λ	wavelength (nm)
σ	Stefan-Boltzmann constant (W m^{-2} K^{-4})
τ	time (s)
ϕ	relative humidity

Subscripts

f	foliage
g	ground
i	indoor
ir	infrared
lim	limit
max	maximum
min	minimum
o	outdoor
op	operative
s	summer
so	outer surface
sol	solar
w	winter

LIST OF FIGURES

Chapter 1

Chapter 2

Chapter 3

Chapter 4

Chapter 5

LIST OF TABLES

Chapter 1

Chapter 2

Chapter 3

Chapter 4

Chapter 5

1. INTRODUCTION

The rapidly growing building energy use has raised concerns globally. The contribution from buildings towards total national energy consumption, both residential and commercial, has steadily increased and reached figures as high as 40% in developed countries, and has exceeded the other major sectors such as industrial and transportation [1]. With the growing population, day-by-day increasing demand for building services and comfort levels, along with the rise in time spent inside buildings, energy demand in buildings will surely stick to the upward trend in the future. For this reason, energy efficiency in buildings is one of the prime objectives in design and retrofit at regional, national, and international levels. Within this framework, the topic of Zero Energy Buildings (ZEB) has received increasing attention in recent years, until becoming part of the energy policy in several countries. However, while new buildings can be constructed with high performance levels, the older buildings represent the vast majority of the building stock and are predominantly of low energy performance and subsequently in need of renovation work. With their potential in terms of energy and CO_2 savings as well as many societal benefits, energy efficient buildings can have a pivotal role in a sustainable future.

The present chapter starts with a brief discussion on ZEB definitions and issues, and then develops considerations on the existing EU building stock and on the potential for its energy retrofit, thus framing the research topic of this thesis.

1.1 Towards nearly (or Net) Zero Energy Buildings

The nearly Zero Energy Building (nZEB) concept is one of many low-energy building movements that respond to the issues of climate change and energy security. The nZEB concept strives to reduce demand for energy and then to offset any residual energy consumption with CO_2 free technologies. The (re-)design focus for nZEBs is to reduce primary energy consumption, so as to be equal to or less than any generated renewable energy. This is an important concept since approximately 40 percent of all energy and emissions worldwide are building-related. If all buildings were designed and operated to be nZE, the energy could be used by other sectors, with a potential increase in energy security.

In Europe, article 9 of the EPBD (2010/31/UE) Recast requires that [2]:

(i) by 31 December 2020, all new buildings are nearly zero energy buildings;

(ii) after 31 December 2018, new buildings occupied and owned by public authorities are nearly zero energy buildings.

A few exemplary non-residential renovation projects have demonstrated that total primary energy consumption can be drastically reduced, together with improvements to indoor environment quality, by means of passive and active systems. Because most (property) owners are not even aware that such savings are possible, they tend to set less ambitious targets: buildings that are renovated to mediocre performance can be a lost opportunity for decades.

Nevertheless, a further step towards the so-called Net Zero Energy Building (NZEB) is the desire to design buildings in a sustainable way [3]. There is considerable debate on how to define this design approach, particularly on how to calculate the balance between energy use and energy generation. Indeed, in principle a NZEB could simply be a traditional building that has its energy supplied by a very large renewable energy generation systems: if these systems deliver an equal or greater amount of energy than the building consumes, then it is a NZEB.

Obviously, this would not imply a reduction of global energy demand, since it would be theoretically possible to deliver as much energy as needed by means of renewable sources, thus *buildings must be low energy* ones, and have enough onsite renewable energy generation.

A graph explaining the concept of NZEB is reported in Fig. 1.1; here it is shown how the reference building energy needs should be first decreased (moving towards left on the energy demand x-axis), then covered by renewable energy sources. This definition was universally agreed.

If the energy supply should overcome the annual energy balance of the building, we talk of *Positive/Plus Energy Buildings*.

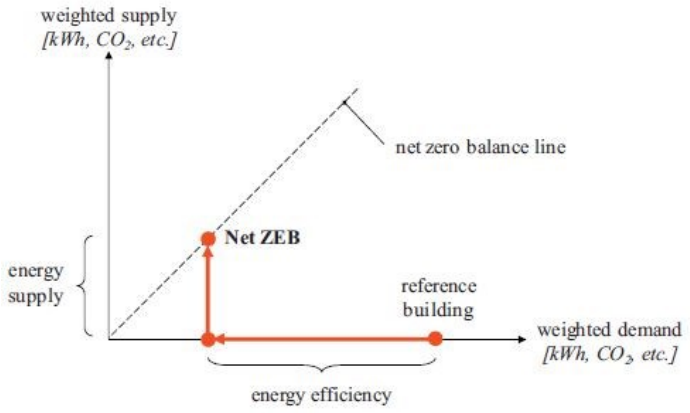

FIGURE 1.1: Graph representing the NZEB balance concept [4]

Where consensus has been harder to find is about the metric (i.e. primary energy, carbon emissions, …) and what to consider in the balance (i.e. energy use due to building operation, embodied

energy in materials, …), as these aspects lead to different definitions and different results as a consequence.

For example, insulation levels, HVAC system performance, photovoltaic or cogeneration system sizing and so on are directly dependent on the NZEB balance.

The biggest dispute concerns if the zero should be measured *on site* or *off site*, and which of the four traditional energy related units or metrics have to be used (see Fig. 1.2 for a scheme depicting the energy boundaries for the calculation).

Torcellini et al. [5] undertook an in-depth analysis about these issues, identifying the following definitions:

(i) *Net Zero Site Energy*: a building that produces at least as much energy on-site as it uses in a year;

(ii) *Net Zero Source (Primary) Energy*: source energy refers to the primary energy used to generate and deliver the energy to the site. It requires the imported/exported energy to be multiplied by appropriate site-to-source conversion factors;

(iii) *Net Zero Energy Costs*: the amount of money the building tenant pays for the energy services should be equal to or less than the amount of money the utility pays for the building energy exports to the grid;

(iv) *Net Zero Energy Emissions/Carbon*: building emissions from emissions-producing energy sources should be less than the equivalent ones produced by renewable energy sources (that are emissions-free).

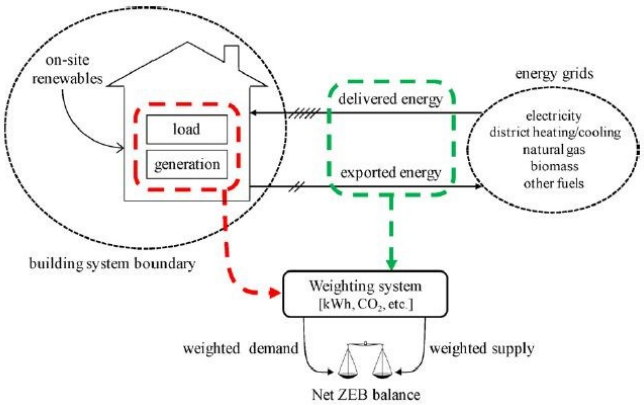

FIGURE 1.2: Connections between buildings and energy grids [4]

The importance of a well-developed NZEB definition is highlighted when considering buildings that are being refurbished: firstly, refurbishment projects are more difficult because the building geometry, size and layout are pre-determined and not necessarily optimized to save energy. Secondly, very often all renewable energy supplies must be situated on site, and there is a lack of space for allocating them.

Some examples of successful NZEB all over the world are given in [6] where 23 selected projects are discussed, ranging across different functional typologies and sizes to illustrate implementation at different scales and in different climates.

For what concerns the office buildings sector (on which this thesis is focused, as will be explained in the next paragraphs), it is worth mentioning the renovation project of the WWF headquarters in Zeist (Netherlands, see Fig. 1.3). This building is regarded as the first carbon-neutral administration building in the Netherlands.

It is efficiently conditioned by using exhaust heat, which is stored in the ground by means of geothermal probes, as well as by a passive cooling system. Solar collectors cover a part of the heat required for the provision of hot water, while the remaining hot water and heating demands are covered by heat pumps.

The façade is clad in glazed ceramic tile supported by a wooden frame and wood panel sheathings, which enclose a 24 cm deep air cavity and a 12 cm thick insulating layer of mineral wool. The inner face is comprised of a vapor barrier and a 5 cm thick adobe render layer.

FIGURE 1.3: WWF headquarters in Zeist [Internet]

As large areas of the façade are glazed, daylight can penetrate deeply into the offices, and they permit an almost unobstructed view of the surroundings. Horizontal wooden louvers shade parts of the south-facing façade in the office wings in the old part of the building.

Openable windows combined with ventilation flaps in the lightweight timber construction elements ensure natural ventilation throughout the year. The large areas available for thermal exchange allow homogeneous temperature shifts and help avoid sudden temperature changes. In addition, the adobe retains moisture and improves the indoor climate.

The calculated demand parameters are strongly reduced with respect to the starting point, being now the total primary energy demand equal to 247 kWh $m^{-2}y^{-1}$ and the total primary energy generated 326 kWh $m^{-2}y^{-1}$.

The Pixel Building in Melbourne (Australia, Fig. 1.4) gives another example of the feasibility of NZEB projects, in a different climate. Here, passive strategies such as sunshade and daylight optimization reduce the need for cooling and heating, while recyclable materials minimize the amount of CO_2 produced during the building construction. The photovoltaic arrays and the micro wind turbine power generators on the roof are sized to offset all climate gas emissions from the gas absorption heat pump and the other building service plants.

FIGURE 1.4: Pixel building in Melbourne [Internet]

The reinforced concrete floor slabs rest on the walls of the solid staircase core and on three precast concrete piers outside the insulated building envelope of the western façade. The windows recede by about a meter to provide architectural sunshade for the façade that receives a lot of sun during working hours.

Sufficient daylight can enter through the full-height windows while preventing direct solar radiation from heating up the rooms excessively. In addition to the intelligent exploitation of daylight, an energy-efficient lighting system (fluorescent tubes) in the office ensures low heat loads: they are

dimmed in accordance with the amount of daylight and connected to presence sensors. In all other rooms apart from the offices LED lighting is used.

To passively cooling the building during the night, the windows of the upper floors open automatically on cool nights, allowing cold air to flow across the solid ceiling slabs and withdraw the heat stored during the day.

The vertical axis wind turbines on the roof are also a unique feature that makes the theme of renewable energy clearly visible; they are not affected by the frequent change in wind direction and allow an even generation of 1.7 kW of electricity at a wind speed of 8 m/s. The renewable energy system is completed by a photovoltaic array measuring 38 m^2, mounted on three solar trackers (dual axis system that follows the sun).

The resulting primary energy demand amounts to 123 kWh $m^{-2}y^{-1}$, while the primary energy generation is equal to 84 kWh $m^{-2}y^{-1}$.

1.2 EU buildings stock

Amongst the current political discussions at EU level, Buildings Performance Institute Europe (BPIE) has undertaken an extensive survey across all EU Member States, Switzerland and Norway reviewing the situation in terms of the building stock characteristics and policies in place. This survey provides an EU-wide picture of the energy performance of the building stock, and is hereafter called as a basis for determining existing buildings features [7].

European countries have been divided up into three regions, according to climatic, building typology and market similarities:

(i) North & West;

(ii) South;

(iii) Central & East.

Each region, together with floor and population distributions, is shown in Fig. 1.5.

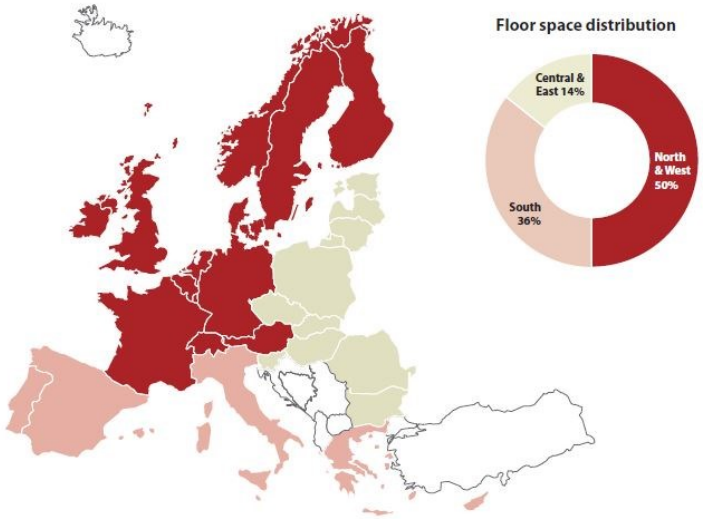

North & West	AT, BE, CH, DE, DK, FI, FR, IE, LU, NL, NO, SE, UK	Population: 281 million
Central & East	BG, CZ, EE, HU, LT, LV, PL, RO, SI, SK	Population: 102 million
South	CY, GR, ES, IT, MT, PT	Population: 129 million

FIGURE 1.5: EU Countries considered within BPIE survey together with population and floor distribution breakdown [7]

The five most populated countries (France, Germany, Italy, Spain and the UK) account for approximately 65% of the total floor space, thus there is no surprise in finding out that the corresponding share of population in these countries is equal to 61% of the total.

The residential stock is the biggest segment, accounting for 75% of the building stock (see Fig. 1.6); an analysis of this sector indicates that 64% of the residential floor area pertains to single-family houses, whereas the remaining 36% to apartment blocks.

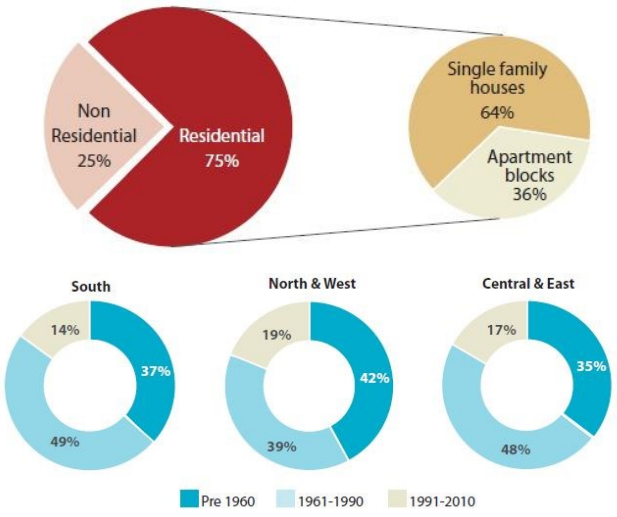

FIGURE 1.6: Breakdown of the floor space typology (top) and age categorization (bottom) in Europe [7]

The split between the two main types of residential buildings vary significantly amongst the countries, but share the same little rate of annual new buildings, which approaches 1% over the period 2005-2010.

It is important to know how a great share of the stock in Europe is older than 50 years, and many buildings still operating nowadays are hundreds of years old, being constructed when energy building regulations where very limited or absent.

The BPIE report also focuses on the final energy use in the residential sector within the period 1990-2010, rebating that European households are responsible for the 68% of the total final energy use in buildings, being space-heating the dominant energy end-use.

The final energy use in the residential sector in Mtoe (*Million tons of oil equivalent*), split into fuels and electricity needs, is shown in Fig. 1.7 together with heating degree days (nominal and actual). By analyzing this picture, it is possible to notice a decrease in the fuels needs (mainly for space heating, which represents about 70% of total final energy use) and a parallel increase in the electricity needs (mainly for space cooling). A likely explanation for these trends could be found in both the increased insulation levels of the building envelopes and the augmented outdoor air temperatures found within the cities (a phenomenon known as *Urban Heat Island effect*).

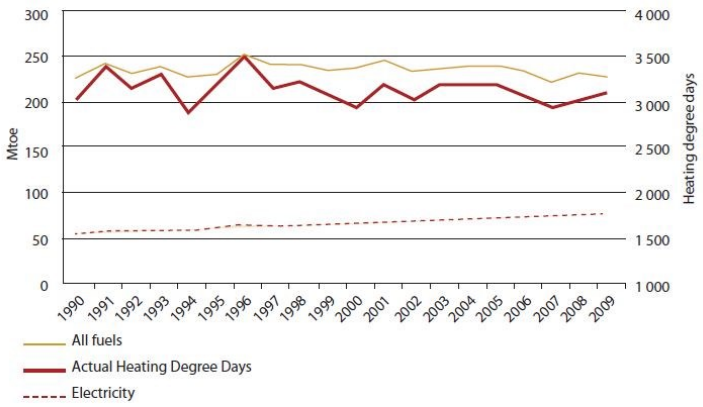

FIGURE 1.7: Final energy use in the residential sector [7]

For what concerns the non-residential sector, understanding its energy use is complex because end-uses such as lighting, ventilation, heating, cooling, refrigeration and appliances vary greatly from sector to sector (sport facilities, wholesale and retail, hotel & restaurants, hospitals, educational buildings and offices).

Nonetheless, it is estimated that the average specific energy consumption (covering all end-uses) of this sector is 280 kWh/m^2, about 40% larger than the equivalent value for the residential sector.

Moreover, the electricity demand within this sector has increased tremendously in the last 20 years, by 74% as shown in Fig. 1.8, probably due to an increasing penetration of IT equipment and air conditioning systems.

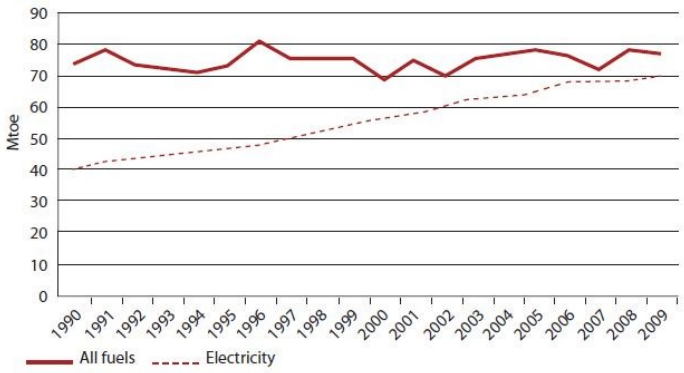

FIGURE 1.8: Final energy use in the non-residential sector [7]

If looking at the share of total energy use per building type (Fig. 1.9), it appears how the office and commercial buildings sectors account for more than 50% of energy needs, thus highlighting a big opportunity for implementing energy saving measures in this kind of buildings, especially for lowering the electricity needs.

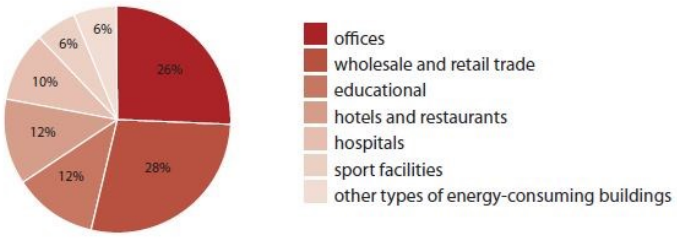

FIGURE 1.9: Share of total energy use for the non-residential sector [7]

1.3 Characteristics of the Office Buildings sector in EU-27 countries

The increasing interest in the office buildings sector is underlined by a recent IEA task (Task 47: Renovation of Non-Residential Buildings towards Sustainable Standards, [8]), aimed at showing how total primary energy consumption can be reduced by means of building's passive and active systems.

The objectives of this task are *"to develop a solid knowledge-base including: how to renovate non-residential buildings towards the Net Zero Energy Building standards in a sustainable and cost efficient way; ways to identify important market and policy issues; and effective marketing strategies for such renovations".*

In a European-based perspective, a very comprehensive and up-to-date study about the EU building stock, with a focus on office buildings, is reported in [9].

Firstly, a recognition of the size, age, type of tenure of the building stock is given, based on previous EU reports such as TABULA, ENTRANZE, BPIE and Odyssee, and on semi-structured interviews with research institutions.

Secondly, a detailed analysis of building types and constructions, as well as their thermal performance and energy consumption, is provided by splitting the stock analyzed into seven different climate zones.

Finally, building energy models representative of different vintage periods are developed as base cases for studying energy efficiency measures.

The information collected during the literature review has been presented in a database specifically created for the Inspire project in Microsoft Excel format, and is attached in Appendix I. Here the main findings are summarized, and most of them are used for creating the base models for the energy assessment carried out in Chapter 4 by means of dynamic thermal simulations.

For what concerns the total floor area, in the EU-27 is approximately 1.25 billion m^2, of which 0.98 billions m^2 are heated; the majority of it (about 70%) lies in the six biggest countries (Spain, Italy, France, Germany, UK and Poland), and this reflects the size of the population in these countries.

Very little is known about the age of the current office stock, and in particular for those buildings constructed pre-1980. However, what is clear from this survey is that although a large proportion of the office stock dates before 1980, the office stock is generally younger than the residential stock (see Fig. 1.10 for the age breakdown).

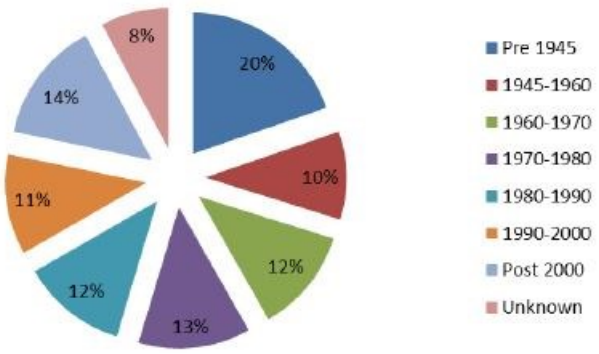

FIGURE 1.10: Age construction breakdown for EU-27 countries [9]

Most of the office stock in EU-27 is privately owned, and this varies across all of the countries from 30% to 84%; the remaining part is publically owned. The type of tenure represents an important aspect for refurbishing programs intended to reduce energy bills, as the costs of installing retrofit measures and the consequent benefits apply to the same individuals.

Construction types are found to be pretty much the same in most countries – concrete structural frame with curtain walls is the most widespread – despite they can show different numbers of floors, different shapes or type of offices. This last aspect makes the office stock very hard to categorize; nevertheless, the iNSPiRe survey found three main construction typologies based on the fact that facades are the components mostly affecting the building thermal behavior.

These typologies are:

(i) Brick structural walls: typically built before 1945 (end of World War II), they are often low-rise blocks;

(ii) Concrete structures: bricks or concrete panels are mainly used within the period 1945-1964, while curtain walls spread during the 1970s and 1980s;

(iii) Concrete structures with reinforced cement: statistics show how these structures dominate the stock and curtain walling is the most common type of façade. The majority of them incorporate glazing.

The three categories represent the base for developing thermal models aimed at giving a broad view of the energy needs for air conditioning (cooling + heating), artificial lighting and ventilating, and thus implementing measures for their effective refurbishment. The models are shown in the following data sheets and will be further discussed in Chapter 4, where the methodology for characterizing the "typical" model used for simulation purposes is detailed.

REFERENCE OFFICE 1	LOW-RISE MASONRY OFFICE BUILDING		
Sketch and picture	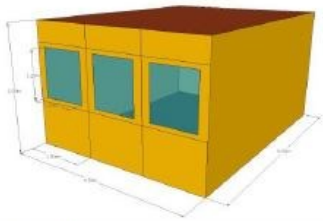		
Attribute	Quantity	Unit	Note
Number of floors	2		
Façade type and materials	Bearing brick walls: Gypsum plaster; Bricks; Air gap; Bricks		
Floor area per floor	1180	[m^2]	
Ceiling height	3.8 / 3	[m]	Ground fl. / Above floors
Building width /depth	70.7 /16.7	[m]	
UA-value of walls and roof / ground floor	3 500 / 5 000	[W/K]	
Roof type and materials	Flat concrete roof with bitumised surface: Ceiling board; Wood beams; Concrete slab; Bitumen		
Windows type	Double glazed		PVC frame
Windows-to-wall ratio / Frame-to-window ratio	50 / 24	[%]	
Windows U-value / g-value	3.1 / 76	[W/m^2K] / [%]	
Ventilation type	Natural ventilation		
Shading	Internal		

FIGURE 1.11: Office building 1 [9]

Reference Office 1 represents a category of buildings built in pre 1970s and most typically during the 1950s and 1960s, however small office buildings continued to be built from masonry. The main construction consists of walls and floor slabs made in situ. The structure consists of brick walls. Most buildings are constituted of usually 2 floors for an average total office of between 1800 and 3000 m^2.

When these buildings were built, no legal energy requirement existed yet as regulations only really started to come into effect during the 1970s. The lack of insulation in the facades and roofs contributes to a high heating demand. The heating generation is accomplished by fuel oil or gas boiler and distributed by radiators. The cooling demand depends on the location, so it is very variable.

The windows are double glazed and have internal shading, while the roof consists of a flat concrete slab on wooden beams, with a bitumised surface.

REFERENCE OFFICE 2	CONCRETE PANELS OFFICE BUILDING		
Sketch and picture	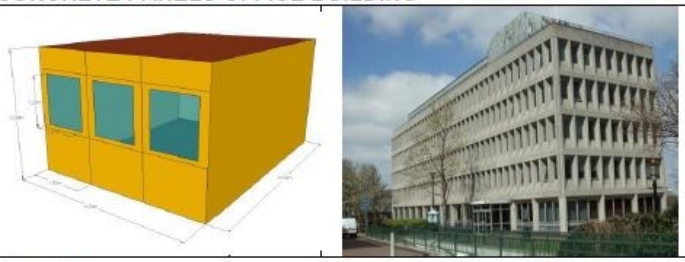		
Attribute	Quantity	Unit	Note
Number of floors	5 + basement		
Façade type and materials	Concrete cladding on concrete pillars and beams: Skim finish; Dry walling plasterboard; Air gap; Concrete panels		
Floor area per floor	793	[m^2]	
Ceiling height	3	[m]	
Building width /depth	61 /13	[m]	
UA-value of walls and roof / ground floor	10 600 / 3 200	[W/K]	
Roof type and materials	Flat concrete roof with bitumised surface: Skim finish; Concrete slab; Bitumen		
Windows type / Frame ratio	Double glazed		Aluminium frame
Windows-to-wall ratio / Frame-to-window ratio	30 / 20	[%]	
Windows U-value / g-value	3.1 / 76	[W/m^2K] / [%]	
Ventilation type	Natural ventilation		
Shading	Internal		

FIGURE 1.12: Office building 2 [9]

The buildings represented by the Reference Office 2 were mainly built between 1945 and 1970, although they became most typical during the 1960s. There is little or no insulation in the buildings in this category, and the number of floors is between two and seven, with an average total floor area of approximately 4000 m^2.

A basement with limited parking, building services, and storage space is also present. Precast concrete cladding panels on a concrete frame form the outer envelope of the building, while the windows are double glazed and have internal shading.

REFERENCE OFFICE 3	METAL AND GLASS FACADE OFFICE BUILDING		
Sketch and picture	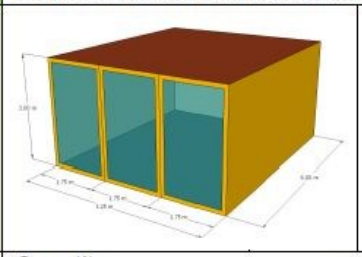		
Attribute	Quantity	Unit	Note
Number of floors	5 + basement		
Façade type and materials	Aluminium and glass façade on concrete pillars and beams		
Floor area per floor	793	[m^2]	
Ceiling height	3	[m]	
Building width / depth	61 / 13	[m]	
UA-value of walls and roof / ground floor	10 000 / 3 200	[W/K]	
Roof type and materials	Flat concrete roof with bitumised surface: Skim finish; Concrete slab; Bitumen		
Windows type / Frame ratio	Double glazed		Aluminium frame
Windows-to-wall ratio / Frame-to-window ratio	55 / 20	[%]	
Windows U-value / g-value	3.1 / 76	[W/m^2K] / [%]	
Ventilation type	Natural ventilation		
Shading	Internal		

FIGURE 1.13: Office building 3 [9]

The statistics showed that concrete structures dominate the stock and curtain walling is the most common type of façade. The majority of curtain walls incorporate glazing. This category is the most recent, with buildings built between 1960 and 1980, and covers buildings with a concrete structure of reinforced cement (Reference Office 3).

Window frames with aluminum panels form the outer envelope of the building, fitted between the concrete pillars and beams. Effectively each façade has three elements to the thermal envelope: concrete, aluminum, and glass. The windows are double glazed and have internal shading.

As far as energy needs are concerned, specific space heating consumption is highest in the Northern Continental region (at 238 kWh m^{-2} $year^{-1}$) and lowest in Southern Dry at 54 kWh m^{-2} $year^{-1}$. The EU-27 weighted average for space heating consumption is 161 kWh m^{-2} $year^{-1}$ and 10 kWh m^{-2} $year^{-1}$ for domestic hot water.

Specific space cooling consumption is highest in Southern Dry region (at 42 kWh m^{-2} $year^{-1}$) and lowest in the Oceanic region at 11 kWh m^{-2} $year^{-1}$. The EU-27 weighted average for space cooling consumption is 22 kWh m^{-2} $year^{-1}$.

Lighting energy consumption ranges between 25-71 kWh m^{-2} $year^{-1}$, being the EU-27 weighted average approximately 39 kWh m^{-2} $year^{-1}$.

Detailed information about the fuel use in office buildings is limited, showing a high degree of variation in the primary and secondary fuels used. However, some fuels are strongly preferred in certain countries, due to availability and geopolitical reasons:

- Coal: Slovakia, Poland and Lithuania;
- Electricity: all countries, but particularly in Cyprus, Greece, Malta and Spain;
- Wood: Bulgaria, Latvia and Portugal;
- Gas: UK, Slovakia, Netherlands, Luxembourg, Germany, Hungary and Czech Republic;
- Oil: Belgium, Cyprus, Ireland, Spain and Slovenia.

1.4 Typical refurbishing actions for office buildings

Several studies have focused generally on the issue of refurbishing existing office buildings. In general, they are based on the concept that the use of an energy-efficient façade is indispensable for reducing the energy demand for air conditioning [10-11].

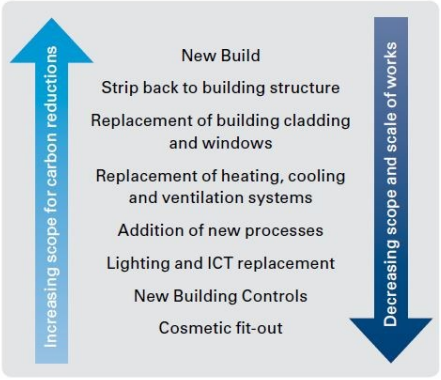

FIGURE 1.14: Relationship between refurbishment scope and ability to influence carbon emissions [10]

In fact, since facades act as a physical barrier between the indoor and outdoor environments, interventions aimed at improving its performance are considered as one of the most effective ways to both reduce energy consumption in buildings and improve their indoor environmental quality.

Additional thermal insulation, installation of high-performance glazing systems, and passive measures such as natural ventilation, shading systems, and the use of daylighting are all beneficial

interventions in that respect. Some authors suggest that an improved insulation is more important than an insulated solar control in existing, poorly insulated office building [12].

There are, however, counter-arguments which suggest that traditional means of improving façade thermal performance are likely to increase cooling loads during warm/hot seasons [13].

The upgrade from standard single or double-glazing to high efficiency double glazing to reduce heating loads has been considered as the most effective way to reduce the negative environmental impacts as a result of poor performance of old façade components, as reduction in space heating in some cases has been recorded to be around 35% [14].

FIGURE 1.15: Example of double skin glass façade (a,c) and green façade (b) [15]

Different retrofitting strategies have also been investigated for different types of office buildings in different climatic conditions. Among these strategies, many relate to elements of the building façade such as the improvement of wall insulation, the replacement of windows and window frames, the use of shading devices and the maximum deployment of natural ventilation.

Such interventions resulted in significant energy reductions for all the office types in all the climatic regions, with values ranging from 20% up to 50% [13, 16].

TABLE 1.1: Different retrofitting scenarios for open plan (Type A) and cellular (Type B) office buildings [13]

Scenario	Type A	Type B
Building envelope	• Improvement of insulation levels • Weather stripping of windows/doors • Replacement of window frames in bad condition • Use of double glazing • Use of additional shading (summer) • Integration of passive solar and daylighting components (atriums—shaded in summer)	• Increase of wall insulation levels • Reduction of the air infiltration rate • Replacement of existing windows
Passive systems and techniques	• Use of additional shading devices in the 1st and 2nd floor (summer) • Night ventilation (summer) • Use of ceiling fans in the major zones (summer) • Use of an economizer cycle (summer) • Use of an evaporative cooler to pre-cool the fresh air (summer)	• Use of mechanical night ventilation (summer) • Use of external shading devices (summer) • Use of ceiling fans (summer) • Use of indirect evaporative cooler (summer)
Lighting	• Use of high-efficiency fluorescent lamps with electronic ballast and daylight compensation • Decrease of the general lighting up to 20 W/m^2 and use task lighting • Use of time-scheduled control • Improvement of luminaries and installation of reflectors	
HVAC	• Use of a BMS • Decrease of the winter set-point • Use of heat recovery of the return air • Recovery of the waste heat from the boiler flue gases • Possible replacement of the existing boiler • Use of a flue gas analyzer and a compensation controller for the burner • Recovery of heat from the condenser	• Use of a BMS • Use of air-to-air heat recovery system
Global retrofit	All the above	All the above

Beneficial effects due to façade improvements, related to heating/cooling loads reduction, natural ventilation and appropriate shading are echoed also by Wong et al. [17] and Jin and Overend [18].

To summarize, three main conclusions related to office buildings refurbishment can be drawn from this brief literature review:

- Notable energy reduction is achievable;
- Significant carbon emissions can be saved;
- Interventions beneficial in one season may have counter effects in other seasons.

1.5 Research topic and significance of the study

Within this context, the present research aims at exploring the benefits stemming from the application of a passive cooling technology, namely the application of *cool materials* to existing office buildings roofs, in terms of improvement of thermal comfort conditions and reduction in the energy needs.

Despite the concept of cool roofs is well known in US since 1990s, many studies focused on their performance in the residential/commercial sectors under various climatic conditions (see Chapter 3) for US countries, while only a few exemplary case studies are analyzed in EU countries.

Given this, after the characterization of the existing buildings stock in the EU (Chapter 1) – with a particular focus on office buildings - the thesis work gives an insight into roof energy balances due to different technological solutions (Chapter 2). Chapter 3 describes in detail the physical properties of cool materials and their availability on the market, thus providing a solid background for the parametric analysis developed in Chapter 4 aimed at evaluating cool roofs performance for various climates and office buildings configurations.

By using detailed numerical models, the thermal behavior of representative office buildings of the existing EU buildings stock is deeply assessed in terms of thermal comfort and energy needs for air conditioning (Chapter 5). Finally, an economic analysis carried out in terms of payback time will discuss the convenience of this solution for passive cooling purposes.

1.6 References of the chapter

[1] International Energy Agency, 2014. Link: www.iea.org/aboutus/faqs/energyefficiency/

[2] Directive 2010/31/EU of the European Parliament and of the Council of 19 May 2010. Link: http://eur-lex.europa.eu/LexUriServ/LexUriServ.do?uri=OJ:L:2010:153:0013:0035:EN:PDF

[3] N. Rajkovich, R. Diamond, B. Burke, Zero net energy myths and modes of thought, Proceedings of ACEE Summer Study on Energy Efficiency in Buildings, Pacific Grove, California, 2010. Link: http://aceee.org/files/proceedings/2010/data/papers/2125.pdf

[4] I. Sartori, A. Napolitano, K. Voss, Net zero energy buildings: A consistent definition framework, Energy and Buildings 48 (2012) 220-232

[5] P. Torcellini, S. Pless, M. Deru, D. Crawley, Zero Energy Buildings: A critical Look at the Definition, Proceedings of ACEE Summer Study, Pacific Grove, California, 2006. Link: http://www.nrel.gov/docs/fy06osti/39833.pdf

[6] K. Voss, E. Musall, Net Zero Energy Buildings, International projects of carbon neutrality in buildings, Detail Green Books, Varennes (Canada), 2011

[7] BPIE, Europe's Building Under the Microscope. A country-by-country review of the energy performance of buildings, 2011. Link: http://www.europeanclimate.org/documents/LR_%20CbC_study.pdf

[8] International Energy Agency Solar Heating and Cooling Task 47, 2014. Renovation of Non-Residential Buildings towards Sustainable Standards. Link: http://task47.iea-shc.org/publications

[9] iNSPiRe Project, Survey on the energy needs and architectural features of the EU buildings stock, 2014.
Link: http://www.inspirefp7.eu/about-inspire/downloadable-reports/

[10] Carbon-Trust, Low Carbon Refurbishment of Buildings, A guide to achieving carbon savings from refurbishment of non-domestic buildings, 2008

[11] CIBSE, CIBSE TM 53: 2013-Refurbishment of non-domestic buildings in Great Britain, 2013

[12] L. Thomas, Evaluating design strategies, performance and occupant satisfaction: a low carbon office refurbishment, Building Research Information 38:6 (2010) 610-624

[13] E. Dascalaki, M. Santamouris, On the potential of retrofitting scenarios for offices, Building and Environment 37:6 (2002) 557-567

[14] I. Blom, L. Itard, A. Meijer, Environmental impact of dwellings in use maintenance of façade components, Building and Environment 45:11 (2010)

[15] S. F. Larsen, L. Rengifo, C. Filippin, Double skin glazed facades in sunny Mediterranean climates, Energy and Buildings 102 (2015) 18-31

[16] M. Santamouris, E. Dascalaki, Passive retrofitting of office buildings to improve their energy performance and indoor environment: the OFFICE Project, Building and Environment 37 (6) (2002) 575-578

[17] I.L. Wong, P.C. Eames, S. Perera, Energy simulations of a transparent-insulated office façade retrofit in London, UK, Smart Sustainable Built Environment 1 (3) (2012) 253-276

[18] Q. Jin, M. Overend, Façade renovation for a public building based on a whole-life value approach, in: Proceedings of Building Simulation and Optimisation Conference 2012, Loughborough, 2012, 378-385

2. ROOF TECHNOLOGIES AND THEIR ENERGY BEHAVIOR

The building's energy demand is closely connected to the efficiency of its envelope; in fact, if the building envelope is not correctly designed, the heat fluxes through the structures (vertical, horizontal, transparent and opaque) are the cause of a large increase in energy consumption. Therefore it is very important to develop alternative construction techniques that guarantee both thermal comfort and low energy use. Generally, thermal building regulations have the aim to reduce the energy needs for air conditioning, but usually the proposed solution is the *overinsulation* of buildings that could reduce the effectiveness of traditional passive strategies (thermal mass, ventilation) and create adverse effects on indoor thermal comfort. In regions with hot climates, such as Mediterranean countries, the roofs during the summer receive large amounts of solar radiation and their superficial temperatures can reach values up to 75°C [1]. Obviously, this causes a significant risk of overheating, making consequently the cooling of the building very expensive [2].

A possible way to cope with this problem is the reduction of heat fluxes through the building envelope by using technologies such as *cool roofs*, *green roofs* and *ventilated roofs*. In the following, an overview of these solutions will be given, together with the energy balance equations that govern the physical problem.

2.1 General overview of Cool Roofs (CR)

"A roof with high solar reflectance (ability to reflect sunlight) and high thermal emissivity (ability to radiate heat) stays cool in the sun, reducing demand for cooling power in conditioned buildings and increasing occupant comfort in unconditioned buildings" [3].

Levinson defines *Cool Roofs* in this way: they are particular materials having a high solar reflectance r - thus reducing heat gains during daytime - and a high thermal emissivity ε that enables them to dissipate the heat absorbed during night. However, while these are key features, other parameters are of main interest for the energy balance of a roof, such as its extension compared to the opaque envelope (known as *roof-to-wall ratio*) and the thermal resistance R of the whole roof components.

As stated in the introduction, traditionally building codes have focused on more roof insulation, i.e. high R-values, but more recently the extent of energy savings and comfort benefits of roofs with a high albedo in warm climates have become prominent.

In fact, the raise of roof *R*-values - and consequently of insulation costs – reduces daytime heat gains but at the expense of nighttime heat losses, and this is inferable from the energy balance reported in Eq. (2.1) for steady-state conditions, that is to say without considering the heat capacitance of the roof:

$$\underbrace{(1-r)\cdot I}_{q_{absorbed}} = [\underbrace{\sigma\cdot\varepsilon\cdot(T_{so}{}^4 - T_{sky}{}^4)}_{q_{radiant}} + \underbrace{h_c\cdot(T_{so}-T_o)}_{q_{convective}}] + \underbrace{\frac{T_o - T_i}{R}}_{q_{transferred}} \qquad (2.1)$$

Eq. (2.1) states that the solar radiation absorbed by the roof surface $q_{absorbed}$ is partially released to the outdoor environment, both by infrared radiation ($q_{radiant}$) and by convection ($q_{convective}$). The contribution of these terms is strongly affected by the roof surface temperature T_{so}. Moreover, heat transfer occurs through the roof by conduction ($q_{transferred}$): this contribution is proportional to the difference between the outdoor air temperature T_o and the indoor temperature T_i, while depending on the thermal resistance *R* associated to the roof layers and to the heat transfer on the inner surface of the roof.

FIGURE 2.1: View of cool roofs in Honolulu, Hawaii [Internet]

It is clear from the previous equation how the main parameters determining the cool roof performance are the solar reflectance *r*, the thermal resistance *R* and thermal emissivity ε, although a significant contribution to the heat balance is provided also by the convective coefficient h_c.

A very interesting study on the influence of the three parameters (*r*, *R*, ε) on the peak heat gains and daily average cooling loads (over six summer months), per 100 m^2 of a flat roof located in Sydney, is carried out by Gentle et al. [4] by means of dynamic simulations.

The main results are reported in Figs. 2.2-2.3, which show the peak cooling load in January (southern hemisphere) and the average cooling load per day over the cooling season, respectively. Eighteen different combinations of the three parameters are taken into account, with the aim of considering reasonable values for all of them. The cooling set point is 25°C, and the figures refer to different combinations of solar absorptance (A_{sol} = 1-r), thermal emissivity (E= ε) and thermal resistance (R).

More in detail, Fig. 2.2 reveals how cooling loads rapidly rise as R decreases at low r, in contrast with the small rise with 1/R that occurs at high r. It is also important to notice how the peak load is smaller at A_{sol} = 0.2 and R = 1.63 compared to all cases with A_{sol} > 0.6 when R = 3.06, thus demonstrating how a low solar absorptance should be the dominant concern. Moreover, these peak loads can be reduced in magnitude by factors of 2.5-3.5 by lowering A_{sol} (i.e. by increasing r), whatever R is considered.

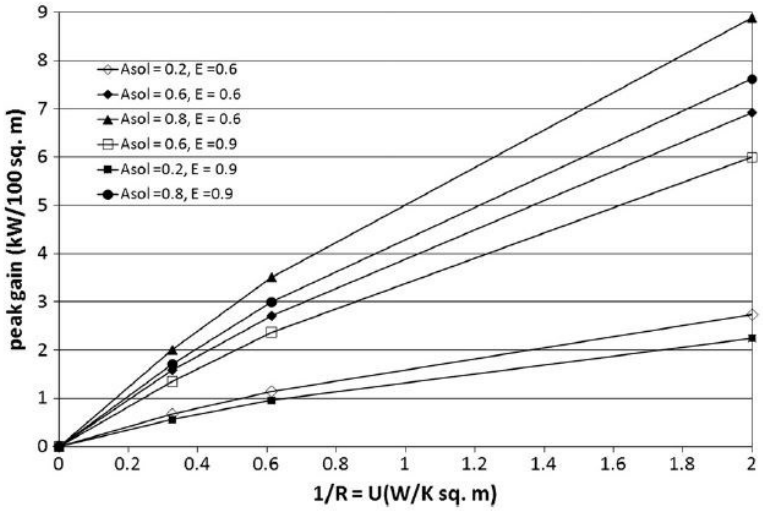

FIGURE 2.2: Peak heat gains (kW) per 100 m^2 of a flat roof as a function of different combinations of A_{sol}, E and R values [4]

For the same parameter set, Fig. 2.3 shows the average cooling load per day over the six months cooling season. It is important to pinpoint that the sensitivity to lowering of the E value from 0.9 to 0.6 increases as both more solar energy is absorbed by the roof and more is transmitted inwards.

Although high E appears less important if A_{sol} is small at all R, the thermal resistance should not get too high to enable night sky cooling to be more effective and to save costs.

Moreover, if comparing Figs. 2.2-2.3 it is possible to observe how they are qualitatively similar in shape, but for each change in thermal resistance A_{sol} have a bigger impact on average daily load than on peak load.

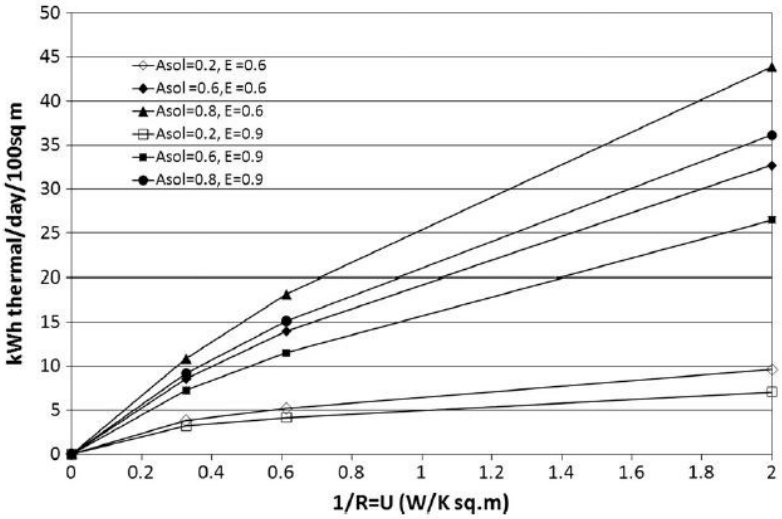

FIGURE 2.3: Daily average cooling loads per 100 m^2 of a flat roof as a function of different combinations of A_{sol}, *E* and *R* values [4]

In order to fully appreciate how much cool roofs can help improve building thermal performance, it is important to focus on the values currently achievable by solar reflectance *r*; these values obviously depend on the chemical agents used to produce a cool paint, and can achieve values higher than 0.8. However, it is well known that cool paints usually undergo soiling and weathering in the first months after installation, which significantly reduce their solar reflectance. As an example, Akbari [5] reported on a reduction of about 10% in only two months in the solar reflectance of a white coating having an initial *r* = 0.8; another field study measuring the effects of aging and weathering on ten roofs in California found that the reflectance of cool materials can decrease by as much as 0.15, due to the deposition of soot and dust, mostly within the first year of service [6].

This aging process is shown in Fig. 2.4, where the effects of two months to six years of accumulation of environmental pollutants on the albedo of different roofs is measured. The data indicate that most of the decrease in albedo occurs in the first year, possibly in the first few months, being the cementitious coating on gravel substrate the technical solution ensuring the smallest and most gradual decrease in albedo.

In order to assess the effects of the cool materials aging process on cooling energy savings, the same authors assume a linear approximation for the relationship between albedo and surface

temperature as an indicator of the magnitude of the heat transfer through the roof. In this way, energy savings are proportional to the reduction in the heat fluxes incoming through the roof.

For testing this hypothesis, the cooling needs of real buildings were monitored over the summer period, at the beginning of which the albedo of the roof was measured at 0.73, and the original value (before the coating) was 0.18. The estimated energy savings reported are about 80% (270 kWh/year).

After one year of exposure, roof albedo had dropped to 0.61, thus they estimate long-term cooling energy savings to be 20% lower than first year savings.

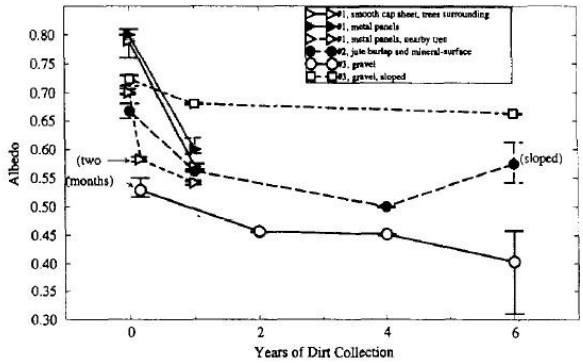

FIGURE 2.4: Variations in albedo for different exposure time for various flat roofs in California [6]

A slightly different message is conveyed by Bretz and Akbari [7], who demonstrated that washing the roof surface could almost restore the original solar reflectance.

In the framework of an experimental campaign, most roofs were washed with soap and water, using a mop while other were washed differently, for the sake of comparison among the different methods.

The restoration in albedo (expressed as a percentage of recovery with respect to the original value) resulting from the washing process was found to be generally significant. When surfaces were rubbed with soap, the albedo was restored to within 90% of the original value, indicating that the loss of albedo is not permanent, and it is caused by dirt accumulation rather than by UV or hydrolytic degradation (see Table 2.1 for details).

TABLE 2.1: Albedo restoration of different roofs for various washing methods [7]

Measurement No.	Substrate type	Pitch (%)	Age of coating (y)	Dirt collection (y)	Washing method	Initial Albedo	Albedo restoration (% of initial albedo)
NA	smooth cap sheet	2	1	1	hose off	0.79	81
21	smooth cap sheet	2	1	1	soap and mop	0.79	92
22	smooth cap sheet	2	2	1	soap and mop	0.79	96
2	metal panels	0	1	1	soap and mop	0.69	100

For further details on this phenomenon, the reader can refer to Section 3.3 where several long-term albedo assessments are described for different cool materials.

As for the values assumed by thermal emissivity ε, it can be assumed almost constant for a great variety of roofing materials and very close in value to that of a grey body (usually $\varepsilon = 0.9$ can be assumed for non-metallic materials).

Finally, Eq. (2.1) states that it is also important to make an appropriate choice for the convective coefficient h_c, as remarked in [8]. Indeed, under typical summer conditions occurring in a hot-humid climate such that of Southern Italy ($I = 800$ W m^{-2}, $\varphi = 60\%$, $25 \leq T_o \leq 35$ °C) - and for a fixed value of the thermal resistance of the roof ($R = 1.40$ m^{-2} K W^{-1}) - it is easy to notice that the choice of h_c has a strong influence on the temperature difference ΔT between the roof surface temperature T_{so} and the outdoor temperature T_o (Fig. 2.5).

This is true for a low reflective coating ($r = 0.25$), for which ΔT differences up to 5°C should be expected when increasing h_c by 5 units step (W m^{-2} K^{-1}), while if looking at the high reflective coating ($r = 0.85$) this temperature difference is extremely less sensitive to h_c. In this case, the roof temperatures are expected to be only few degrees above the outdoor air temperature.

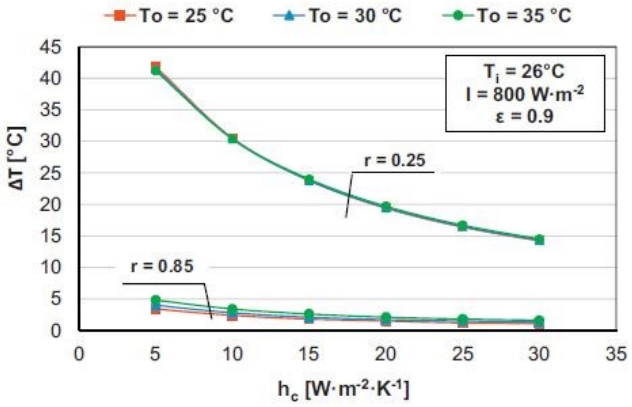

FIGURE 2.5: Difference between roof outer surface temperature and outdoor temperature as a function of h_c [8]

Moreover, the increase in h_c also affects the heat flux q incoming through the roof, as shown in Fig. 2.6 for the same r values seen in the previous graph. Here both the low and high reflective finishing layers of the roof follow a trend very close to that shown in Fig. 2.5. This rebates how important is a correct evaluation of the convective heat transfer coefficient, especially for low to moderate reflective

roofs, for making reliable predictions on the potentiality of cool roofs as a strategy to improve thermal performance of existing buildings.

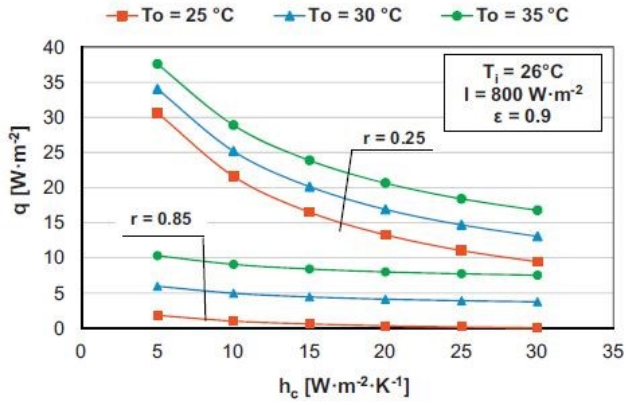

FIGURE 2.6: Heat flux incoming through the roof as a function of h_c [8]

2.2 General overview of Green Roofs (GR)

Green roofs represent a promising adaptation strategy for facing climate changes, and the number of green roof studies has consequently increased in recent years. The thermal effects of a green roof mainly result from the shading, insulation, evapotranspiration and thermal mass of the plants and their substrate, with the additional contribution of the high specific heat of the water contained in the substrate to the thermal inertia of the whole "green" package.

In addition, evapotranspiration from a green roof brings a cooling effect, since experiments demonstrate that latent heat can override sensible heat on a green surface, and leaf transpiration accounts for almost 30% of rooftop cooling.

Moreover, the insulation role of green roofs can mitigate indoor peak temperatures, saving both cooling and heating loads, and decreases the heat flux entering the roof by 60% according to the roof design.

FIGURE 2.7: View of green roofs in Stuttgart, Germany [Internet]

Parizotto and Lamberts [9] investigated the thermal performance of a green roof in Florianopolis (Brazil) for both warm and cold periods by means of field measurements. Heat fluxes, green roof's temperature profile and water volumetric content in substrate layer were monitored, together with internal air temperature of rooms.

They found out that during the warm period (1-7 March 2008), the green roof reduced heat gain by 92%-97% in comparison to ceramic and metallic roofs respectively, and enhanced the heat loss to 49% and 20%. During the cold period (25-31 May 2008), the green roof reduced heat gain by 70% and 84%, and reduced the heat loss by 44% and 52% in comparison to ceramic and metallic roofs, respectively. From the derived data, it has been confirmed that green roof contributes to the thermal benefits and energy efficiency of the building in temperate climate conditions.

A comparison among different passive cooling technologies under hot-humid climatic conditions and for highly-insulated slabs has been carried out by D'Orazio et al. [10], who performed an experimental assessment of the yearly performance of all of the different technologies. The goal was to understand whether in summer the passive cooling effects are inhibited by the low thermal transmittance recently introduced in many southern Europe countries to meet the demands of the energy savings regulations for the winter heating season.

The results of this field study show that, despite thermal fluxes do not turn out to be very different from those of other roof solutions - because of low transmittance of the systems - passive cooling effects are not negligible. This is due to the presence of fluxes going out of the slab 40% of the time during the summer season considered, and by significant delay of incoming heat fluxes waves.

During winter, the green roof produces a further insulating effect in the covering that contributes to reducing thermal dispersion also in wet or saturated conditions.

Similar results are obtained by Lazzarin et al. [11], who performed a series of measurement sessions on a green roof installed on the Vicenza Hospital roof (northern Italy), finding how relevant is the role played by the latent flux of the evapotranspiration process. In fact, during summer – with the soil in almost dry conditions – the green roof allows an attenuation of the thermal gain entering the underneath room of about 60% with respect to a traditional roofing with an insulating layer.

That is due to the higher solar reflection of the greenery, while the evapotranspiration contribution is quite limited. When the soil is in a wet condition, not only the entering flux is cancelled, but also a slight outgoing flux is produced so that the green roof works as a passive cooler, thanks to the cooling effect of evapotranspiration. During winter, the evapotranspiration process is driven above all by the air vapor pressure deficit, able to produce an outgoing thermal flux from the roof that is 40% higher than the corresponding one of a high solar absorbing and insulated roof.

As briefly described above, green roofs can achieve the expected goals if properly designed, but it is necessary to simulate their effectiveness in relation to local conditions before construction.

Modeling green roofs involves the study of mass and heat transfer through the different layers, as well as plant physiology. Several models are available in the literature: the simplest models only consider the reduction of roof thermal transmittance based on in-situ measurements (Fig. 2.8, [10]), while other studies analyze more in detail the complex phenomena due to foliage shading and evapotranspiration [9].

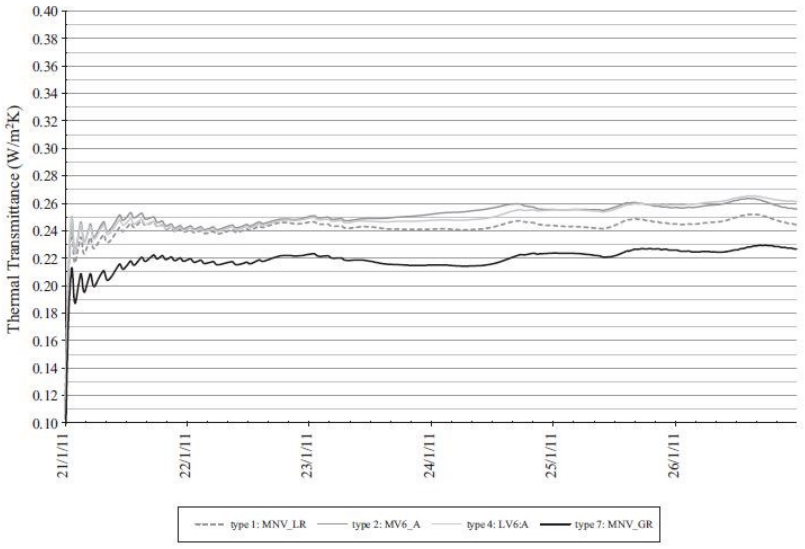

FIGURE 2.8: In situ thermal transmittance assessment for various green roof solutions [10]

Among all of the models proposed in the literature, the mono-dimensional one developed by Del Barrio [12] divides a green roof in three different layers: the canopy, the soil and the support. By imposing the horizontal homogeneity of the roof slab, heat and mass fluxes are assumed to be mainly vertical, so one-dimensional equations can be adopted to describe the thermal behavior of each layer. This model has been validated through a sensitivity analysis using Athens meteorological data and a concrete roof slab of 10 cm. Its approach represents the main reference for other one-dimensional models, such as those developed by Kumar and Kaushik [13] or by Lazzarin et al [11].

On the other hand, two-dimensional models are much less common: an example in the literature is given by Alexandri and Jones [14], aimed to evaluate the thermal effect of green roofs and green walls. Anyway, nowadays the one-dimensional EcoRoof model developed by Sailor [15] is maybe the most used one, and thanks to its high reliability it has been implemented in the software tool EnergyPlus (Fig. 2.9 gives a representation of the heat fluxes occurring at different layers).

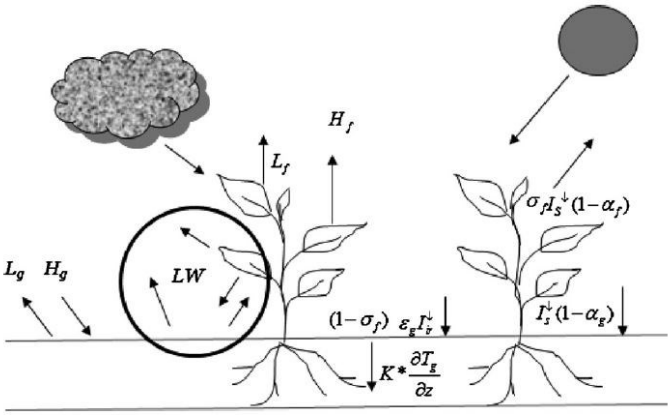

FIGURE 2.9: Energy balance for a green roof, including latent heat flux (L), sensible heat flux G, shortwave (I) and longwave radiation (LW) [15]

Based on the previous work of Frankenstein and Koenig [16], who developed the FASST (Fast All-Season Soil Strength) model, Sailor considers two heat fluxes for the green roof, respectively at the foliage surface F_f (see Eq. 1) and at the ground surface F_g (see Eq. 2.2):

$$F_f = \underbrace{\sigma_f[I_{sol}\cdot(1-r_f)+\varepsilon_f\cdot I_{ir}-\varepsilon_f\cdot\sigma\cdot T_f^4]}_{radiative\_sky}+\underbrace{\frac{\sigma_f\cdot\varepsilon_g\cdot\varepsilon_f\cdot\sigma}{\varepsilon_1}\cdot(T_g^4-T_f^4)}_{radiative\_ground}+\underbrace{H_f}_{sensible}+\underbrace{L_f}_{latent} \qquad (2.2)$$

$$F_g = \underbrace{(1-\sigma_f)\cdot[I_{sol}\cdot(1-r_g)+\varepsilon_g\cdot I_{ir}-\varepsilon_g\cdot\sigma\cdot T_g^4]}_{radiative\_sky}-\underbrace{\frac{\sigma_f\cdot\varepsilon_g\cdot\varepsilon_f\cdot\sigma}{\varepsilon_1}\cdot(T_g^4-T_f^4)}_{radiative\_foliage}+\underbrace{H_g}_{sensible}+\underbrace{L_g}_{latent}+\underbrace{K\cdot\frac{\partial T_g}{\partial z}}_{conductive\_soil}$$

(2.3)

As it is possible to observe from Eq. (2.2) and Eq. (2.3), in both cases the energy balance is split into a radiant term, a sensible and latent heat exchange and a conductive heat flux for the soil. The radiant term considers the heat exchange with the sky (at short and long wavelengths) and the mutual heat transfer between foliage and ground layers. Actually, this model does not allow the soil thermal properties (specifically solar reflectance, thermal conductivity, specific heat capacity and density for dry soil) to vary according to the moisture content of the soil media, because of stability issues during the calculation [17]. However, a simplified moisture balance that allows to consider precipitation, irrigation and moisture transport between two soil layers (top and root zones) is already implemented; future improvements in this direction are in any case necessary, as highlighted in [18]. In fact, moisture can leave the soil by means of evaporation, and the vegetation by evapotranspiration: these phenomena are influenced by water runoff in the soil layer due to saturation-excess and infiltration-excess [19]. Given this, EnergyPlus allows the user to define a series of parameters, for both the soil layer and the foliage, to fully characterize the green roof.

Olivieri et al. [20] have carried out a sensitivity analysis by varying all the parameters that define the EcoRoof routine in the range allowed by the software, and have found that, for an extensive green roof in the Mediterranean coastal climate, only four parameters have a strong influence on the roof performance and must be carefully considered.

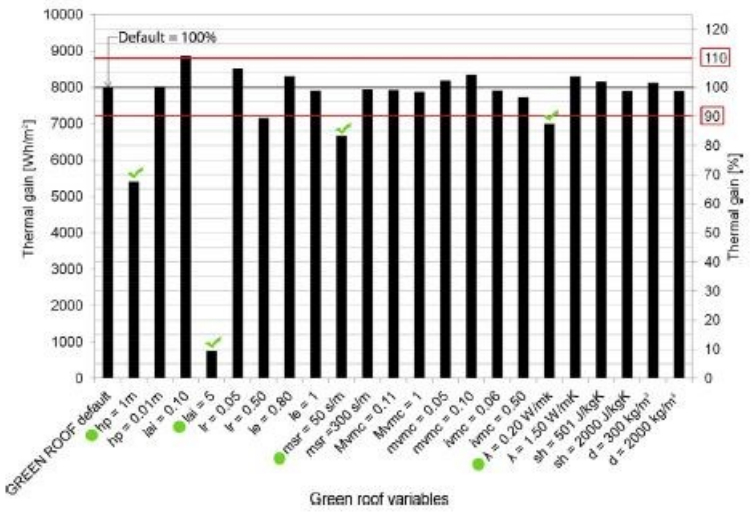

FIGURE 2.10: Results of the sensitivity analysis of the EcoRoof routine on predicted thermal gain [20]

More in detail, the thermal gain entering the roof for the maximum and minimum value of each variable is found (see Fig. 2.10), leaving the other variables at default values. These values are then

compared with the value obtained using all default variables; a variation of less than 10% compared with the default value was considered not significant.

The most important parameters are found to be:

- the height of plants (h_p);
- the Leaf Area Index (LAI), defined as the ratio of the projected leaf area to the overall ground area;
- the minimum stomatal resistance (m_{sr}), which represents the resistance of the plants to moisture transport;
- the dry soil conductivity (K).

2.3 General overview of Ventilated Roofs (VR)

Natural ventilation of a roof cavity seems to be an attractive measure to dissipate solar radiation outdoors before excessive heat is transferred into the occupied space indoors.

The ventilation of a roof or an attic has become one of the greatest interests for building researchers in the last several decades as a measure to decrease attic temperatures and cooling load in an occupied space.

When naturally ventilating a roof, induced air movement by solar irradiation must be pursued in depth, considering the buoyancy of hot air as a self-induction force acting favorably even when wind force is not available [21].

Ventilated roofs may adapt to the geometry configuration of existing flat or tilted roofs (see Figure 2.11); however, in order to evacuate accumulated hot air from an attic, several studies indicates that the most effective form of ventilation is given by a combination of ridge and soffit vents [22].

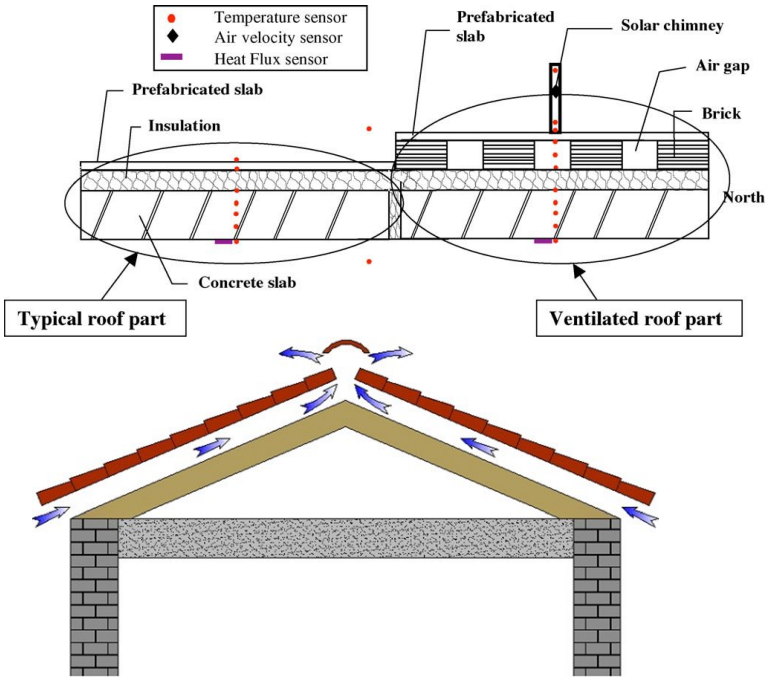

FIGURE 2.11: Schematic representation of flat (top, [21]) and pitched (bottom, [22]) ventilated roofs

The ventilation of the roof may be created by natural or forced convection: natural convection (buoyancy effect) is generated by difference of temperatures; mechanical apparatus (i.e. fans) generates forced convection.

Solar radiation heats the outdoor air within the air gap; the warm air becomes lighter and creates an upward flow. This airflow produces advantageous effects because it reduces the heat storage in the structure while reducing the heat flux through the roof. This is shown in Fig. 2.12, where the upper and lower surface temperatures of a metallic cavity roof and of a single roof are compared for the Japanese city of Toyohashi City [21].

In daytime, the upper surface temperatures of the cavity are significantly lower than those of the single roof: the highest temperature difference is registered at noon, and amounts to about 20°C. During the night, the upper surface temperatures of both roofs fell slightly below the outdoor air temperature.

Moreover, the lower surface temperature of the cavity roof was much lower than that of the single roof in the daytime, being approximately the same during night.

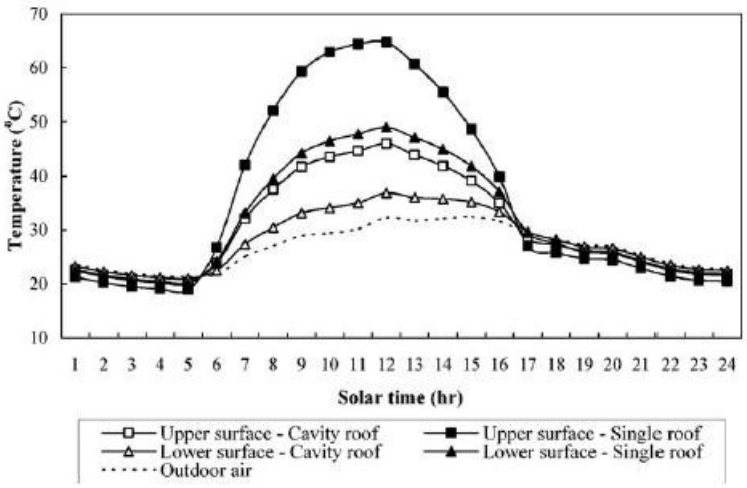

FIGURE 2.12: Comparison of upper and lower roof surface temperatures [21]

If looking at the corresponding hourly cooling load (Fig. 2.13), it can be observed how they became negative at night for the ventilated roof, thus theoretically requesting some heating, while peak values are almost split in half.

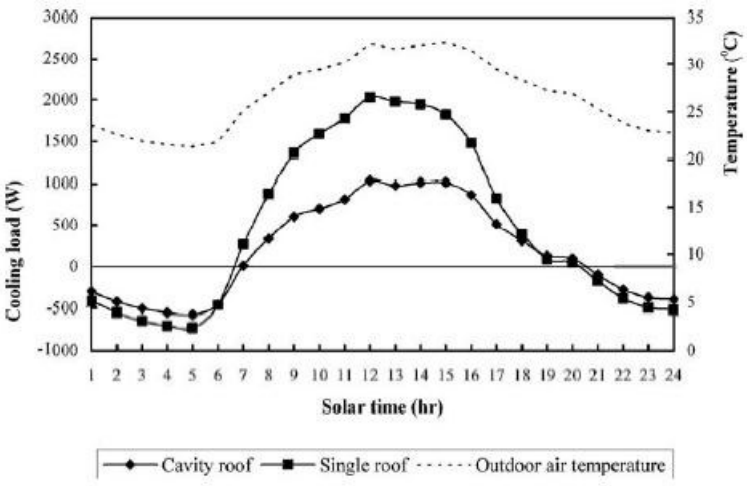

FIGURE 2.13: Comparison of cooling loads [21]

During the winter season, the air temperature within the ventilated roof is approximately the same as of the outdoor environment, because the solar radiation has low intensity resulting with much reduced stack effect.

A study aimed at comparing the thermal performance of ventilated and traditional flat roofs for the hot-arid climate of Athens (Greece), with the help of well-insulated test cells, was undertaken by Dimoudi et al. [23].

The ventilated roof component consisted of a 12 cm reinforced concrete slab in direct contact with the underneath room, 5 cm thick layer of extruded polystyrene placed on top of the concrete slab, the ventilation air gap (6 cm and 8 cm gap heights are tested) and 2.5 cm reinforced concrete slab facing outdoor.

In the center of the ventilated roof, a circular chimney of 35 cm height and 5 cm diameter made of metal sheet and painted black externally, was used for improving the extraction of hot air from the gap.

A constant room temperature of 27°C was applied in the interior of the test cell during the whole testing period.

The relative difference of the heat flow for different layout configurations (Phases 2-3 refer to an air gap height of 8 cm, while Phases 4-5 to an air gap height of 6 cm) - considering also the presence of a radiant barrier (Phases 3 and 4) - is shown in Table 2.2.

Here, the percentage difference of the ventilated roofs heat fluxes with respect to the traditional roof ones (performance indicator *A*) is reported for daytime, nighttime and for the whole 24 hours.

TABLE 2.2: Comparison of heat flows between ventilated and typical roofs [23]

	Daytime	Night-time	24 h
Performance indicator $A = (Q_T - Q_V)/\|Q_T\|$ (%)			
Phase 2	45	−18	49
Phase 3	58	−38	110
Phase 4	68	−33	281
Phase 5	56	−13	61

It can be inferred that the ventilated roof performs better than the typical during summer daytime, while the opposite is true for summer nighttime; on a 24 h basis, the ventilated roof presents better thermal performance than the typical one.

The radiant barrier (Phases 3 and 4) enhances the performance of the ventilated roof during summer daytime by reducing thermal gains, while during nighttime it is unfavorable for the performance of the ventilated roof. Anyway, the overall daily performance is still favorable for both air gaps.

Not negligible is also the role played by roof tile permeability on thermal performance of ventilation ducts typically used in south European countries under the layer of tiles.

By analyzing 14 different types of roofs, D'Orazio et al. [24] proved that the air permeability of the layer of tiles determines a certain amount of heat to be released, in addition to the release connected with the stack effect, in ventilation ducts that have the same characteristics but are perfectly airtight.

The main finding of this study is that there are no substantial differences in performance between perfectly and not-perfectly airtight ventilation ducts, thereby confirming that the very high permeability of the tiles used tends to counter the differences in the cross section of the ventilation duct.

On the other hand, the numerical study of ventilated structures is a very complex procedure that requires a detailed knowledge of the airflow rate and its thermodynamic properties, thermophysical properties of materials, convective coefficients values and outdoor boundary conditions (solar radiation intensity, outdoor air temperature, outdoor relative humidity, velocity and wind direction).

An example of a ventilated roof energy balance is given in Figure 2.14 [25], where the surface temperatures of the upper and lower roofs slabs (T_1, T_2, T_3 and T_4), the outdoor and indoor air temperatures T_o and T_i represent the nodes of the thermal network shown in Fig. 2.15; thermal resistances are given by interior/exterior air films, slabs thicknesses and radiative/convective resistances within the air gap.

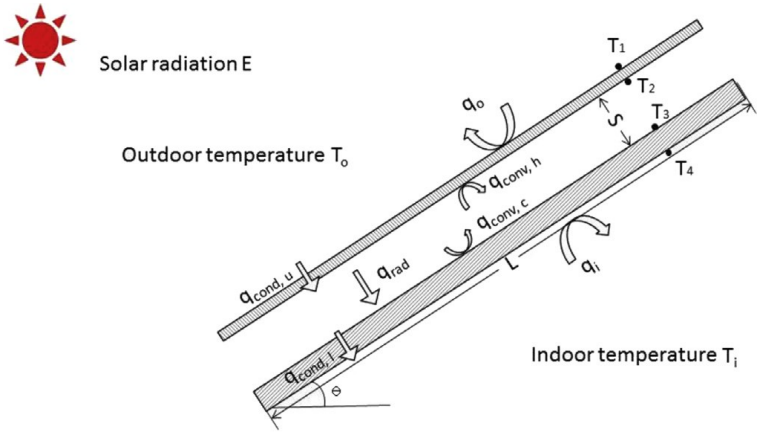

FIGURE 2.14: Heat fluxes across a ventilated roof [25]

For solving these circuits, thus finding the nodal temperatures and estimating the heat fluxes incoming through the roof, the use of Computational Fluid Dynamics (CFD) simulations is very often employed.

These simulations are used also to calculate the airflow and thermodynamic properties of the air within the gap, by solving the time-averaged Navier-Stokes equations of motion for steady, compressible flows.

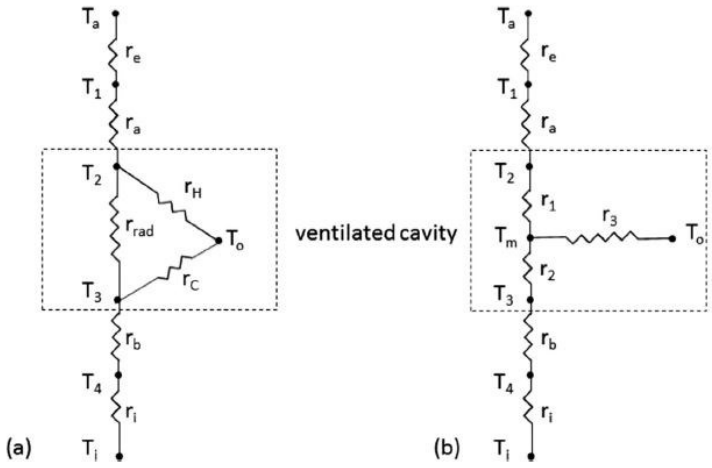

FIGURE 2.15: Two possible thermal networks for the ventilated roof: a triangular circuit (a) and a Y-circuit (b) [25]

Based on simulation results, correlations are proposed for the convective thermal resistances between air and cavity walls; the proposed correlations are implemented in the developed model to predict the transferred heat flux.

It is possible to find a very close agreement between predictions and measurements for a specific experimental setup, as shown in Fig. 2.16 when comparing air velocity and temperature within the sloped cavity investigated by Tong et al. [25].

The main limitation of such an approach is that these correlations keep valid only for one specific cavity configuration; different layouts need to be investigated separately.

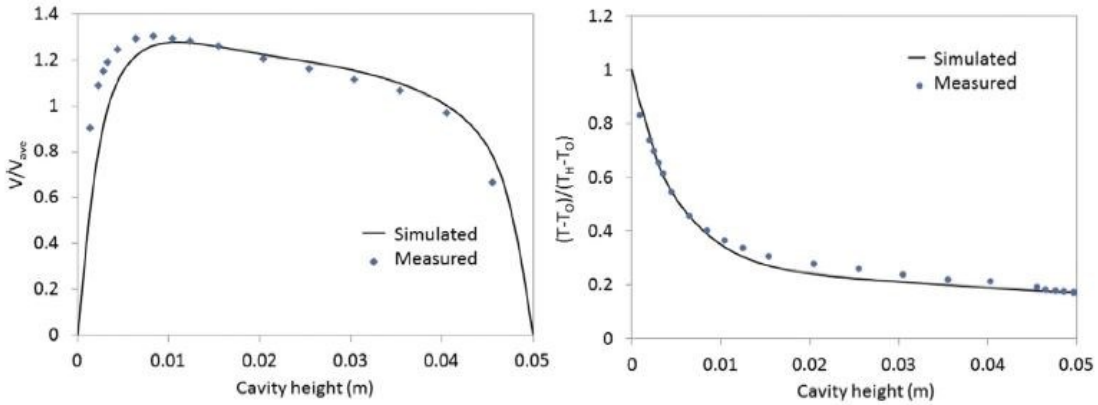

FIGURE 2.16: Comparison between simulated and measured air velocity and temperature in the ventilated cavity [25]

2.6 References of the chapter

[1] B. Cerne, S. Medved, Determination of transient two-dimensional heat transfer in ventilated lightweight low sloped roof using Fourier series, Building and Environment 41 (2007) 2279-2288

[2] A. Dimoudi, A. Androutsopolous, S. Lycoudis, Thermal performance of innovative roof component, Renewable Energy 31 (2006) 2257-2271

[3] R. Levinson, P. Berdahl, H. Akbari, W. Miller, I. Joedicke, J. Reilly, Y. Suzuki, M. Vondran, Methods of creating solar-reflective nonwhite surfaces and their application to residential roofing materials, Solar Energy Materials and Solar Cells 91 (2007) 304-314

[4] A.R. Gentle, J-L.C. Aguilar, G.B. Smith, Optimized cool roofs: Integrating albedo and thermal emittance with R-value, Solar Energy Materials & Solar Cells 95 (2011) 3207-3215

[5] H. Akbari, Measured energy savings from the application of reflective roofs in two small non-residential buildings, Energy 28 (2003) 953-967

[6] P. Berdahl, S.E. Bretz, Preliminary survey of the solar reflectance of cool roofing materials, Energy and Buildings 25 (1997) 149-158

[7] S.E. Bretz, H. Akbari, Long-term performance of high-albedo roof coatings, Energy and Buildings 25 (1997) 159-167

[8] V. Costanzo, G. Evola, L. Marletta, A. Gagliano, Proper evaluation of the external convective heat transfer for the thermal analysis of cool roofs, Energy and Buildings 77 (2014) 467-477

[9] S. Parizotto, R. Lamberts, Investigation of green roof thermal performance in temperate climate: A case study of an experimental building in Florianópolis city, Southern Brazil, Energy and Buildings 43 (2011) 1712-1722

[10] M. D'Orazio, C. Di Perna, E. Di Giuseppe, Green roof yearly performance: A case study in a highly insulated building under temperate climate, Energy and Buildings 55 (2012) 439-451

[11] R.M. Lazzarin, F. Castellotti, F. Busato, Experimental measurements and numerical modelling of a green roof, Energy and Buildings 37 (2005) 1260-1267

[12] E.P. Del Barrio, Analysis of the green roofs cooling potential in buildings, Energy and Buildings 27 (1998) 179-193

[13] R. Kumar, S.C. Kaushik, Performance evaluation of green roof and shading for thermal protection of buildings, Building and Environment 40 (2005) 1505-1511

[14] E. Alexandri, P. Jones, Temperature decreases in an urban canyon due to green walls and green roofs in diverse climates, Building and Environment 43 (2008) 480-493

[15] D.J. Sailor, A green roof model for building energy simulation programs, Energy and Buildings 40 (2008) 1466-1478

[16] S. Frankenstein, G. Koenig, Fast all-season soil strength (FASST), U.S. Army Engineer Research and Development Center, Cold Regions Research and Engineering Laboratory (ERDC/CRREL), Special Report SR-04-01 (2004). Washington, DC

[17] US Department of Energy, EnergyPlus version 8.1, 2014. Link: http://apps1.eere.energy.gov/buildings/energyplus/?utm_source=EnergyPlus&utm_medium=redirect&utm_campaign=EnergyPlus%2Bredirect%2B1

[18] Chen Pei-Yuan, Li Yuan-Hua, Lo Wei-Hsuan, Tung Ching-pin, Toward the practicability of a heat transfer model for green roofs, Ecological Engineering 74 (2015) 266-273

[19] Yang Wen-Yu, Li Dan, Sun Ting, Ni Guang-Heng, Saturation-excess and infiltration-excess runoff on green roofs, Ecological Engineering 74 (2015) 327-336

[20] F. Olivieri, C. Di Perna, M. D'Orazio, L. Olivieri, J. Neila, Experimental measurements and numerical model for the summer performance assessment of extensive green roofs in a Mediterranean coastal climate, Energy and Buildings 63 (2013) 1-14

[21] L. Susanti, H. Homma, H. Matsumoto, A naturally ventilated cavity roof as potential benefits for improving thermal environment and cooling load of a factory building, Energy and Buildings 43 (2011) 211-218

[22] A. Gagliano, F. Patania, F. Nocera, A. Ferlito, A. Galesi, Thermal performance of ventilated roofs during summer period, Energy and Buildings 49 (2012) 611-618

[23] A. Dimoudi, A. Androutsopoulos, S. Lykoudis, Summer performance of a ventilated roof component, Energy and Buildings 38 (2006) 610-617

[24] M. D'Orazio, C. Di Perna, P. Principi, A. Stazi, Effects of roof tile permeability on the thermal performance of ventilated roofs: analysis of annual performance, Energy and Buildings 40 (2008) 911-916

[25] S. Tong, H. Li, An efficient model development and experimental study for the heat transfer in naturally ventilated inclined roofs, Building and Environment 81 (2014) 296-308

3. COOL ROOFS: STATE OF THE ART

The present chapter provides an insight on:

(i) the physical optical properties (albedo and thermal emissivity namely) to be held by cool materials;

(ii) the current technologies and products available on the market;

(iii) the aging process effects on their performance;

(iv) the policies implemented worldwide to disseminate their knowledge and use.

3.1 Optical properties: values and measurements

As shown in Chapter 2, when a surface with high *solar reflectance* and *thermal emissivity* is exposed to solar radiation, it will have a lower surface temperature compared to a similar one with lower reflectance and emissivity values.

This in turns leads to a lower amount of the heat flux released by convection during the day and by radiation during the night, as well as to a reduction in the conductive heat flux through the roof layers and a faster release of the heat stored during daytime.

Both solar reflectance and thermal emissivity are physical properties that depend on the wavelength and angle of incidence of the radiative flux, as well as on the temperature of the body.

Analytically speaking, the equations for the calculation of their global values, starting from the monochromatic ones and neglecting their spatial dependence, are the following:

$$r = \frac{\int_{250}^{2500} G(\lambda, T)\, r(\lambda, T)\, d\lambda}{\int_{250}^{2500} G(\lambda, T)\, d\lambda} \tag{3.1}$$

$$\varepsilon = \frac{\int_{IR} e_n(\lambda, T)\, \varepsilon(\lambda, T)\, d\lambda}{\sigma T^4} \tag{3.2}$$

Eq. (3.1) gives the operative formulation for global solar reflectance estimation; it is measured on a scale of 0 to 1 (or 0 to 100%) and it is calculated with reference to a solar spectral radiation distribution *G(λ,T)*. Actually, different profiles are reported in literature for its estimation: for the US countries, Levinson et al. [2] report seven different solar spectral irradiances specified by the American Society for

Testing Materials (ASTM), whereas in EU countries the irradiances distribution specified by the EN 410 European Standard [3] is the most used, also because it is prescribed for the characterization of the optical properties of glazing.

As highlighted by Ferrari et al. [4], in principle different spectra should be used to integrate the spectral reflectivity for surfaces having different orientation and inclination: for example, vertical and north facing surfaces mostly collect diffuse irradiance, whereas horizontal or south facing surfaces mostly collect direct irradiance. Moreover, each spectrum is suitable for different climate conditions, such as sky air mass (i.e. the ratio between the direct optical path length through the atmosphere to the zenith path length) and sky clearness, as well as for different sun beam angles of incidence.

On the other hand, unique values are preferred by both manufacturers and building designers, in order to more easily define the product and calculate its performance, respectively.

Ferrari et al. [4] also highlighted how for ceramic materials – and for all materials with a flat reflectivity spectrum – discrepancies among the predicted solar reflectance values as high as a couple of percentage points should be expected when using different spectra. This is due to different fractions of total radiant energy that fall in the UV, Vis and NIR ranges; as an example, the AM1GH [2] and the ASTM G173-3 spectra [5] are depicted in Fig. 3.1, where it is possible to appreciate some discrepancies in the UV and Vis fields.

In any case, the wavelength field considered spans from 250 nm to 2500 nm, where approximately 99% of the sunlight incident on an unshaded horizontal surface illuminated by a zenith sun arrives, and a large consensus on this point exists.

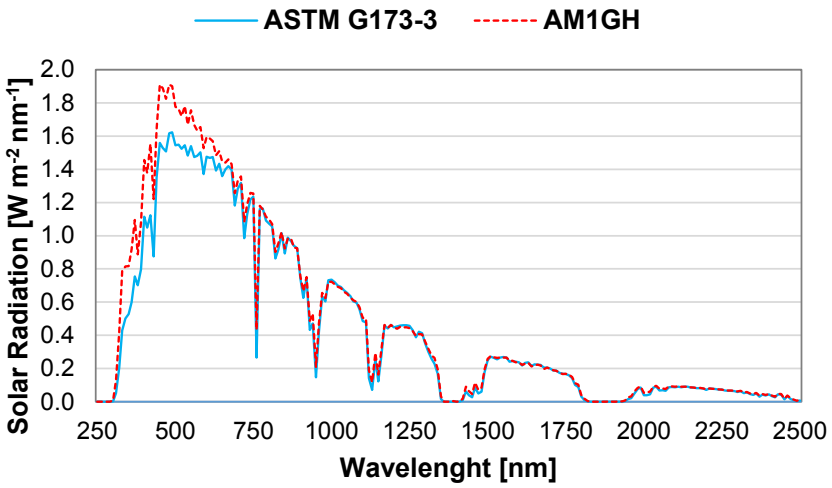

FIGURE 3.1: Solar spectral irradiances according to ASTM G173-3 and AM1GH spectra [Author]

A field study aimed at determining the optic-energetic properties of innovative waterproof membranes has been recently carried out by Pisello et al. [6], with the help of both laboratory measurements and full scale models. The in-field experimental campaign allowed to characterize the product under real boundary conditions (the period of the year, the cloudiness and the time interval of measurement, namely), showing how it is difficult to measure the in-field albedo with a variability less than 1% if compared to laboratory tests.

Therefore, such in-field measurements are not suitable to detect relatively small performance differences, and laboratory assessment of solar reflectance following well-consolidated International Standards (ASTM E903-6 and ASTM C1371-04A) is preferred when characterizing cool materials to be sold on the market.

For what concerns thermal emissivity, it can be defined as the fraction of energy emitted from the surface of a material at a finite temperature following a hemispherical flux, as compared to an ideal black body emission at the same temperature (Eq. 3.2).

Emissivity depends on the material and on other parameters, such as temperature, surface conditions (roughness mainly) and radiation wavelength [7]. It is measured on a scale of 0 to 1.

For the sake of characterizing building materials, the wavelengths usually investigated are those falling in the range $8 \leq \lambda \leq 12$ μm (sometimes also in the mid-infrared range $3 \leq \lambda \leq 5.4$ μm, especially when dealing with historical buildings), since these materials usually emit heat at IR wavelengths [7-8].

Most common building materials (i.e. plaster, stone, concrete) have high emissivity values (usually higher than 0.8), while non-treated metallic materials can present values less than 0.5.

A summary of typical values for solar reflectance (albedo) and thermal emissivity values, for common roof covering materials, is provided in Table 3.1.

TABLE 3.1: Typical solar reflectance and thermal emissivity values for roof covering materials [8]

Roof coverings	Solar reflectance	Infrared emittance
Clay-cement		
Clay tile - white	0.60–0.80	0.90–0.93
Clay tile - red	0.16–0.45	0.83–0.95
Concrete tile - white	0.65–0.80	0.85–0.90
Concrete tile - red	0.10–0.12	0.85–0.90
Metal		
Unpainted	0.20–0.60	0.05–0.35
Painted - white	0.60–0.75	0.80–0.90
Painted – red	0.25–0.45	0.80–0.90
Bitumen		
Modified bitumen, mineral surface	0.10–0.20	0.85–0.95
Shingle, white	0.20–0.30	0.80–0.90
Shingle, red	0.25–0.30	0.80–0.90
Shingle, black	0.04–0.05	0.80–0.90

It is interesting to remark that the standard ASTM E1980-01 [9] introduces a parameter, called *Solar Reflectance Index (SRI)*, aimed to allow a direct comparison amongst different roof surfaces exposed to the sun, in relation to the temperature potentially reached on their external surface. The *SRI* is defined so as to result *SRI*=100 for a standard white surface (r = 0.80, ε = 0.90), and *SRI*= 0 for a standard black surface (r = 0.10, ε = 0.90).

Now, under the hypotheses of standard solar and ambient conditions (I = 1000 W m^{-2}, T_o = 310 K and T_{sky} = 300 K), the *SRI* can be calculated with good approximation as follows:

$$SRI = 123.97 - 141.35 \cdot \chi + 9.655 \cdot \chi^2 \tag{3.3}$$

where

$$\chi = \frac{(1 - r - 0.029 \cdot \varepsilon) \cdot (8.797 + h_c)}{9.5205 \cdot \varepsilon + h_c} \tag{3.4}$$

Here, *SRI* depends not only on solar reflectance r and on thermal emissivity ε values, but also on the convective heat transfer coefficient h_c. However, as discussed by Costanzo et al. [10], *SRI* is not sensitive to changes in h_c - at least for very performing cool materials. As an example, in the case of a cool paint having r = 0.85 and ε = 0.9, the Solar Reflectance Index would be *SRI* = 106 with h_c = 5 W m^{-2} K^{-1}, and *SRI* = 106.2 with h_c = 30 W m^{-2} K^{-1}. The two selected values of h_c correspond to those suggested in the standard ASTM E1980-01 for low-wind and high-wind condition, respectively.

Moreover, as shown in Section 2.1, roof surface temperatures and heat fluxes through the roof are greatly affected by h_c, and thus its correct evaluation is fundamental for thermal load calculation purposes.

3.2 Cool materials

The intensive research carried out in the last two decades has led to the development of a new-generation materials and techniques that present advanced thermal characteristics, able to mitigate the UHI phenomenon.

Among these, cool materials can be divided into two main categories: cool materials for roofs and cool materials for roads and pavements [11].

3.2.1 Cool materials for roofs

Main roof products include single ply membranes, modified bitumen, coatings (elastomeric, acrylic), shingles and tiles (Fig. 3.2).

FIGURE 3.2: Typical cool roofs solutions: single ply membranes and modified bitumen in the first row, coatings in the second row and tiles and shingles in the last row [Internet]

An up-to-date summary of representative optical values for each of them, in terms of solar reflectance *r*, thermal emissivity *ε* and Solar Reflectance Index *SRI* is provided in Table 3.2.

The values reported in the table highlight a great variability in terms of *r* values, whereas *ε* values can be always assumed (except for aluminum finishing layers) greater than 0.80 and very often equal to that of a grey body (i.e. equal to 0.90).

TABLE 3.2: Summary of the optical properties for cool materials to be applied to the roofs [11]

Material	Solar reflectance	Infrared emittance	Solar reflectance index
Coatings			
White	0.70–0.85	0.80–0.90	84–113
Aluminum	0.20–0.65	0.25–0.65	−25 to 72
Conventional black	0.04–0.05	0.80–0.90	−7 to 0
Cool black	0.20–0.29	0.80–0.90	14–31
Conventional dark colored coatings	0.04–0.20	0.80–0.90	−7 to 19
Cool dark colored coatings	0.25–0.4	0.80–0.90	21–45
Asphalt shingles			
White asphalt shingle	0.20–0.30	0.80–0.90	15–28
Black	0.04	0.80–0.90	−7 to −1
Dark colored conventional asphalt shingles (using a two-layer process)	0.05–0.10	0.80–0.90	−6 to 6
Cool colored asphalt shingles (using a two-layer process)	0.18–0.34	0.80–0.90	11–37
Tiles			
Terracotta ceramic tile	0.25–0.40	0.85–0.90	23–45
White clay tile	0.60–0.75	0.85–0.90	71–93
White concrete tile	0.60–0.75	0.85–0.90	71–93
Grey concrete tile	0.18–0.25	0.85–0.90	14–25
Dark colored concrete tile	0.04–0.40	0.85–0.90	−4 to 45
Cool dark colored concrete tile	0.40–0.60	0.85–0.90	43–72
Membranes			
White membrane	0.65–0.85	0.8–0.90	76–107
Black	0.04–0.05	0.8–0.90	−7 to 0
Metal roof			
Unpainted	0.20–0.60	0.05–0.35	−48 to 53
Painted white	0.60–0.75	0.8–0.90	69–93
Dark conventionally colored	0.05–0.10	0.8–0.90	−6 to 6
Dark cool colored	0.25–0.70	0.8–0.90	21–86
Build up roof			
With asphalt	0.04	0.85–0.90	−4 to −1
With dark gravel	0.08–0.20	0.8–0.90	−2 to 19
With white gravel	0.30–0.50	0.8–0.90	27–58
With white coating	0.75–0.85	0.8–0.90	93–113
Modified bitumen			
With mineral surface capsheet	0.10–0.20	0.85–0.95	4–21
White coating over mineral surface	0.60–0.75	0.85–0.95	71–94

The products listed above derive from an intense laboratory research on the development of cool products for different roofing systems. Among them, it is worth mentioning the work of Levinson et al. [12] in creating prototypical solar-reflective non-white concrete tile and asphalt shingle roofing materials. They used a two-layer spray coating process intended to maximize both solar reflectance and factory-line throughput. Each layer is a thin, quick-drying pigmented latex paint based on acrylic aqueous polyvinylidene fluoride (PVDF)/acrylic technology: the first layer is a white basecoat with weak absorption and strong backscattering from about 500 to 2000 nm, which spans most of the Vis and NIR spectra. The second layer is a color topcoat with weak NIR absorption and strong NIR backscattering.

This effort follows a previous one of Levinson et al. [13] on the development of selective non-white coatings to be applied on pitched roofs. In fact, owners of homes with pitched roofs visible from the ground prefer non-white roofing products for aesthetic considerations.

Given this, six experimental NIR reflective coatings (terracotta, chocolate, gray, green, blue and black) were prepared, each similar in appearance to a conventional coating (see Fig. 3.3).

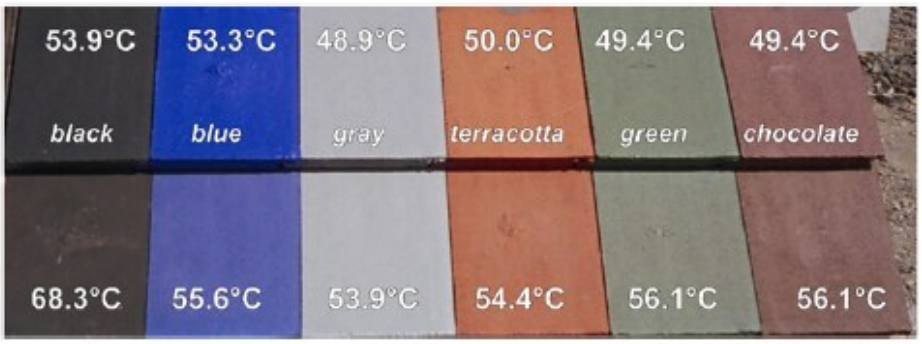

FIGURE 3.3: Surface temperature reached by standard (bottom row) and cool (upper row) prototypical tiles developed by Levinson et al. [13] under the same outdoor conditions

These formulations provided a reasonably full color palette; the first four NIR-reflective coatings are single-layer systems (i.e. color on gray tile), while the blue and black ones are formed by applying a NIR-transmitting layer of color over an opaque, highly reflective white undercoating.

The resulting specimens showed a thermal emissivity value of 0.9 and solar reflectance values between 0.41 and 0.48.

Again, issues related to aesthetic reasons - as well as to heritage buildings in most EU countries - led Libbra et al. [14] to develop a cool colored red clay tile by applying a pigmented topcoat highly transparent in the NIR onto a basecoat highly reflective over the whole range of solar radiation.

The topcoat is basically made of a material transparent to solar radiation, to which a proper selective pigment is added; this pigment produces the desired reflection spectrum of visible radiation but allows NIR to pass through the topcoat, be reflected by the basecoat and pass back through the topcoat. Availability and ease of application were specifically considered in the selection of the materials, but the color produced by the pigment is relatively unnatural for clay tiles (see Fig. 3.4).

FIGURE 3.4: Cool clay tile (on the left) and original clay tile appearances [14]

Nonetheless, in spite of the difficulties in producing a "cool" tile with a visual appearance as close as possible to traditional ones, solar reflectance values as high as 0.42 were achieved (the spectral distribution is shown in Fig. 3.5); this is an excellent result for a clay tile and much better than common terracotta surfaces with a similar or slightly darker color (see also Table 3.2 as reference).

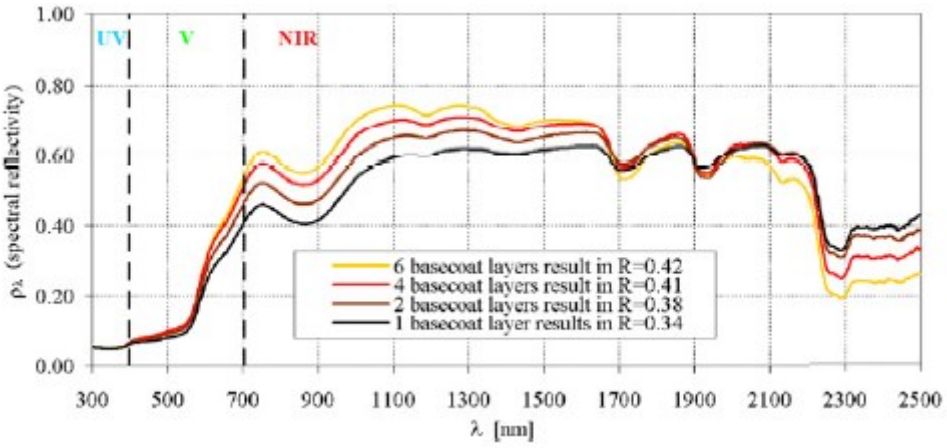

FIGURE 3.5: Reflectivity spectrum of coated fire clay tiles for increasing number of coating layers [14]

3.2.2 Cool materials for roads and pavements

Conventional pavements are usually made of concrete and asphalt (see Fig. 3.6) with *r* values ranging from 0.05 to 0.45; other materials used to pave surfaces of the urban environment, such as stone, rubber, granite, marble and pebble are less common, but show similar solar reflectance values.

In order to increase the solar reflectance of a pavement several methods have been proposed: for asphalt pavement one technique is to use white or light colored aggregate (gravel, white stone) or

pigment in the asphalt mix. Other techniques, mainly used in the US, are white topping (overlaying a thin layer of concrete over existing pavements) and chip seals (pressing rock chips over an asphalt binder so that the solar reflectance of the road is determined by the reflectance of the light color aggregate).

FIGURE 3.6: Cool pavements (on the left) and cool asphalt (on the right) [Internet]

Carnielo and Zinzi [15], by means of both laboratory and in situ measurements, tested a premixed powder made of photocatalytic cement based on titanium dioxide, with the addition of pigments to give the products special coloration.

Moreover, increasing the albedo of pavements can cause glare issues - when driving for example – so there is an effort to develop pavements that absorb in the visible part of the spectrum in order to be dark in appearance but with high reflectance in the NIR part of the solar spectrum (similarly to cool roofing materials).

To this aim, Kinouchi et al. [16] have developed a new type of pavement that satisfies both high albedo and low brightness based on the application of an innovative paint coating on conventional asphalt pavement. The pigments and coating structure used are effective in achieving low reflectivity in the visible part of the spectrum (23%) and high near-infrared reflectivity (86%). Field measurements show that the maximum surface temperature of the paint-coated asphalt pavement is about 15°C lower than that of the conventional asphalt pavement.

A palette of cool colored coatings has been developed by Synnefa et al. [17] at the University of Athens with the help of an industrial partner: special infrared reflecting color pigments were used for testing 10 prototype cool colored acrylic coatings, to be applied on white concrete pavement tiles. The final results were very promising, also for the visual appearance of the final product, if compared to that of standard materials (see Figure 3.7).

FIGURE 3.7: Standard and cool coatings for pavement tiles tested at the University of Athens [17]

For the sake of comparison, Table 3.3 reports solar reflectance values for commonly used and cool paving materials, showing how very low values have to be expected for conventional paving materials ($r < 0.20$) while cool ones can attain values as high as 0.75.

TABLE 3.3: Solar reflectance values of standard and cool paving materials [11]

Material	Solar reflectance
Black conventional asphalt	0.04–0.06
Aged conventional asphalt	0.09–0.18
White topping on asphalt	0.3–0.45
Cool colored thin layer asphalt	0.27–0.55
Gray concrete slab	0.12–0.2
White concrete slab	0.6–0.77
Cool colored pigmented concrete tile (grey, green, beige)	0.61–0.68
Cool colored pigmented concrete block (red, yellow, grey)	0.45–0.49
Photocatalytic white cobcrete tile	0.77
White marble	0.65–0.75
Dark colored marble	0.2–0.4
Red rubber tile	0.07–0.1
Dark colored granite	0.08–0.12

However, it is worth to notice that the energy balance of a surface in contact with the ground is more complex than the one for roofs and other parameters such as permeability, thermal conductivity and heat capacity need to be taken into account for the assessment of their performance [18].

3.3 The aging effect

The solar reflectance and the thermal emissivity of a surface exposed to outdoor conditions may change over time because of aging, weathering and soiling. For assessing the long-term performance of cool materials, changes in solar reflectance and emissivity over time and not only the initial values must be taken into consideration. Synnefa [17] reports that the coatings showing the highest initial solar reflectance are the ones that demonstrate the highest decrease in solar reflectance, while cool and standard black coatings have maintained their initial value. Regarding the thermal emissivity of the samples, it was found that after three months of natural weathering, they maintained their initial values.

Kültür and Türkeri [19] presented the assessment of long term solar reflectance performance of commonly used roof coverings in Turkey by means of field monitoring of test specimens using two pyranometers acting as an albedometer for one year (see Figure 3.8 for the experimental apparatus).

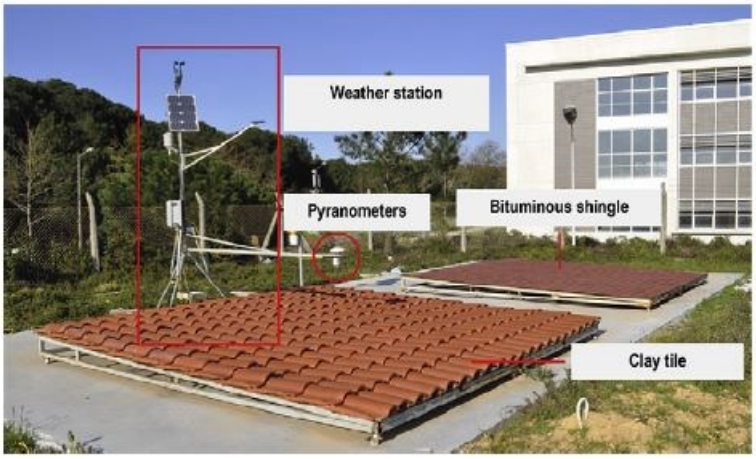

FIGURE 3.8: Test setup for the assessment of long-term solar reflectance used in Turkey [19]

The findings of their research can be summarized in Table 3.4, where solar reflectance values of new and one year aged test specimens are reported for each portion of the solar spectrum (UV, Vis and NIR), as well as for the global value.

It is possible to notice how, after one year of outdoor exposure, total reflectance values are the same (or slightly higher) for red clay tiles, for which small increase in the UV and Vis reflectance values occur.

Other tested materials, such as white ceramic tiles, show a slight decrease of total solar reflectance due to UV degradation of the material. Overall, no significant differences are expected for these materials under climatic conditions of Istanbul for one year of exposure.

TABLE 3.4: Solar reflectance rates for each spectral range of new and one year aged specimens [19]

Test specimens	Solar reflectance, R							
	New (unexposed)				Aged (1-year exposed)			
	Spectrum (NM)				Spectrum (NM)			
	UV	VIS	IR	Total	UV	VIS	IR	Total
	300–380	380–780	780–2500	300–2500	300–380	380–780	780–2500	300–2500
Clay - cement								
Clay tile, red	0.06	0.15	0.62	0.36	0.07	0.16	0.62	0.37
Ceramic tile, white, shiny	0.54	0.84	0.77	0.80	0.50	0.81	0.77	0.78
Concrete tile, red	0.07	0.19	0.42	0.30	0.08	0.19	0.42	0.30
Metal								
Metal tile, red	0.03	0.07	0.31	0.18	–	–	–	–
Galvanized sheet, white	0.08	0.84	0.68	0.71	–	–	–	–
Aluminum sheet, silver	0.50	0.62	0.72	0.65	–	–	–	–
Copper sheet, bronze	0.08	0.19	0.53	0.34	–	–	–	–
Titanium-zinc, black	0.06	0.06	0.07	0.07	–	–	–	–
Titanium-zinc, silver	0.51	0.57	0.56	0.56	–	–	–	–
Bitumen								
Mineral covered membrane-red	0.06	0.11	0.20	0.15	0.06	0.11	0.21	0.16
Shingle, red	0.04	0.07	0.11	0.10	0.04	0.08	0.12	0.10
Corrugated sheet, black	0.04	0.04	0.04	0.04	0.05	0.05	0.07	0.05

Different results are presented in the work of Paolini et al. [20], who tested the spectral solar reflectance of 12 roofing membranes whose initial *r* values range from 0.26 to 0.85, before outdoor exposure and after 3, 6, 12, 18 and 24 months of natural aging in Rome and Milan (Italy).

In both cities, the exposures occurred approximately halfway between the city centres and the peripheries on two non-shaded roofs, and were distant from primary sources of pollution; the main weather data needed for the assessment were collected in loco by means of a weather station (see Figure 3.9 for the experimental setup).

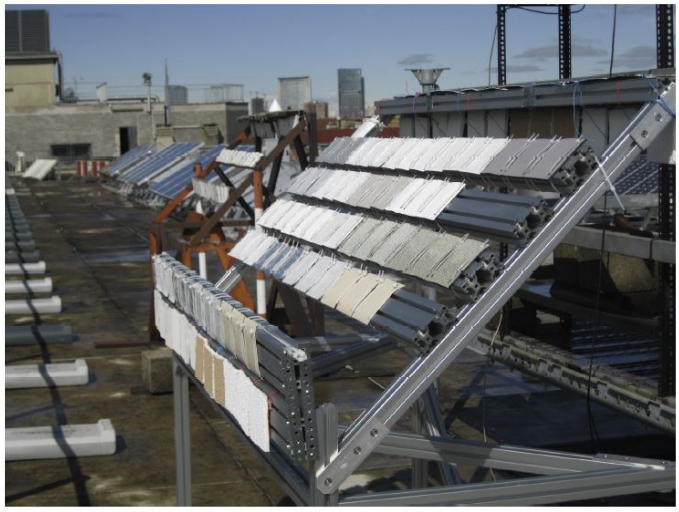

FIGURE 3.9: Test setup for the assessment of long-term solar reflectance used in Milan [20]

The authors found that in Milan, after 3 months of exposure, the membranes with highest initial solar reflectance values ($r > 0.80$) lost an average of 0.13 (about 16% relative decrease) in solar

reflectance, while low reflectivity membranes ($0.20 < r < 0.30$) show modest absolute variations (ranging from 0.02 to 0.05).

All the membranes showed a standard deviation of less than 0.035 (median < 0.008) after 24 months of exposure in Milan and less than 0.017 in Rome (median < 0.010).

Although the absolute values of the reflectance of samples at the two sites were different (see Figure 3.10), the shapes of the spectra of the aged membranes were almost the same in both cities, suggesting that in metropolitan areas the intensity of the deposition is different but ingredients of soiling are pretty much the same (products of combustion from vehicles' engines and heating plants mainly).

The loss of reflectance also impacts the energy needs of buildings and the surface temperatures of the roofing membranes: to quantify these aspects, representative commercial buildings in Rome and Milan were modelled. The results of these simulations show that in all considered cases (poorly or well insulated buildings), aging yields a reduction in annual cooling load savings from 4.1 to 7.1 MJ m^{-2} y^{-1} per 0.1 loss in reflectance.

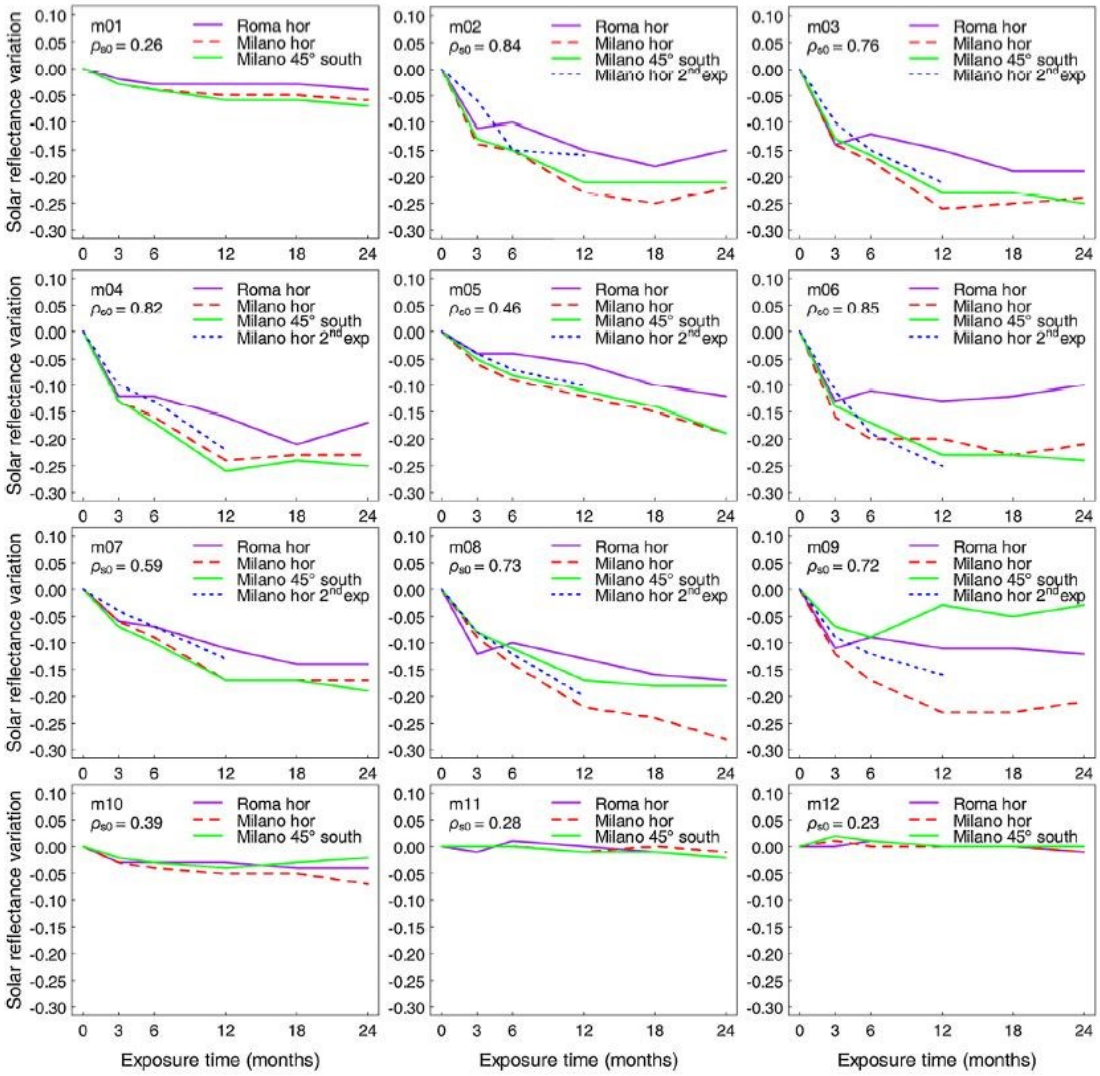

FIGURE 3.10: Solar reflectance variation (aged less initial) of different roofing membranes as a function of exposure time and for two different sites [20]

Similar findings concerning the albedo variation of high-reflective coatings are inferable from the experimental campaign carried out by by Mastrapostoli et al. [21] in two school buildings in Athens (Greece).

Here, white coatings were applied in 2008 (initial roofs albedo of 0.70) and a measurement campaign for assessing how weatherization affects the optical properties of cool roofs was performed in 2012. The main findings are reported in Table 3.5, were albedo measurements results are shown for the two buildings and for existing, cleaned and new cool roofs respectively.

TABLE 3.5: Albedo measurements for the two case study buildings [21]

	Albedo measurements		
	Existing cool roof	Cleaned cool roof	New cool roof
School A	0.50	0.55	0.74
School B	0.54	–	0.71

For building A the cleaning process is able to restore about 7% of the original albedo value, while a new installation would increase it of about 25% compared to the aged cool roof. The last result is pretty much the same for building B.

It is interesting to highlight how significant roof temperature differences have to be expected amongst aged, cleaned and new cool roofs, and this is clearly shown in Figure 3.11 where surface temperatures are compared by means of infrared thermography pictures.

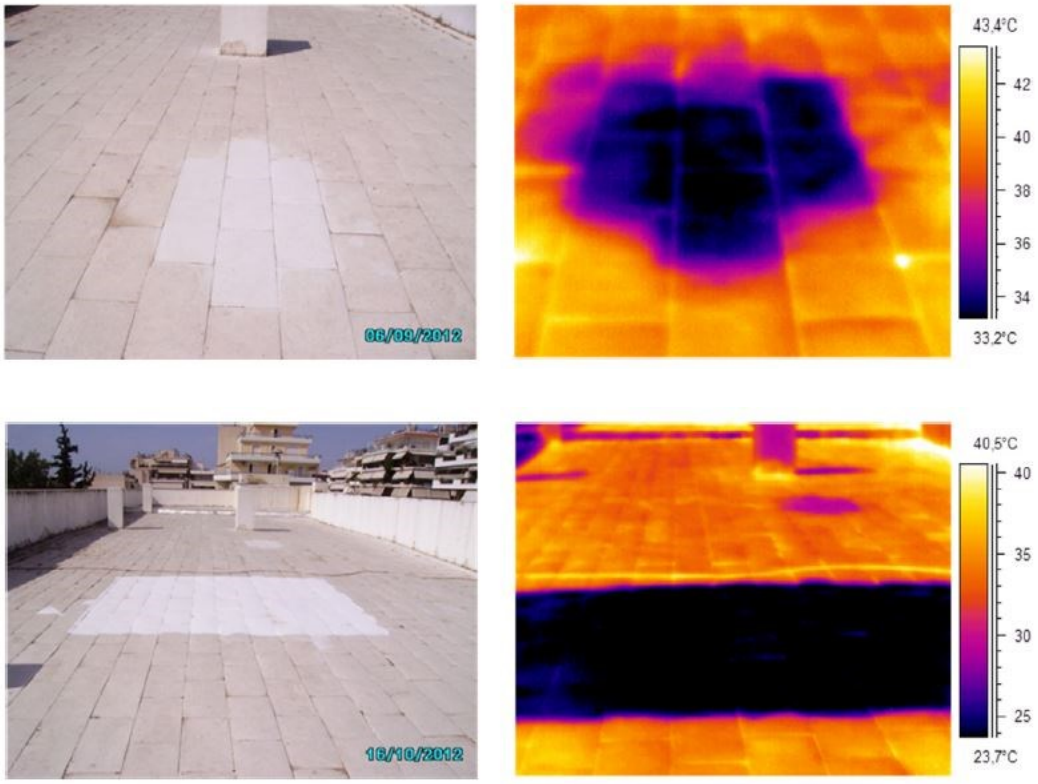

FIGURE 3.11: Visible and infrared pictures of the roof depicting the different surface temperatures achieved by the aged, the cleaned (first row) and new (second row) cool roofs [21]

The temperature difference between the aged cool roof and the cleaned part of it was about 8°C, while the surface temperature difference between the existing and new cool roofs reaches 12°C; the outdoor dry bulb temperature during the measurement process was 24.3°C.

A mineralogical analysis is also carried out to quantify the deposition of pollutants on the roof's surface.

The outdoor pollutants that mainly affect the degradation of albedo are found to be Quartz, Illite, Dolomite and Epsomite, while the microbiological analysis showed high bacterial and fungi load in the aged cool roof. These results highlight how a regular roofs' cleaning and maintenance is necessary in order to fulfil the cool materials contribution in energy efficiency and indoor thermal comfort.

Finally, long-term assessment of solar reflectance for roofs coated up to 8 years before has been tackled by Takebayashi et al. [22] for 8 different cool roofs installation in Japan.

Reduction of solar reflectance is confirmed for samples several months after coating, and varies about 0.10-0.25 several years after coating (see Table 3.6), depending on dirt deposition conditions. Solar reflectance after wiping the target surface with a wet cloth is usually recovered less than 0.10, but for most of the surfaces recovery is not able to reach the initial value, maybe due to dirt adhering to irregularities in the coated surface.

TABLE 3.6: Field measurements of roof albedo after several years of coating [22]

City	Kobe	Osaka	Osaka	Ryuo	Kato	Himeji	Osaka	Koriyama
Form	Flat	Flat	Flat	Folded	Folded	Folded	Flat	Folded
Initial value	0.87	0.73	0.73	0.87	0.87	0.87	0.73	0.87
Years after coating	0.2	0.4	2.5	4	4	4	6	7
Measurement point 1	0.65	0.66	0.67	0.60	0.79	0.64	0.71	0.72
Measurement point 2	0.88	0.65	0.69	0.59	0.74	0.66	0.76	0.71
Measurement point 3	0.86	0.66	0.69	0.61	0.70	0.66	0.72	0.74
Averaged value	0.79	0.66	0.68	0.60	0.74	0.65	0.73	0.72
Initial – averaged value	0.08	0.08	0.05	0.27	0.13	0.22	0.00	0.15
After wiping	–	–	0.67	0.69	0.88	0.71	0.72	0.81
After wiping – point 1	–	–	0.00	0.09	0.09	0.07	0.01	0.09

Interestingly, the authors suggest that it would be more appropriate to use solar reflectance values after an aging process of three months for urban heat island and thermal load calculations, and this is consistent with the above mentioned studies that all identify this time period as the most representative of the aging process.

To this aim, the authors propose an accelerated laboratory-aging test able to predict the solar reflectance value of a coating after 3 months and 1 year of outdoor exposure.

3.4 Cool materials as a passive cooling technology: case studies

A number of experimental and computational studies have been carried out to demonstrate the benefits of cool roofs in improving summer thermal comfort as well as in the energy efficiency of buildings.

A pioneering effort is that made by Akbari in promoting the diffusion of cool roofs in US, starting from the hot humid climate of California [23]: six commercial buildings in California have been monitored in terms of energy use and environmental parameters (surface temperatures and air temperatures) for two consecutive summer months (before and after cool roof installation).

Results showed that installing a cool roof reduced the daily peak roof temperature of each building by 32-42°C by using white coatings, the average peak demand for cooling is reduced to 5-10 W m^{-2} and the estimated savings in average chiller energy use span from 40 Wh m^{-2} to 80 Wh m^{-2}, depending on building typology (school, retail store or cold storage facility).

Based on these results, the authors extend the study on the applicability of this technology to all of the 16 California climate zones by means of dynamic simulations, finding similar results but neglecting potential penalties for space heating (see Table 3.7 for a summary).

TABLE 3.7: Estimated annual energy savings and peak reduction in July for all the 16 California climate zones [23]

Climate zone	Retail store[a]		School building[b]		Cold storage facility[c]	
	kWh/m²	W/m²	kWh/m²	W/m²	kWh/m²	W/m²
CZ01	0.6	0.6	1.1	2.6	4.5	3.9
CZ02	11.5	4.9	4.2	3.9	6.0	5.4
CZ03	4.0	2.9	3.7	3.2	5.9	5.1
CZ04	10.5	4.6	5.1	3.6	6.3	5.5
CZ05	5.9	3.4	3.0	3.2	5.9	5.2
CZ06	11.2	4.3	5.1	2.8	5.7	5.1
CZ07	9.9	3.6	5.2	2.7	5.3	4.7
CZ08	12.7	4.6	6.1	3.4	5.8	5.3
CZ09	11.8	4.3	5.4	3.3	5.5	5.3
CZ10	15.3	5.4	5.8	3.8	5.5	5.1
CZ11	10.8	4.8	4.5	3.6	7.2	6.6
CZ12	10.8	4.9	4.6	3.7	7.4	6.6
CZ13	13.9	5.8	5.3	3.8	7.4	6.6
CZ14	14.0	5.3	4.5	3.2	7.4	6.3
CZ15	16.4	5.5	6.5	3.4	6.2	4.8
CZ16	6.7	4.0	2.5	3.4	6.8	6.2

In EU Countries, five demonstration projects of cool roofs' capabilities in improving thermal conditions and reducing the energy consumption in buildings (both residential and commercial) were carried out within the framework of the project *"Cool Roofs"*.

The case studies were monitored, concerning their energy performance and indoor environment, before and after the application of a cool roof. The buildings selected cover a great geographical and

typological range, but share the same methodological approach: first an experimental monitoring is carried out, then numerical simulations of the same buildings with a number of variations are performed.

In the following, a brief summary of the main findings for each of them will be given, starting from the hottest climates of Greece and Italy and ending to moderate ones of France and UK.

Kolokotsa et al. [24] investigated a building located in Iraklion, Crete (Greece), used as an administrative office for the local technological campus. The monitoring period started in December 2008 and ended on October 2009, covering both the periods before and after the application of a cool white paint with r = 0.89 and ε = 0.89 (the starting values for the concrete slab used as a roof were r = 0.20 and ε = 0.80).

FIGURE 3.12: The house investigated for the Iraklion case study [24]

The model calibration was performed when the cooling system was switched off, for avoiding to add more uncertainties for the model calibration, and then used for comparing the energy efficiency achieved by different energy conservation measures that are commonly used in that region.

To give a snapshot of the results in terms of roof surface temperatures achieved by the untreated and painted roof respectively, Fig. 3.13 depicts the daily trend for the months of September and October 2009.

It is possible to see how the peak values are cut by 30°C when a white coating is used instead of a standard bitumen covering, while dynamic simulations identify this technological solution as the most

promising for reducing annual air conditioning loads (cooling+heating), if compared to the increase of roof's insulation or to the decrease of windows' U-value.

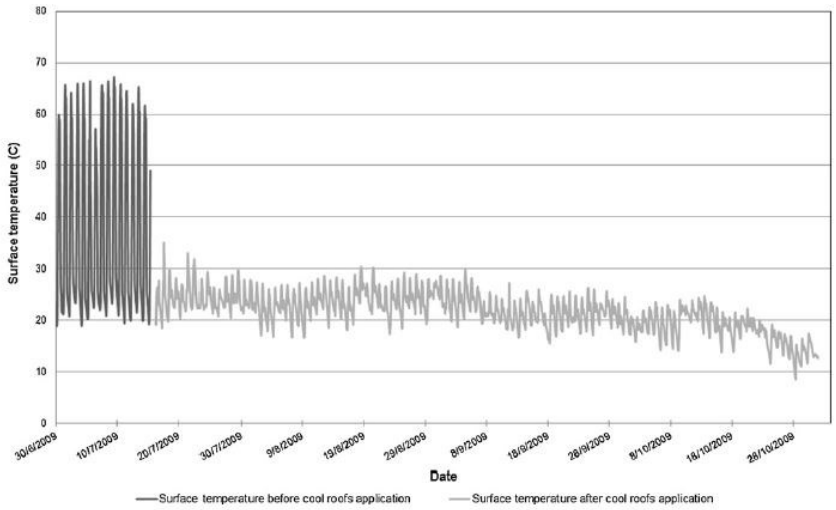

FIGURE 3.13: Roof surface temperatures before and after cool coating [24

Another building in Greece (a school building in Athens, Fig. 3.14) was studied by Synnefa et al. [25], where the existing grey concrete surface (r = 0.20) was replaced again with a cool white paint of solar reflectance r = 0.89.

An analysis combining results from an onsite monitoring campaign and a numerical analysis were performed with the aim to assess thermal comfort conditions and energy performance of the school building before and after the application of the cool roof. The results achieved by the building in Crete are here confirmed in terms of roof surface temperatures (investigated by using infrared pictures), because of similar climatic conditions and of the use of the same white coating. Nevertheless, the study casts light on the effective energy needs experienced before the application of the cool coating thanks to an analysis of heating and electricity bills.

FIGURE 3.14: The school building in Athens [25]

Set point for cooling is set to 26°C and for heating is set to 20°C (both are representative values for the European Mediterranean Countries), and the results of the calculation are reported in Fig. 3.15 for the uninsulated and the insulated cases, as well as for the reference roof and the cool roof.

The application of the cool roof results to a decrease in the annual cooling load by 40% for the reference uninsulated building, being 35% the reduction for the insulated building. Non-negligible heating penalties should be expected for the uninsulated (10% increase) and insulated building cases (+4%): as expected, the cool roof application has a larger impact on uninsulated buildings than on the insulated ones.

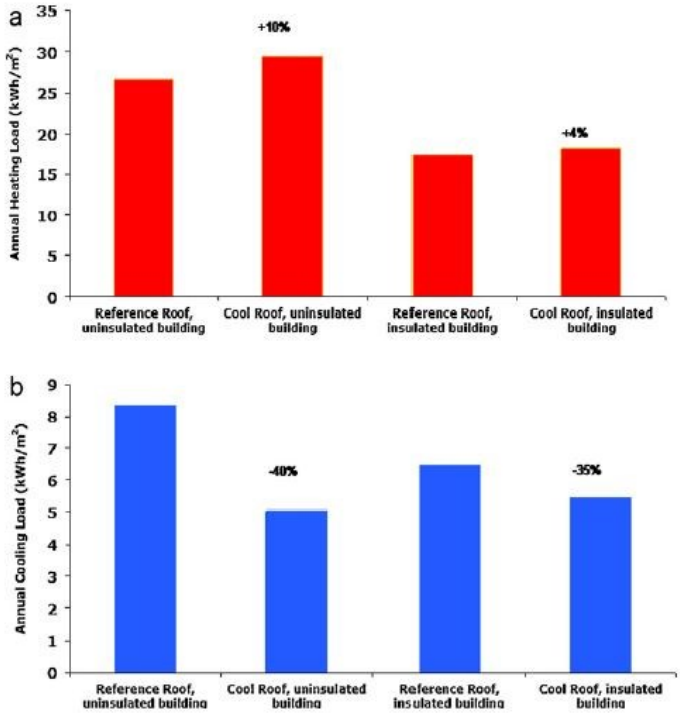

FIGURE 3.15: Annual heating (red bars) and cooling (blue bars) loads of the school building in Athens [25]

Moving to Italy, Romeo and Zinzi [26] considered a school located in Trapani (Sicily) covered by concrete tiles (r = 0.25) and by a white "ecofriendly" cool coating (r = 0.82) in a wing of the building (see Fig. 3.16).

The procedure followed was putting up the cool roof application in the middle of the cooling season and monitoring the building behavior before and after the roof coating.

The outdoor monitoring included air temperature, relative humidity, global horizontal solar radiation and roof surface temperatures, while indoor monitoring recorded air temperature, mean radiant temperature, relative humidity and air velocity.

A simulation and calculation work was needed in order to have extensive results about the building performance through the whole cooling season and longer; the software TRNSYS was selected to perform such calculations.

FIGURE 3.16: Cool roof application in a school building in Trapani [26]

Looking at the thermal comfort conditions in summertime, the cumulative distribution of the number of hours during which the operative temperature is above threshold values (25°C, 27°C and 29°C namely) is reported in Fig. 3.17. Here one can see the strong reduction of discomfort hours in room 2 (north-east oriented) and room 3 (south-east oriented), since a temperature of 27°C was reached for less than 15% of the period. Worse results were obtained for room 5 (west oriented) because of the high solar gains through wide windows in the afternoon.

If considering the yearly energy performance, a parametric study considering various albedo values for the roof has been performed and the results pinpoint how the actual scarcely-insulated building is still heating dominated. In this case, the use of coatings with solar reflectance values higher than r = 0.70 is counterproductive, since heating penalties would overcome cooling savings. On the other hand, by insulating the building shell, the lowest energy needs pertain to the paint with the highest albedo (r = 0.82).

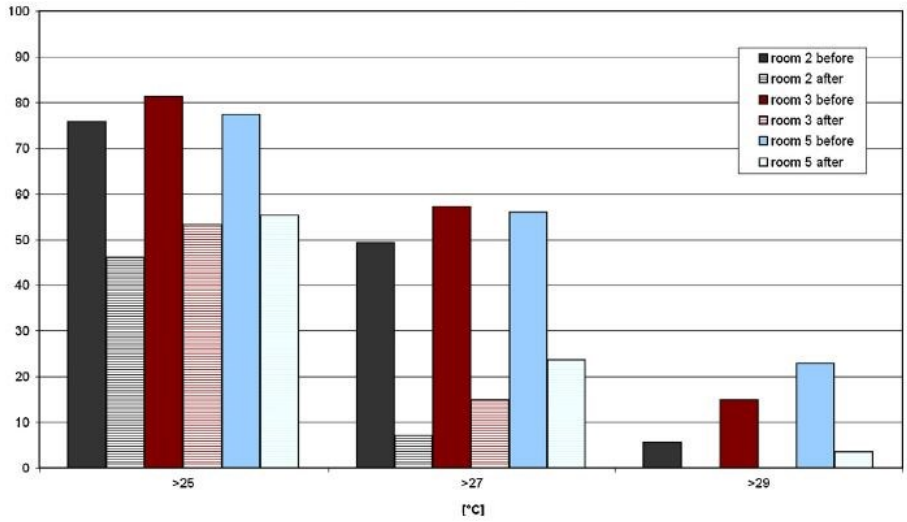

FIGURE 3.17: Cumulative distribution of the operative temperature in different rooms of the school building in Trapani before and after the application of a cool coating [26]

Bozonnet et al. [27] considered typical continental climatic conditions by assessing the performance of a collective dwelling in Poitiers (France).

Following the current specifications in France, the highly insulated building envelopes are designed for winter conditions with few solar radiations and few concerns for summer comfort, thus cool selective surfaces should be evaluated accurately.

The terrace roof before the refurbishment was covered by asphalt (r = 0.20), while after the application of a white elastomeric coating the roof albedo reached the value of 0.88.

What is important to highlight from this study is that, even for a moderate climate like the central part of France, the cool roof decreases the mean outside surface temperature by more than 10°C, with low differences for lower temperatures but a strong impact on the highest temperatures.

The effect on the indoor operative temperature appears to be very low for the building in question, due to the strong insulation consistent with building standards in France for all new constructions.

FIGURE 3.18: Collective dwelling studied by Bozonnet et al. in Poitiers [27]

Finally, Kolokotroni et al. [28] assessed the performance of the estates office at Brunel University (London), located at the topfloor of a four storey building (see Fig. 3.19). The existing roof finishing layer shows a very low solar reflectance value (r = 0.10), while after the coating process it is increased by 0.5 (r = 0.60); the envelope is well insulated, by means of 4 cm thick insulation layer on top of the roof slab and 18 cm on the outer face of the walls.

One aspect highlighted in this work, which is strictly related to roof thermal stress, is the analysis of surface temperature differences between roof and ceiling before and after the application of the cool coating.

As depicted in Fig. 3.20, during early morning and evening the roof is cooler than internal ceiling while during mid-day the opposite occurs. However, after coating the roof internal ceiling surface temperatures are always higher than roof surface temperatures, indicating the cooling effect of cool paint on the external roof surface.

FIGURE 3.19: External view of the case study building in London [28]

A parametric analysis was also carried out using the case study as the reference building and by varying roof albedo in the range 0.1-1, set-point temperatures in summer (23°C or 25°C) and winter (21°C or 23°C) and air changes per hour (2 or 4).

The results, in terms of energy needs for air-conditioning, shows how the optimal albedo value should fall within the range 0.6-0.7, with air change rate of 2 ACH and by maintaining the existing levels of insulation. In this optimal configuration, an overall energy needs reduction of 3-6% is expected, depending on the set-point temperature.

Increasing insulation levels would decrease potential energy benefits in heating and cooling demand, and this is consistent with the other case studies for which energy benefits are higher for lower insulation of the roof.

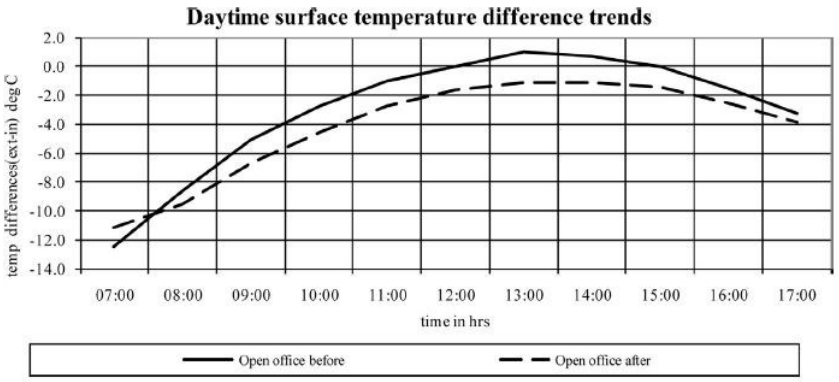

FIGURE 3.20: Measured daytime surface temperature differences (outer-inner roof surface temperatures) for the building in London [28]

3.5 Cool materials policies and markets

In much of the world, the design, construction, and materials used for residential and commercial buildings are guided by building codes. The bulk of these codes are dedicated to ensuring the integrity of the building from a health and safety perspective, but they also cover energy use and recently have become inclusive of requirements that are both energy-saving and cost-effective. Because building codes are focused on the energy savings potential of individual buildings, they do not consider the climate benefits of cool roofs or the micro-climate benefits stemming from the reduction of the urban heat island.

Akbari and Matthews [29] reviewed cool roofs standards, building codes, rating and labeling programs in the US (see Table 3.8), as well as in other parts of the world.

The process for updates and level of enforcement of building codes vary greatly by country. For example, in China there is just one single national code with three climate zones, in India there is a single national code too but it is voluntary, in the EU building codes are determined at country level. Because of large population and significant economic growth, China and India may present the greatest opportunities for promoting the adoption of cool roofs through building codes.

TABLE 3.8: Summary of US policies prescribing or suggesting the use of cool roofs [29]

Standards, codes, labeling programs	Remarks
ASHRAE Standard 90.1-2007	Prescribes cool materials for low-sloped roofs on non residential buildings in some U.S. climate zones
ASHRAE Standard 90.1-2004 and 1999	Offer credits for cool materials for low-sloped roofs on non residential buildings in some U.S. climate zones
ASHRAE Standard 90.2-2004	Offers credits for cool materials for all roofs on residential buildings in some U.S. climate zones
California Title 24 Standards 2008	Prescribes cool materials for all roofs on residential and non residential buildings in California by climate zone
California Title 24 Standards 2005	Prescribes cool materials for low-sloped roofs on non residential buildings and offers credits for all other roofs on residential and non residential buildings by climate zone
California Title 24 Standards 2001	Offers credits for cool materials for all roofs on residential buildings in California by climate zone
International Energy Conservation Code 2003	Allows commercial buildings to comply with the 2003 IECC by satisfying the requirements of ASHRAE Standard 90.1, which offers cool-roof credits
Chicago, IL energy conservation code	Prescribes a minimum solar reflectance and thermal emittance for low-sloped roofs
Florida code 2004	Prescribes cool materials for all roofs on non residential buildings that are essentially the same as those in ASHRAE Standard 90.1-2004
Hawaii	In 2001, 2002, and 2005, respectively, the counties of Honolulu, Kauai, and Maui adopted cool-roof credits for commercial and high-rise residential buildings based on ASHRAE Standard 90.1-1999
U.S. EPA Energy Star™ label	Requires that low-sloped roofing products have initial and three-year-aged solar reflectances not less than 0.65 and 0.50, respectively. Steep-sloped roofing products must have initial and three-year-aged solar reflectances not less than 0.25 and 0.15, respectively
LEED green building rating system	Assigns one rating point for the use of a cool roof in its Sustainable Sites Credit
Cool Roof Rating Council	Develops accurate and credible methods for evaluating and labeling the solar reflectance and thermal emittance of roofing products

However, US countries have played a pioneering role in the use and diffusion of the cool roof technology, as demonstrated by the several codes/prescriptions reported in Table 3.8.

Among them, it is worth to notice the role played by the Cool Roof Rating Council (CRRC) in evaluating and labeling the radiative properties of roofing products and to disseminate the information to all interested parties [30].

By browsing their website, it is possible to access to a rated products directory sorted by product type, color and minimum radiative properties that allows to choose the best performing solution for every roof configuration.

An example of the rating label that certifies the optical properties of the product, both initial and after 3 years of weathering, is given in Figure 3.21.

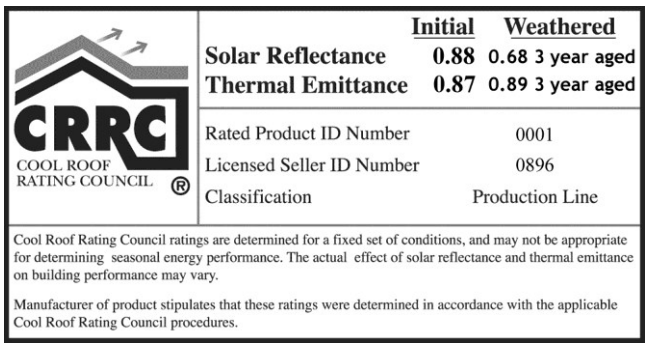

FIGURE 3.21: Measured Cool Roof Rating Council label for test cool roof products [30]

In EU countries, a similar body has been established in 2011 with the name of European Cool Roofs Council (ECRC). It merges all the driving forces for the promotion and adoption of cool roofs in the EU, targeting to accelerate the transfer of knowledge, to remove the market barriers, to help manufacturers to develop cool roofs products, to educate the public and develop incentives and programs [31].

The ECRC's website offers a technical glossary, articles on various aspects of cool roofs usage, publications related to this technology and a database of rated cool roofing materials sorted by country and product type.

It is important to highlight that till now a labeling mechanism, comparable to that implemented by the CRRC in the US, is not in use.

3.6 References of the chapter

[1] R. Levinson, P. Berdahl, H. Akbari, W. Miller, I. Joedicke, J. Reilly, Y. Suzuki, M. Vondran, Methods of creating solar-reflective nonwhite surfaces and their application to residential roofing materials, Solar Energy Materials and Solar Cells 91 (2007) 304-314

[2] R. Levinson, H. Akbari, P. Berdahl, Measuring solar reflectance - Part I: Defining a metric that accurately predicts solar heat gain, Solar Energy 84 (2010) 1717-1744

[3] EN 410 European Standard, Glass in building – Determination of luminous and solar characteristics of glazing, 2011

[4] C. Ferrari, A. Libbra, A. Muscio, C. Siligardi, Influence of the irradiance on solar reflectance measurements, Advances in Building Energy Research 7-2 (2013) 244-253

[5] ASTM G 173-03, Standard Tables for Reference Solar Spectral Irradiances: Direct Normal and Hemispherical on 37° Tilted Surface, 2012

[6] A.L. Pisello et al., Experimental in-lab and in-field analysis of waterproof membranes for cool roof application and urban heat island mitigation, Energy and Buildings (2015), http://dx.doi.org/10.1016/j.enbuild.2015.05.026

[7] R. Albatici, F. Passerini, A. Tonelli, S. Gialanella, Assessment of the thermal emissivity value of building materials using an infrared thermovision technique emissometer, Energy and Buildings 66 (2013), 33-40

[8] N.P. Avdelidis, A. Moropoulou, Emissivity considerations in building thermography, Energy and Buildings 35 (2003) 663-667

[9] ASTM E 1980-01, Standard Practice for Calculating Solar Reflectance Index of Horizontal and Low-Sloped Opaque Surfaces, 2005

[10] V. Costanzo, G. Evola, L. Marletta, A. Gagliano, Proper evaluation of the external convective heat transfer for the thermal analysis of cool roofs, Energy and Buildings 77 (2014) 467-477

[11] M. Santamouris, A. Synnefa, T. Karlessi, Using advanced cool materials in the urban built environment to mitigate heat islands and improve thermal comfort conditions, Solar Energy 85 (2011) 3085-3102

[12] R. Levinson, H. Akbari, P. Berdahl, K. Wood, W. Skilton, J. Petersheim, A novel technique for the production of cool colored concrete tile and asphalt shingle roofing products, Solar Energy Materials & Solar Cells 94 (2010) 946-954

[13] R. Levinson, H. Akbari, J.C. Reilly, Cooler tile-roofed buildings with near-infrared-reflective non-white coatings, Building and Environment 42 (2007) 2591-2605

[14] A. Libbra, L. Tarozzi, A. Muscio, M. Corticelli, Spectral response data for development of cool coloured tile coverings, Optics & Laser Technology 43 (2011) 394-400

[15] E. Carnielo, M. Zinzi, Optical and thermal characterization of cool asphalts to mitigate urban temperatures and building cooling demand, Building and Environment 60 (2013) 56-65

[16] T. Kinouchi, T. Yoshinaka, N. Fukae, M. Kanda, Development of cool pavement with dark colored high albedo coating. Fifth Conference for the Urban Environment, Vancouver (2004)

[17] A. Synnefa, M. Santamouris, K. Apostolakis, On the development, optical properties and thermal performance of cool colored coatings for the urban environment, Solar Energy 81 (2007) 488-497

[18] T. Asaeda, A. Wake, Heat storage of pavement and its effect on the lower atmosphere, Atmospheric Environment 30-3 (1996) 413-427

[19] S. Kültür, N. Türkeri, Assessment of long term solar reflectance performance of roof coverings measured in laboratory and in field, Building and Environment 48 (2012) 164-172

[20] R. Paolini, M. Zinzi, T. Poli, E. Carnielo, A.G. Mainini, Effect of ageing on solar spectral reflectance of roofing membranes: Natural exposure in Roma and Milano and the impact on the energy needs of commercial buildings, Energy and Buildings 84 (2014) 333-343

[21] E. Mastrapostoli at al., On the ageing of cool roofs: Measure of the optical degradation, chemical and biological analysis and assessment of the energy impact, Energy and Buildings (2015), http://dx.doi.org/10.1016/j.enbuild.2015.05.030

[22] H. Takebayashi et al., Experimental examination of solar reflectance of high-reflectance paint in Japan with natural and accelerated aging, Energy and Buildings (2015), http://dx.doi.org/10.1016/j.enbuild.2015.06.019

[23] H. Akbari, R. Levinson, L. Rainer, Monitoring the energy-use effects of cool roofs on California commercial buildings, Energy and Buildings 37 (2005) 1007-1016

[24] D. Kolokotsa, C. Diakaki, S. Papantoniou, A. Vlissidis, Numerical and experimental analysis of cool roofs application on a laboratory building in Iraklion, Crete, Greece, Energy and Buildings 55 (2012) 85-93

[25] A. Synnefa, M. Saliari, M. Santamouris, Experimental and numerical assessment of the impact of increased roof reflectance on a school building in Athens, Energy and Buildings 55 (2012) 7-15

[26] C. Romeo, M. Zinzi, Impact of a cool roof application on the energy and comfort performance in an existing non-residential building. A Sicilian case study, Energy and Buildings 67 (2013) 647-657

[27] E.Bozonnet, M. Doya, F. Allard, Cool roofs impact on building thermal response: A French case study, Energy and Buildings 43 (2011) 3006-3012

[28] M. Kolokotroni, B.L. Gowreesunker, R.Giridharan, Cool roof technology in London: An experimental and modelling study, Energy and Buildings 67 (2013) 658-667

[29] H. Akbari, H.D. Matthews, Global cooling updates: Reflective roofs and pavements, Energy and Buildings 55 (2012) 2-6

[30] Cool Roof Rating Council. Link: http://coolroofs.org/

[31] European Cool Roofs Council. Link: http://coolroofcouncil.eu/index.php

4. DISCOVERING THE POTENTIAL FOR COOL ROOFS APPLICABILITY: METHODOLOGY

In order to generalize as much as possible the findings of the cool roof assessment proposed in this thesis, a representative geometrical building model of the existing EU office buildings stock is derived from an extensive empirical survey.

Several climates are investigated, from the hot Mediterranean to the cold north European one, with the aim of exploring if or to which extent winter heating penalties may overcome summer cooling benefits stemming from the application of cool roofs.

Within each climate, and each vintage period, the thermal characterization of the outer shell (both opaque and glazed components) is varied according to their typical features.

Then, a parametric analysis that takes into account different cool roof design features (roof shape, optical properties and thermal resistance) is performed by means of dynamic simulations. The outcomes of this analysis are reported in terms of thermal comfort conditions and energy needs for air conditioning, taking into account the expected aging process of the cool paint due to weathering and soiling.

4.1 A "typical" office building model for EU countries

The definition of a typical building geometrical model, aimed at bracketing the largest possible amount of different existing configurations, is somewhat tricky and very often not "truly representative", given the huge amount of building layouts observed.

In general, *reference* buildings represent "average" buildings that are modelled/simulated specifically for estimating heating and cooling consumption.

In this thesis, based upon an empirical survey on the existing buildings stock in the EU [1], an *open plan office building of three storey* is used as reference for modelling purposes.

In reality, the iNSPiRe project [1] (see also Chapter 1) proposes a cellular office building layout where six zones are considered: two mid-row office cells with one external wall and one cell in each corner of the building with two external walls, while all internal walls are assumed adiabatic. The mid-row cells are thus multiplied in post-processing to obtain results for the whole building, and the number of floors is varied (up to seven) by multiplying results for the entire floor. All office cells are of the same size and shape (rectangular).

The floors considered are the bottom floor, a middle floor and the top floor, by assuming no heat transfer between two identical floors above and below.

However, two important notes suggest not following such an approach:

(i) It is well known that cool roofs represent an effective energy-saving solution for buildings with up to two-three storey (low-rise buildings). For tall buildings, the benefits deriving from cool roofs application is negligible. Moreover, it is found that the vast majority of the existing office buildings in EU is 2-3 storey (see Table 4.1);

(ii) The use of an open plan layout is consistent with the models proposed by another extensive survey carried in the US [2], especially when talking about medium-to-large office buildings (about 1000 m^2 per floor). These are the floor dimensions most diffused in the EU, and allow comparison with the corresponding ones in the US also in terms of construction period (see Table 4.2), thus extending the validity of the proposed methodology to existing office buildings in the US.

TABLE 4.1: Share of floor area for climate zone, construction period and number of floors [1]

	OFFICES - Period						OFFICE - nr floors		
	pre 1945	1945-1970	1970-1980	1980-1990	1990-2000	post 2000	2-3	4-5	>5
Southern Dry	32%	21%	11%	11%	12%	12%	76%	13%	11%
Mediterranean	25%	20%	9%	14%	16%	16%	76%	13%	11%
Southern Continental	5%	53%	11%	10%	10%	12%	58%	38%	3%
Oceanic	24%	22%	13%	19%	9%	12%	93%	7%	0%
Continental	20%	16%	15%	12%	20%	17%	60%	20%	20%
Northern Continental	20%	22%	14%	15%	11%	19%	78%	20%	2%
Nordic	19%	30%	20%	16%	6%	9%	80%	10%	10%

TABLE 4.2: Amount of floor area built within each reference period [1-2]

	Pre-1980	Post-1980	New construction (after 2000)
EU	56%	28%	16%
US	46%	38%	16%

Under these premises, the reference building has each floor rectangular in shape and 1000 m^2 large (67 x 15 m^2), is glazed on the two main facades (oriented due north and south, respectively) and show a Window to Wall Ratio (WWR) of 0.4, a typical value for this building typology [3]. The Roof to Walls Ratio (RWR), defined as the ratio of roof area to walls area, is 0.70. A sketch of this base configuration is given in Fig. 4.1.

For what concerns building fabric, the survey revealed that the main material used in the structure of office buildings across the EU-27 is concrete, with a brick or concrete façade. Curtain walls are also diffused, especially for buildings constructed after 1960s, when prefabricated sandwich walls were introduced. Glass curtain walls and/or aluminum panel became fairly typical during and after the 1980s.

Table 4.3 summarizes the construction types for each vintage period shown in Table 4.2, and city representative of different climates within the EU. The choice of the cities will be discussed in detail in section 4.3 thanks to an in-depth climatic analysis. The thermophysical properties of the materials forming the various constructions are listed in Table 4.4, while the resulting U-values are summarized in Table 4.5.

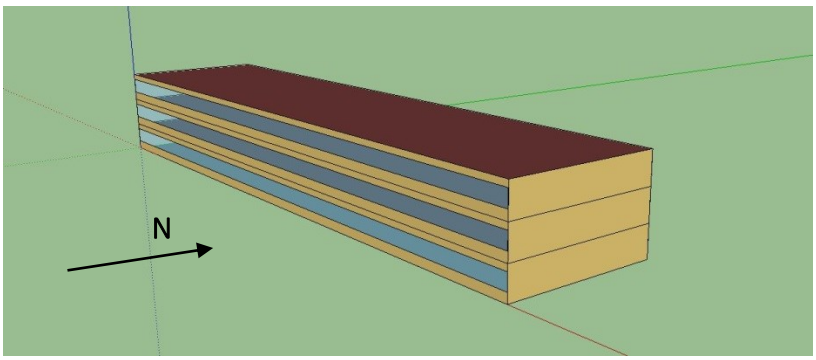

FIGURE 4.1: Prospective view of the reference office building model (base configuration) [Author]

TABLE 4.3: Construction types for vintage period [1]

	Pre-1980	*Post-1980*	*New construction (after 2000)*
Walls	Concrete cladding on concrete pillars and beams	Concrete cladding on concrete pillars and beams	Aluminum and glass façade on concrete pillars and beams
Roof	Flat concrete roof with bitumised surface	Flat concrete roof with bitumised surface	Flat concrete roof with bitumised surface
Floors	As for roof, but with tiles in place of bitumen	As for roof, but with tiles in place of bitumen	As for roof, but with tiles in place of bitumen
Windows	Double-glazed with PVC frame	Double-glazed with aluminum frame	Double-glazed with aluminum frame (thermal cutting)

TABLE 4.4: Thermophysical properties of opaque construction materials [Author]

Materials	*Thickness* [cm]	*Density* [kg·m^{-3}]	*Specific heat* [J·kg^{-1}·K^{-1}]	*Conductivity* [W·m^{-1}·K^{-1}]
Walls – concrete cladding				
Lightweight concrete	10	1280	840	0.53
Wall insulation	variable	90	840	0.043
Gypsum board	2	800	1100	0.16
Walls – aluminum facade				
Aluminum	3	7820	500	45
Wall insulation	variable	90	840	0.043
*Air gap		R = 0.15 m^2 K W^{-1}		
Gypsum board	2	800	1100	0.16
Roof				
Roof membrane	1	1120	1460	0.16
Roof insulation	variable	265	840	0.057
Concrete	10	2250	840	1.311
Stucco	2	1860	840	0.69

*the air gap is modelled by means of its thermal resistance R

It is important to notice that the U-values listed in Table 4.5 are achieved by properly varying the insulating layer thickness of the construction. For the complete list of values reported in [1], the reader can refer to Appendix I.

For what concerns the windows, they are inputted as simple glazing systems by detailing their U-value and Solar Heat Gain Coefficent (SHGC), as gathered from the ASHRAE Handbook of Fundamentals [4] for the typologies detailed in Table 4.3.

TABLE 4.5: U-values for construction types, vintage period and city [1]

		Walls	Roof	Windows
Pre-1980	Athens	2.20	2.70	5.00
	Madrid	2.20	1.40	5.80
	Rome	1.20	1.30	5.50
	Lyon	2.10	1.80	5
	London	1.70	1.80	4.90
	Stuttgart	1.50	1	2.90
Post-1980	Athens	0.80	0.70	3.70
	Madrid	1.80	1	3.30
	Rome	0.80	0.80	4.20
	Lyon	1.20	0.80	3.40
	London	0.70	0.50	4.60
	Stuttgart	0.90	0.50	1.90
New construction (after 2000)	Athens	0.60	0.60	2.80
	Madrid	0.90	0.60	2.80
	Rome	0.60	0.60	3.60
	Lyon	0.40	0.30	2.70
	London	0.40	0.20	1.80
	Stuttgart	0.40	0.30	1.30

4.2 Simulations assumptions and parameters description

The assessment of the thermal comfort conditions and of the energy performance are carried out using the dynamic thermal analysis software EnergyPlus v.8.1 [5].

The solution of the thermal field inside the walls in EnergyPlus is based on the Conduction Finite Difference algorithm. As concerns the discretization of the time variable, in this work a time step $\Delta\tau$ = 3 minutes was adopted, as additional simulations permitted to verify that no changes in the results occur if

using smaller time steps. On the other hand, the space interval Δx is determined by the software itself for each material as a function of the *space discretization constant* C:

$$C = \frac{\Delta x^2}{a \cdot \Delta \tau} \tag{4.1}$$

where *a* is the thermal diffusivity.

The value of this coefficient can be introduced by the user, and corresponds to the inverse of the Fourier number. In this work, C = 2 was chosen, to assure a good stability of the solution [6].

The main simulation assumptions, regarding internal heat gains (people + electric appliances + artificial lighting), infiltrations and ventilation rates and occupancy period of the offices, are provided in Table 4.6 and are desumed from [1].

TABLE 4.6: Common simulation assumptions for all of the models [1]

People	Appliances	Artificial lighting	Infiltrations	Ventilation	Occupancy period
10 m^2/person)	12.5 W/m^2	10.8 W/m^2 (*)	0.15 ACH	40 m^3/h person from outside air	Weekdays: 8:30-12:30 and 13:30-17:30

* the original value of 16 W/m^2 was changed to 10.8 W/m^2, which is considered more suitable for halogen incandescent bulbs typically used in offices. Lights are supposed to be on only during the occupancy period

For ground-contact surfaces, it is important to specify appropriate ground temperatures, especially when modelling low-rise buildings with extended plant shapes. To accurately predicting the surface temperature of the ground floor, the Slab pre-processor embedded within EnergyPlus is used. In this way, average monthly surface temperatures – different for each climate according to the weather files - are used for the floor surface in contact with the ground, and not a simplistic constant value throughout the year.

As for the estimation of the energy needs, it is necessary to define both heating and cooling set point temperatures. This is a very hard task, since the choice of set points would strongly affect the energy consumption for air conditioning.

Moreover, when taking into account different climatic conditions, a too low cooling set point temperature would be detrimental for the cooling needs of a hot climate, while not significantly

affecting those of a cold climate. Vice versa, a too high heating set point temperature would worsen the heating needs of a cold climate while those for a hot one would remain quite the same.

Finally, the choice of different set point temperatures for each climate would mask the performance achieved by cool roofs, thus not allowing for a genuine comparison among several climates.

For all these reasons, a heating set point of 18°C and a cooling one of 26°C are used everywhere, according to the default values used in [1]. In order to compare the energy needs due to different set points, and with the aim of assessing the robustness of the simulation results presented in the next chapter, the reader can refer to Appendix II where energy needs of the models used in [1] are reported.

With the aim of assessing to what extent a cool roof may improve the thermal performance of existing buildings, a parametric analysis about key roof features is carried out.

The main parameters to be varied, listed in Table 4.7, are:

(i) Insulation levels: these values are gathered from Table 4.5, according to the construction age and climate;

(ii) Roof to Walls Ratio (RWR): by retaining a floor area of 1000 m^2 per storey, floor dimensions are varied (67x15 m^2, 50x20 m^2 and 40x25 m^2), and thus different RWR values are obtained;

(iii) Roof solar reflectance (r): values between 0.3 and 0.8 - with a step of 0.1 – are considered for modelling both traditional roofing materials (low reflective) and cool roofing materials (high reflective), as well as the aging process of them;

(iv) Roof thermal emissivity (ε): values ranging from 0.8 to 0.9, with a 0.02 step, are analyzed for studying the role of the long wave radiative heat exchange.

TABLE 4.7: Building features used for the parametric analysis [Author]

Parameters	*Values*	*Variations*
Roof insulation levels	pre 1980; Post 1980; New (post 2000)	3
Roof to Walls Ratio (RWR)	RWR=0.7; RWR=0.8; RWR=0.9	3
Roof solar reflectance (r)	From r=0.3 to r=0.8, with 0.1 step	6
Roof thermal emissivity (ε)	From ε=0.8 to ε=0.9, with 0.02 step	6
	Number of models per city – *free running models*	*324*
	Number of models per city – *with HVAC system*	*324*
	Total number of models per city	***648***

4.3 Climate analysis

In order to study the climatic parameters that affect cool roof performance, 6 cities representative of different EU climate zones have been chosen: Athens (mixed dry), Madrid (hot dry), Rome (hot humid), Lyon (mixed humid), London (marine) and Stuttgart (cold).

The updated Köppen-Geiger climate classification [7] is too simplistic for comparing the effects of the climates of different cities scattered all over the world on passive building performance. Köppen-Geiger focuses on the outdoor environment very much from a plant physiology viewpoint; what is needed in building physics is a focus on the likely effect of the Air Temperature, Humidity, Wind Speed and Solar Radiation on the performance of a particular building. For example, if a building is a small house, with a small internal heat gain from people and lights, and a high heat loss surface area relative to its surface area, then a cool climate might well require mostly heating; but if it is large office building with a large internal heat gain from people and lights and a small surface area relative to its conditioned volume, the same Köppen-Geiger 'cool' climate would still lead to a requirement for a lot of cooling to get rid of the internal heat gains.

For the sake of comparison, a combined approach that takes into account both the Ecotect psychometric classification [8] and the summer monthly averaged values of dry bulb temperature, relative humidity, wind speed and global horizontal radiation – as gathered from TMY2 weather files [9] has been adopted. Table 4.8 lists the cities selected; their latitude (LAT), longitude (LON), Heating Degree Days (HDD) and Cooling Degree Days (CDD) are also shown. The HDD and CDD were calculated on a baseline of 18.3 °C, according to the Climate Design Data 2009 ASHRAE Handbook [4]. Table 4.9 lists the summer monthly (from June to September) and winter (January to March) averaged values of a selection of representative climate variables.

TABLE 4.8: Cities representative of different mid-latitude climates with Köppen-Geiger style classifications [Author]

Mixed dry	**Hot dry**	**Hot humid**	**Mixed humid**	**Marine**	**Cold**
Athens	*Madrid*	*Rome*	*Lyon*	*London*	*Stuttgart*
LAT: 37.90N LON: 23.73E HDD: 1534°C CDD: 994°C	LAT: 40.27N LON: 3.32W HDD: 2023°C CDD: 612°C	LAT: 41.47N LON: 12.13E HDD: 1525°C CDD: 555°C	LAT: 45.43N LON: 5.40E HDD: 2588°C CDD: 309°C	LAT: 51.90N LON: 0.10W HDD: 2968°C CDD: 44°C	LAT: 48.40N LON: 9.13E HDD: 3490°C CDD: 106°C

TABLE 4.9: Climatic characteristics of different sites (summer and winter daily averages) [Author]

Standard "Koppen-Geiger" style Classes	Weather station	Dry bulb temperature (°C)	Relative humidity (%)	Global horizontal radiation (Wh m^{-2} hr^{-1})	Wind speed (m s^{-1})
		SUMMER			
Mixed dry	Athens Eleftherios Intl Arpt	25.2	51.7	493.2	2.7
Hot dry	Madrid Barajas Intl Arpt	23.6	45.6	487.4	2.7
Hot humid	Rome Fiumicino Intl Arpt	23.3	76.0	437.2	3.3
Mixed humid	Lyon Satolas Intl Arpt	20.3	69.4	378.2	2.7
Marine	London Gatwick Intl Arpt	16.3	73.8	307.7	2.9
Cold	Stuttgart Echterdingen Intl Arpt	17.2	68.8	338.3	2.3
		WINTER			
Mixed dry	Athens Eleftherios Intl Arpt	10	66.3	272.7	3.0
Hot dry	Madrid Barajas Intl Arpt	6.1	75.2	209.9	2.6
Hot humid	Rome Fiumicino Intl Arpt	8.9	79.4	196.0	3.8
Mixed humid	Lyon Satolas Intl Arpt	3.4	86.1	124.0	2.8
Marine	London Gatwick Intl Arpt	4.5	84.8	94.3	3.3
Cold	Stuttgart Echterdingen Intl Arpt	0.9	81.9	113.3	3.3

Part of the classification of the climates involved visual examination of the Typical Meteorological Year (TMY) data for each city on a psychometric chart using the Climate Consultant software [10]. It is clear from these charts that the much greater extremes of climate that the Koppen-Geiger approach is intended to document are not found in Europe, thus the simplistic climate typologies are at best indications.

By analyzing Figs. 4.2-4.7, where a psychometric representation of the outdoor air conditions (temperature and relative humidity) and the frequency distribution of annual values of global horizontal

radiation and wind velocity is given for each city, it is possible to notice the peculiarities of the different climates.

Indeed, Athens (mixed dry), Madrid (hot dry) and Rome (hot humid) share a very similar outdoor air temperature and global horizontal radiation distributions, but a different relative humidity range (the "cloud" of points for Athens and Rome is closer to the saturation curve than the Madrid one). Moreover, Athens is characterized by lower wind speeds than Madrid and Rome.

These three cities represent the hottest climate conditions found within EU countries, and thus are potentially the places in which cool roofs application could be most beneficial for reducing overheating issues.

As for Lyon (mixed humid) and London (marine), they share similar values of outdoor air temperature and global horizontal radiation, but different humidity levels since Lyon experiences a wider range of humidity values (the points are more scattered within the chart than for London).

These two climates are considered for representing mild conditions typical of middle-Europe countries.

Finally, the low outdoor air temperature ranges in Stuttgart allow to characterize this city as representative of a "cold" climate, different from the previous ones. Coldest climates such those of Poland, Norway and Sweden are not considered because they are clearly heating-dominated, and the application of cool roofs to existing buildings would likely increase the energy needs for air conditioning, while improving summer comfort to a negligible extent.

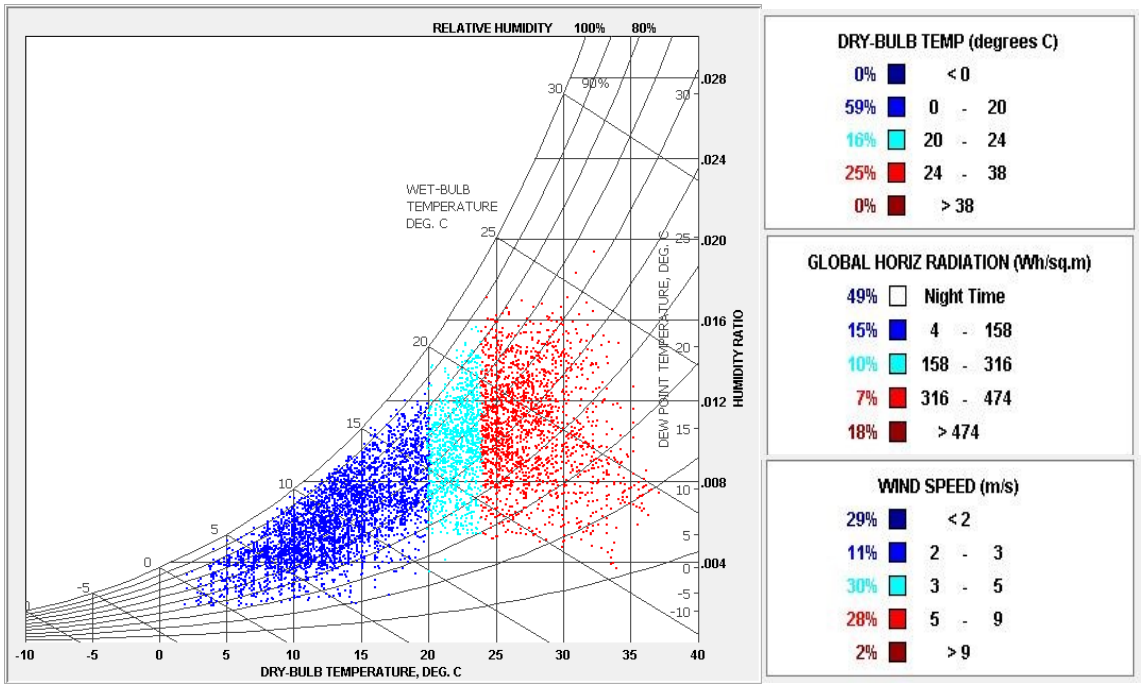

FIGURE 4.2: Athens psychometric chart and outdoor temperature, global horizontal radiation and wind speed annual frequency distributions [Author]

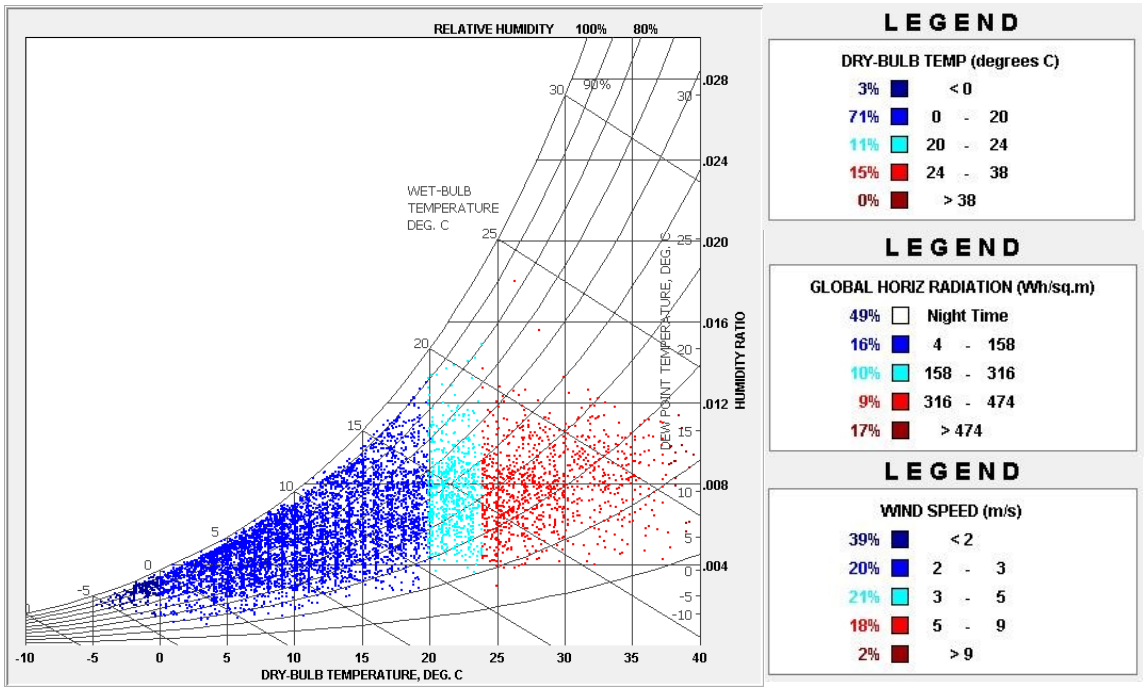

FIGURE 4.3: Madrid psychometric chart and outdoor temperature, global horizontal radiation and wind speed annual frequency distributions [Author]

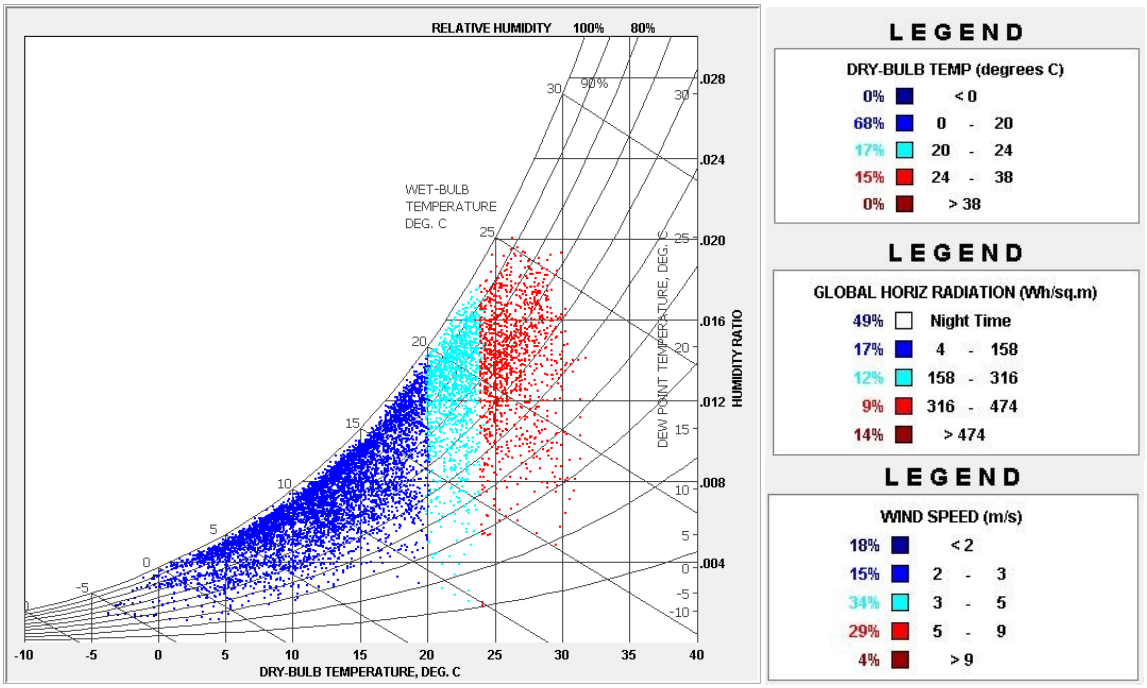

FIGURE 4.4: Rome psychometric chart and outdoor temperature, global horizontal radiation and wind speed annual frequency distributions [Author]

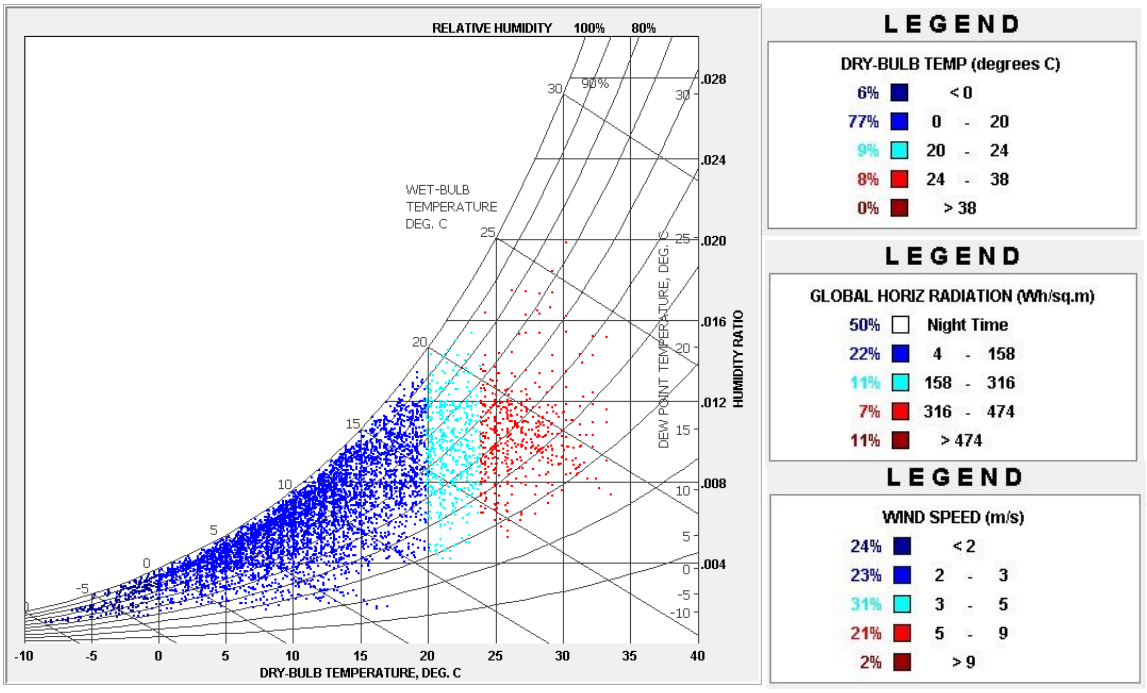

FIGURE 4.5: Lyon psychometric chart and outdoor temperature, global horizontal radiation and wind speed annual frequency distributions [Author]

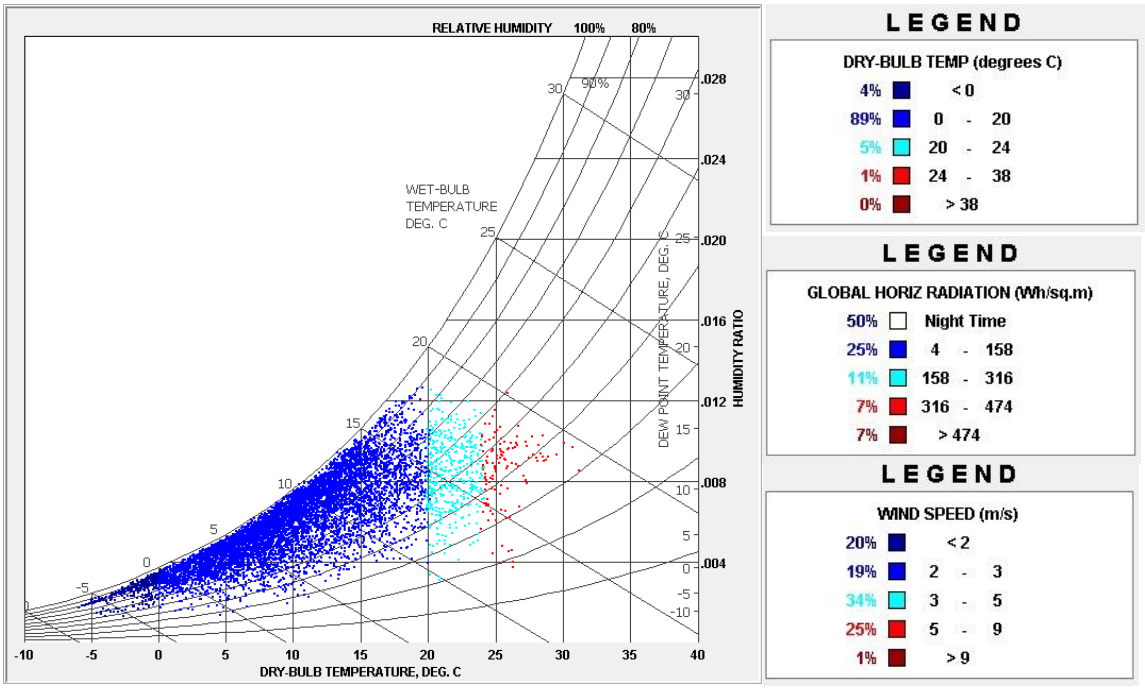

FIGURE 4.6: London psychometric chart and outdoor temperature, global horizontal radiation and wind speed annual frequency distributions [Author]

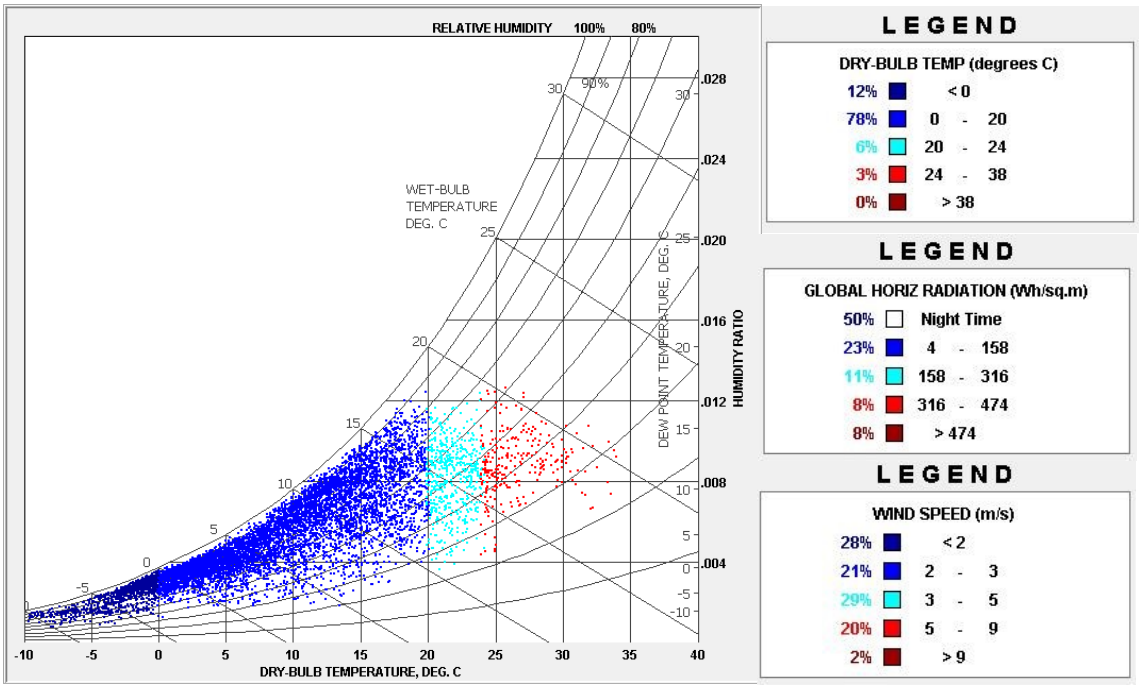

FIGURE 4.7: Stuttgart psychometric chart and outdoor temperature, global horizontal radiation and wind speed annual frequency distributions [Author]

4.4 Thermal comfort assessment: operative temperature and Intensity of Thermal Discomfort Index (ITD)

Traditionally, the PMV-PPD model for comfort proposed by Fanger [11] is considered the first endeavor in predicting building occupants' comfort sensations.

This approach, based on a steady-state energy balance on the human body, allows the prediction of thermal sensation and comfort satisfaction of the human body as a function of four parameters related to the indoor environment (internal temperature, air velocity, humidity, mean radiant temperature) and two parameters related to the occupants (activity and clothing). No correlation with the external environmental conditions are taken into account. This model, developed by using the results of interviews carried out under controlled micro-climatic conditions (typical of buildings provided with HVAC systems), is not suitable to manage the transient state that occurs, for instance, in naturally ventilated buildings, in buildings without HVAC systems or where occupants vary their behavior and activity. This means that for most bioclimatic buildings as well as for a large number of renewed buildings Fanger's approach might not be suitable.

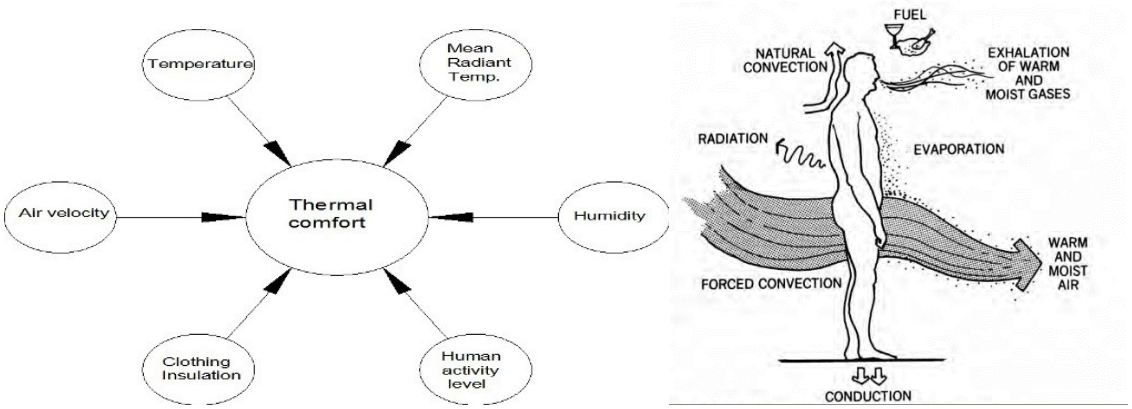

FIGURE 4.8: The six variables affecting thermal comfort under Fanger's theory (left) and the energy balance on a human body (right) [Internet]

On the other hand, in the same years the adaptive model proposed by Nicol and Humphreys [12] stated that people's interaction with the external and internal environment allows a range of thermal comfort conditions which is wider than that admitted by a steady-state model. Actually, people can react to changes in the environment by taking appropriate actions or by changing their attitudes, in order to restore a comfortable condition even if the environment where they are placed has undergone appreciable changes. De Dear and Brager [13] also underlined that people who live or work in naturally

ventilated buildings, where they are able to open windows, get used to thermal variations reflecting local climatic patterns.

By analyzing a great number of surveys conducted world-wide on free-running buildings, Nicol and Humphreys [14] found a clear correlation between the comfort *operative temperature* and the *running mean outdoor temperature* measured over the previous days. Therefore, they stated that thermal comfort in free-running buildings could be assessed just as a function of the indoor operative temperature, thus neglecting all the other parameters accounted for in Fanger's model, which would have a minor importance.

Then, while Fanger's approach intrinsically postulates the need of a system to provide and keep optimal thermal conditions inside the building, the adaptive approach just defines a range of temperatures in which an occupant can find his own comfort without the aid of any air-conditioning system, if he is free of adapting his behavior.

When studying low energy demand buildings, the adaptive approach appears more appropriate, since no HVAC is postulated and a link is created among human behavior, its interaction with the environment and, as a consequence, the building energy demand. The importance of this approach has increased in the last ten years so that it was first included in the ASHRAE standard 55 [15] and more recently in the EN standard 15251 [16].

For all these reasons, the *operative temperature* is regarded as the physical parameter that expresses thermal comfort occurrences within the building, under free-floating conditions (i.e. without any HVAC system operating).

An effective way to quantify the intensity of uncomfortable thermal sensation due to overheating in a living space is the measure of the difference between the room operative temperature and a threshold value; however, the duration of such overheating should also be taken into account.

The value of the threshold temperature T_{lim} depends on the choice of a specific thermal comfort theory. As stated before, the adaptive approach is chosen, as described in the ISO EN 15251 Standard [16]; hence, the threshold value is not constant in time, but it should be determined daily as a function of the running mean outdoor air temperature T_{rm} (see Fig. 4.8). The formulation of the threshold temperature is given in Eq. (4.2), and corresponds to the upper limit T_{lim}^{I} of Category I as introduced by the EN Standard (high level of expectation):

$$\begin{cases} T_{lim}^{I} = 20.8 + 0.33 T_{rm} \\ T_{lim}^{II} = 16.8 + 0.33 T_{rm} \end{cases} \tag{4.2}$$

As for the running mean external temperature T_{rm}, the EN Standard defines it as an exponentially weighted of the daily mean external air temperature of the previous day T_{ed-1}:

$$T_{rm} = (1-\alpha)\,\mathrm{T}_{ed-1} + \alpha T_{rm-1} \tag{4.3}$$

where α is a constant between 0 and 1 (0.8 is recommended) and T_{rm-1} is the running mean temperature of the previous day.

Figure 4.9 provides an example of the adaptive comfort boundaries – from the most restrictive category I to the most tolerant category III – for the city of Lyon in August. The outdoor running mean temperature is also reported to give an example of how outdoor thermal conditions are very often out of the boundaries of comfort.

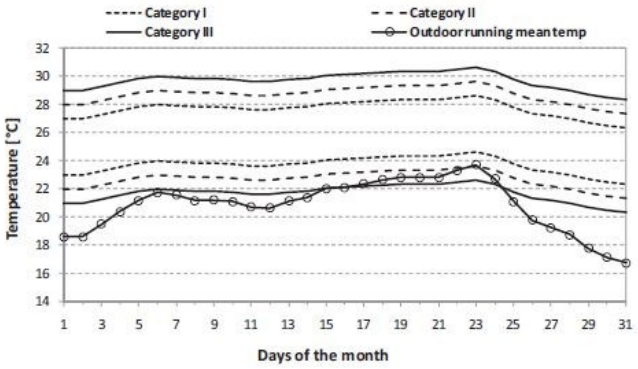

FIGURE 4.9: Adaptive comfort categories for the city of Lyon, August [17]

With the aim of giving a concise information about overheating occurrences during the year in a room, an indicator called Intensity of Thermal Discomfort for overheating (ITD_{over}), introduced by Sicurella et al. [17], will be adopted.

It is defined as the time integral, over the occupancy period *P* (defined in Table 4.6), of the positive differences between the current operative temperature and the upper threshold for comfort defined for the Category I:

$$\mathrm{ITD}_{\mathrm{over}} = \int_{\mathrm{P}} \Delta\mathrm{T}^{+}(\tau)\ \mathrm{d}\tau \tag{4.4}$$

where

$$\Delta\mathrm{T}^{+} = \begin{cases} \mathrm{T}_{\mathrm{op}}(\tau) - \mathrm{T}^{\mathrm{I}}_{\mathrm{lim}}(\tau) & \text{if } \mathrm{T}_{\mathrm{op}}(\tau) > \mathrm{T}^{\mathrm{I}}_{\mathrm{lim}}(\tau) \\ 0 & \text{if } \mathrm{T}_{\mathrm{op}}(\tau) < \mathrm{T}^{\mathrm{I}}_{\mathrm{lim}}(\tau) \end{cases} \tag{4.5}$$

For further clarifying this concept, a graphical representation of the ITD physical meaning is provided in Fig. 4.10.

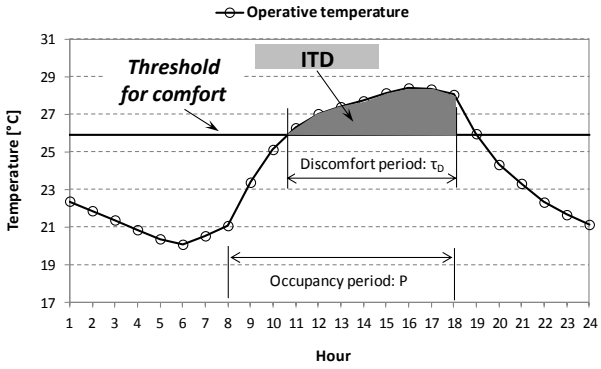

FIGURE 4.10: Definition of the Intensity of Thermal Discomfort (ITD) index [17]

4.5 Energy needs assessment: Primary Energy (PE) consumption

The energy needs assessment is first accomplished by estimating the heating and cooling loads of the building - as reported in output by the dynamic simulations - assuming an ideal plant always able to meet thermal load.

Then, the calculation of the overall (heating + cooling) Primary Energy (PE) consumption is carried out.

To this aim, one needs to define the plant solutions adopted to provide both heating and cooling to the sample building. In fact, the PE consumption depends highly on the efficiency of the energy technology in use, which is expressed by the Primary Energy Ratio (PER). Now, in this study air-conditioning in summer is supposed to be based on fan-coil units fed by a reversible electric air-to-water vapor-compression chiller. As concerns space heating, air-to-water electric reversible heat pumps are considered. In fact, these are two of the most widespread plant solutions for office buildings within EU countries.

Furthermore, the results of such an investigation are also likely to depend on the local weather conditions, and especially on the duration of the heating and cooling seasons. For sake of comparison among different climates, the calculation of the PE consumption will be performed for all of the cities previously discussed on an annual basis.

The overall annual PE needs for both space cooling and heating are expressed by Equation (4.6):

$$PE = \frac{Q_s}{PER_s} + \frac{Q_w}{PER_w} \tag{4.6}$$

Here, the first addend is the PE consumption for cooling in summer (s), while the second one is the PE consumption for heating in winter (w). The primary energy ratios PERs and PERw depend on the plant configuration and are summarized in Table 4.10, where the value 0.46 represents the average efficiency for the production and distribution of the electric energy within the EU [18].

TABLE 4.10: Primary Energy Ratio (PER) for different plant solutions [Author]

Air-cooled vapour-compression chiller	PER_s = EER·0.46
Air-to-water Heat Pump	PER_w = COP·0.46

For the calculation of the system efficiency, the mean values reported in Table 4.11 were assumed. In fact, EER and COP values strongly depend on the outdoor boundary conditions for air-to-water heat pumps.

With the aim of taking into proper consideration this phenomenon, the mean performance coefficients listed in Table 4.11 are calculated by regressing the hourly efficiency values of an existing reversible electric heat pump as a function of the outdoor temperature T_o.

The regressing equations, for the calculation of both average EER and COP values are shown in Eqs. (4.7-4.8), respectively.

$$EER = 0.0022T_o^2 - 0.3665T_o + 10.72 \tag{4.7}$$

$$COP = 0.0823\mathrm{T}_o + 2.772 \tag{4.8}$$

As one can observe, the Energy Efficiency Ratio (EER) of the chiller and the Coefficient Of Performance (COP) of the heat pump are not the same. In cold climates (London and Stuttgart) the chiller behaves better than in hot climates (Athens, Madrid and Rome). On the other hand, the heat pump is highly penalized in a cold climate such as Stuttgart (COP = 2.93), whereas it is very efficient in hot climates (Athens, COP = 3.71).

These differences could affect the global energy performance of buildings provided with cool roofs, and thus their convenience, as shown in the next Chapter.

TABLE 4.11: Mean performance coefficients for summer and winter air conditioning devices [Author]

	Athens	Madrid	Rome	Lyon	London	Stuttgart
EER	2.73	3.43	3.48	4.13	4.71	4.56
COP	3.71	3.34	3.58	3.13	3.21	2.93

4.6 References of the chapter

[1] iNSPiRe Project reports D2.1a-D2.1c (2014). Survey on the energy needs and architectural features of the EU building stock. Retrieved on March 2015 from http://www.inspirefp7.eu/about-inspire/downloadable-reports/

[2] NREL report (2011). U.S. Department of Energy Commercial Reference Building Models of the National Building Stock. Retrieved on March 2015 from http://energy.gov/eere/buildings/commercial-reference-buildings

[3] L. Bellia, F. De Falco, F. Minichiello, Effects of solar shading devices on energy requirements of standalone office buildings for Italian climates, Applied Thermal Energy 54 (2013) 190-201

[4] ASHRAE Handbook of Fundamentals, American Society of Heating , Refrigerating and Air Conditioning Engineers, The Society, Atlanta, 2009

[5] US Department of Energy, EnergyPlus version 8.1, 2014. http://apps1.eere.energy.gov/buildings/energyplus

[6] PC. Tabares-Velasco, C. Christensen, M. Bianchi, Verification and validation of EnergyPlus phase changing material model for opaque wall assemblies, Building and Environment 54 (2012) 186-196

[7] M. Kottek, J. Grieser, C. Beck, B. Rudolf, F. Rubel, World map of the Köppen-Geiger climate classification updated, Meteorologische Zeitschrift 15-3 (2006) 259-263

[8] Natural Frequency. WeatherTool: Psychometry. Retrieved on March 2015 from http://wiki.naturalfrequency.com/wiki/WeatherTool/Psychrometry

[9] Marion W, Urban K. User's manual for TMY2s Typical Meteorological Years (1995). Retrieved on March 2015 on http://rredc.nrel.gov/solar/pubs/tmy2/

[10] UCLA Energy Design Tools Group, Climate Consultant v.6.0, 2015. http://www.energy-design-tools.aud.ucla.edu/

[11] P.O. Fanger, Thermal Comfort-Analysis and Applications in Environmental Engineering Copenhagen, Danish Technical Press, 1970

[12] J. F. Nicol, M.A. Humphreys, Thermal comfort as part of a self-regulating system, in: Proceedings of the CIB Symposium on Thermal Comfort, Building Research Establishment, Watford, UK, 1972

[13] R.J. De Dear, G.S. Brager, Thermal comfort in naturally ventilated buildings: revisions to ASHRAE Standard 55, Energy and Buildings 34 (2002) 549-561

[14] J.F. Nicol, M.A. Humphreys, Adaptive Thermal comfort and sustainable thermal standards for buildings, Energy and Buildings 34 (2002) 563-572

[15] ASHRARE Standard 55, 2004, Thermal Environmental Condition for Human Occupancy, Atlanta, ASHARAE Inc.

[16] EN Standard 15251, 2007, Indoor environmental input parameters for design and assessment of energy performance of buildings addressing indoor air quality, thermal environment, lighting and acoustics

[17] F. Sicurella, G. Evola, E. Wurtz, A statistical approach for the evaluation of thermal and visual comfort in free-running buildings, Energy and Buildings 47 (2012) 402-410

[18] Energy Efficiency Trends and Policies in the Household and Tertiary Sectors. Ana analysis based on the ODYSSEE and MURE Databases (2015). Retrieved on October 2015 from http://www.odyssee-mure.eu/publications/br/energy-efficiency-trends-policies-buildings.pdf

5. YEAR-ROUND ASSESSMENT: DYNAMIC SIMULATIONS

The assessment of the yearly performance of different roof solutions, for several European climates and roof features, will be shown in this Chapter in terms of both thermal comfort (Section 5.1) and Primary Energy needs (Section 5.2).

The methodology followed, described in detail in Chapter 4, is that of an extensive parametric analysis regarding the main features affecting cool roofs performance (i.e. their optical properties such as solar reflectance and thermal emissivity) and roofs energy balance in general (roof to walls ratio and thermal transmittance namely).

The great amount of models simulated – 648 per each city, thus resulting in 3888 final models - raised the issue of filtering in some way the results, while retaining the greatest possible amount of information. This problem will be tackled in each of the following sections, discussing to which extent some parameters have a negligible influence on the results.

Finally, Section 5.3 will deal with an economic feasibility study of cool roofs application to existing office buildings, based on the expected energy savings as highlighted by simulations.

5.1 Thermal comfort and reduction of overheating occurrences

Thermal comfort simulations aim at showing how cool roofs could improve summer comfort conditions in free-running operation, i.e. without the help of any HVAC system operating.

Given the great number of models taken into account (648 per each city) a filter criterion is needed. To this aim, the following procedure has been adopted:

(i) the first 10% of models (32 models) showing the lowest number of hours during which the operative temperature exceeds the threshold value T_{op} = 26°C have been referenced as "*best comfort models*". On the other hand, the last 10% of models showing the highest number of hours for which the operative temperature exceeds the threshold value have been named "*worst comfort models*";

(ii) common features among best and worst models have been studied, respectively. This task gave the opportunity to neglect some parameters that have little influence on the results;

(iii) the resulting models have been parametrically analyzed by varying the most important features. This led to consider 54 models per city.

The results of the filtering procedure described above showed how the best comfort models share the same features for each city analyzed. More in detail, the best-performing buildings are those with a Roof to Walls Ratio (RWR) of 0.9, a good but not excessively insulated envelope (pre-1980 and post-1980 vintage periods), and the highest possible values of both solar reflectance (r = 0.8) and thermal emissivity (ε = 0.9). Indeed, a high RWR value would increase the weight of the roof in the building energy balance, while a scarcely insulated envelope (both opaque and glazed components) would allow an easier and faster heat release to the outdoor. High solar reflectance and thermal emissivity values of the cool material applied to the roof would in turn strongly reduce the amount of the heat flux entering through the roof (daytime) and increase the heat discharge by irradiation (mainly during night), although the influence of thermal emissivity is found to be of secondary importance.

Conversely, the worst comfort models are those with RWR = 0.7, constructed after 2000 (new construction vintage period) and with the lowest values for both solar reflectance (r = 0.3) and thermal emissivity (ε = 0.8). In fact, for these models the contribution of the roof surface to the building energy balance is the lowest, and the optical properties of the cool material are the worst considered. Moreover, a well-insulated envelope would reduce the amount of the heat flux entering the building but at the expense of a lower release to the outdoor, thus enhancing overheating discomfort.

In the following subsections, only the best comfort models will be discussed for each city by plotting the operative temperature distribution for a representative summer month and by calculating the Index of Thermal Discomfort (ITD) for the entire year. In this way, both a detailed (but time-limited) and long-term representation of the thermal performance due to the use of cool materials are provided.

The thermal zone chosen for these analyses is the top floor, since both intermediate and ground floors are only slightly influenced by the application of a cool roof.

5.1.1 Operative temperature distribution over a typical summer month

The operative temperature distribution over the month of July will be plotted in a graph showing the comfort boundaries suggested in EN 15251.

As already remarked in Chapter 4, these boundaries are climate-dependent by means of the running mean outdoor temperature, thus the threshold values for the operative temperature classification – from the most restrictive Category I (red lines) to the most permissive Category III (green

lines) – vary across the cities. Each point of the graph represents the operative temperature value reached in the top floor thermal zone for every simulated hour.

The models chosen for this kind of representation are those with the highest/lowest values of solar reflectance *r* within the best comfort group of models (*r* = 0.8 and *r* = 0.3). In fact, from preliminary analyses, it has been found that *r* is the parameter mostly affecting thermal comfort, followed by thermal insulation level (i.e. age of construction) and RWR value. No appreciable differences are observed by changing thermal emissivity values within the range 0.8-0.9.

If looking at the results of the mixed dry climate of Athens (Fig. 5.1), it is possible to notice how, when *r* = 0.8 (top graph), for a great extent of time (almost 50%) the operative temperature falls within Category I comfort limits (26°C <T_{op}< 30°C), while being outside of the largest comfort band defined by Category III (T_{op}> 32°C) for 13% of time.

On the other hand, when using a roofing material with *r* = 0.3 (bottom graph), the operative temperature is very often above the upper limit of comfort (64% of time) and seldom (10%) within Category I of comfort.

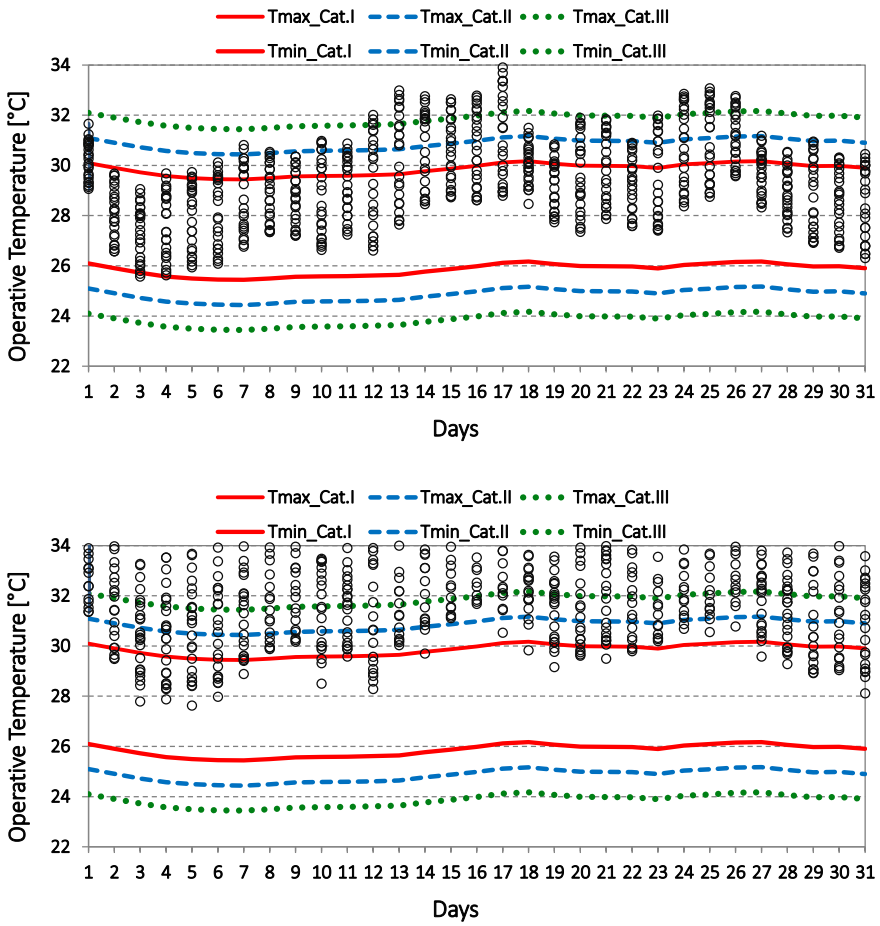

FIGURE 5.1: Operative temperature distribution over the month of July for the best thermal models of Athens. Top: r = 0.8. Bottom: r = 0.3 [Author]

Similar results are found for the hot dry climate of Madrid (Fig. 5.2), where for 40% of time the operative temperature is within Category I limits (25°C <T_{op}< 29°C) and for 28% of time is above the upper comfort threshold (T_{op}> 31°C), when a high-reflective coating (r = 0.8) is employed.

If roof solar reflectance drops to 0.3 (bottom graph), for half of the time temperature is too hot ($T_{op} > T_{max\_Cat\,III}$) and for just 11% of time is within the most restrictive boundaries of Category I.

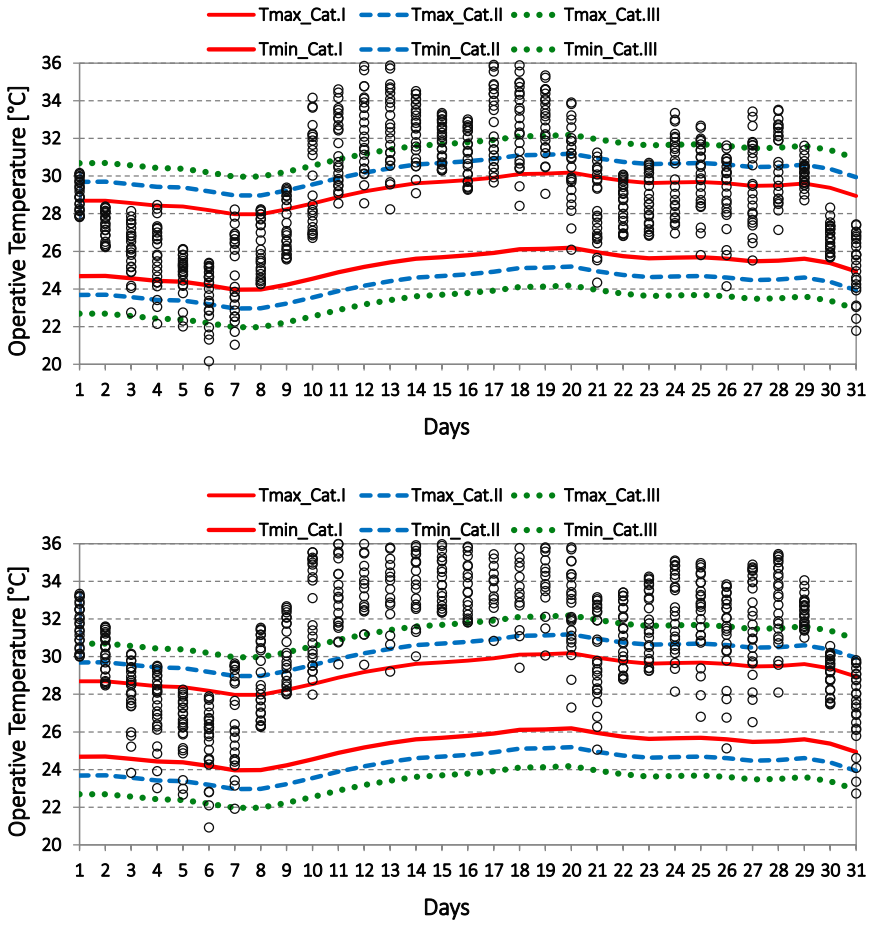

FIGURE 5.2: Operative temperature distribution over the month of July for the best thermal models of Madrid. Top: r = 0.8. Bottom: r = 0.3 [Author]

The adoption of a cool paint with r = 0.8 is a very impressive strategy for improving comfort conditions in a hot-humid climate such that of Rome. In fact, if looking at the top of Fig. 5.3, it is clearly visible how operative temperature is very often (about 71% of time) within the comfort boundaries of Category I (24°C <T_{op}< 28°C), while being for the remaining time within Category II limits.

On the contrary, if a roof finishing layer with r = 0.3 is used (Fig. 5.3 bottom), the results are strongly worsened since T_{op} is outside the comfort boundaries for 20% of time because it is too high, and for the rest of time is within the other Comfort Categories in almost equal proportions.

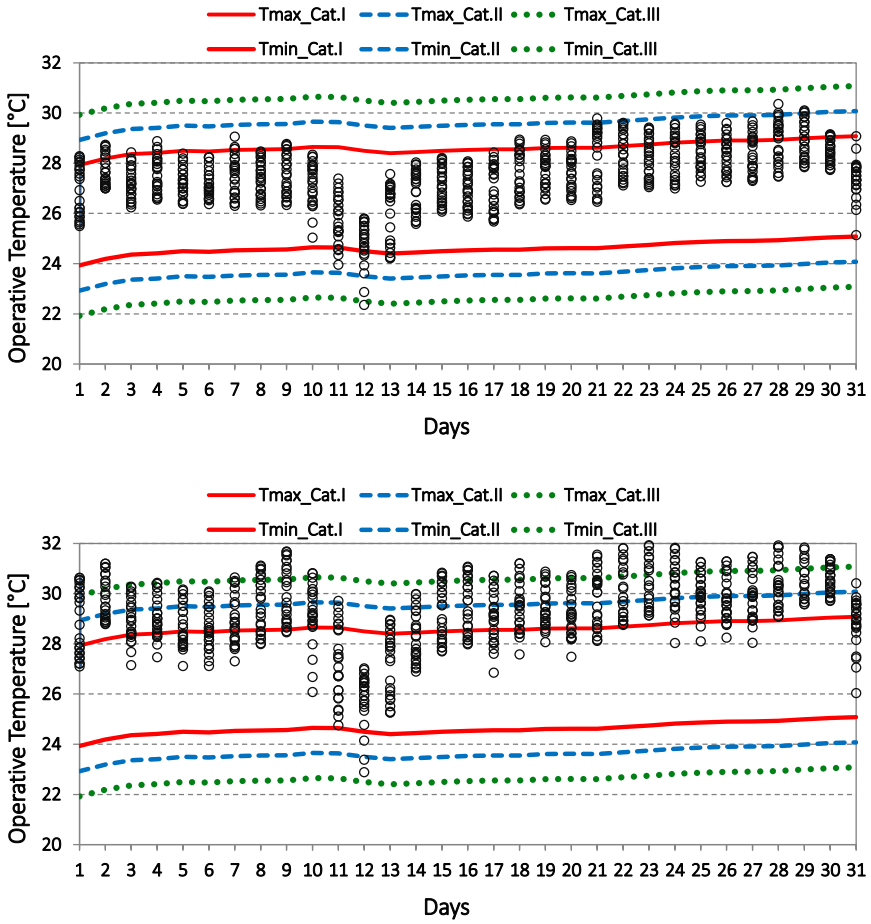

FIGURE 5.3: Operative temperature distribution over the month of July for the best thermal models of Rome. Top: r = 0.8. Bottom: r = 0.3 [Author]

Smaller differences stemming from the use of high-reflective materials instead of low-reflective ones are expected for mild and cold climates. In fact, when considering the mixed humid climate of Lyon (Fig. 5.4), the operative temperature is expected to be within Category I limits (23°C< T_{op} <27°C) for 43% of time and outside of the boundaries for overheating ($T_{op} > T_{max\_Cat\,III}$) for just 8% of time when r = 0.8.

On the other hand, there are hours (20% of the total) during which Top is below the comfort threshold defined by $T_{min\_Cat\,III}$, and thus too low temperatures should be expected.

If considering r = 0.3 (Fig. 5.4 bottom), the hours of discomfort for overheating are increased up to 22%, while those of discomfort for too low temperatures are reduced to 9% of time.

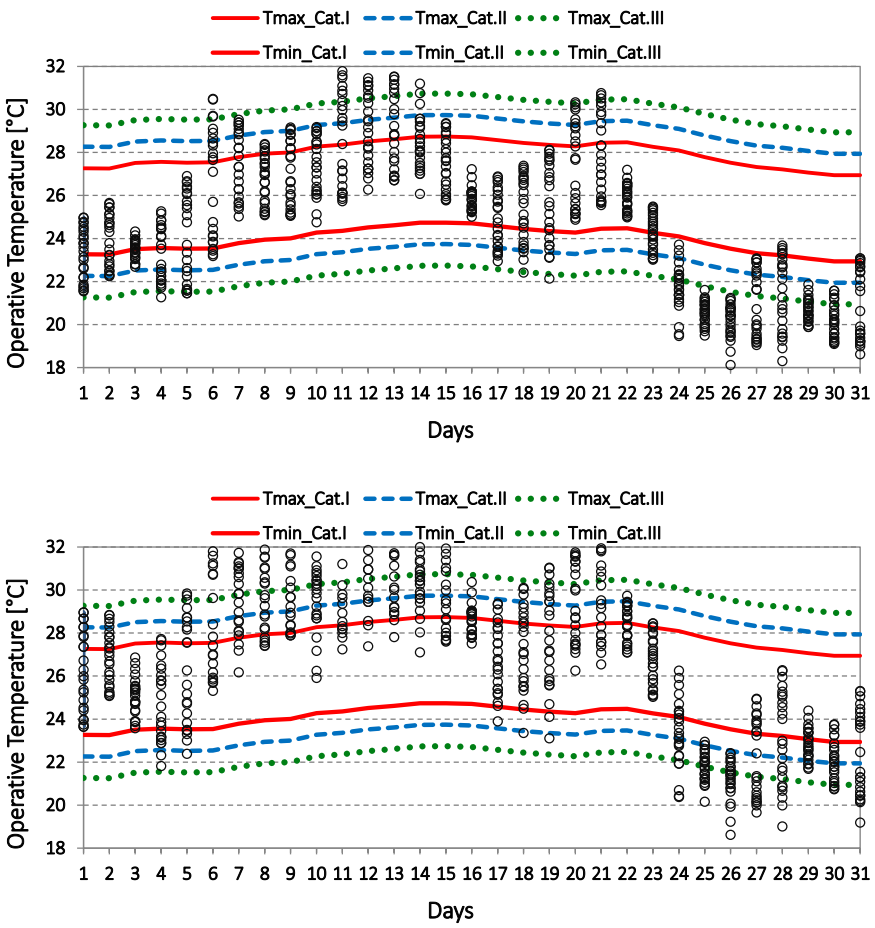

FIGURE 5.4: Operative temperature distribution over the month of July for the best thermal models of Lyon. Top: r = 0.8. Bottom: r = 0.3 [Author]

When considering the marine climate of London (Fig. 5.5), temperatures are found to be within the most restrictive boundaries of comfort (23°C <T_{op} <27°C) for 35% of time and outside of the limit defined by $T_{min\_Cat\,III}$ (too low temperatures) for 29% of time, when a cool material with *r* = 0.8 is used.

If using a roof external layer with *r* = 0.3 (Fig. 5.5 bottom), comfort conditions are even improved since now T_{op} is within Category I range for 52% of time and the number hours of discomfort due to low temperatures are reduced from 29% to 21%.

This a very interesting finding that suggests how cool materials could be detrimental for comfort purposes if applied to buildings located in mild-to-cold climates, and this is rebated by analyzing the results for the city of Stuttgart (Fig. 5.6).

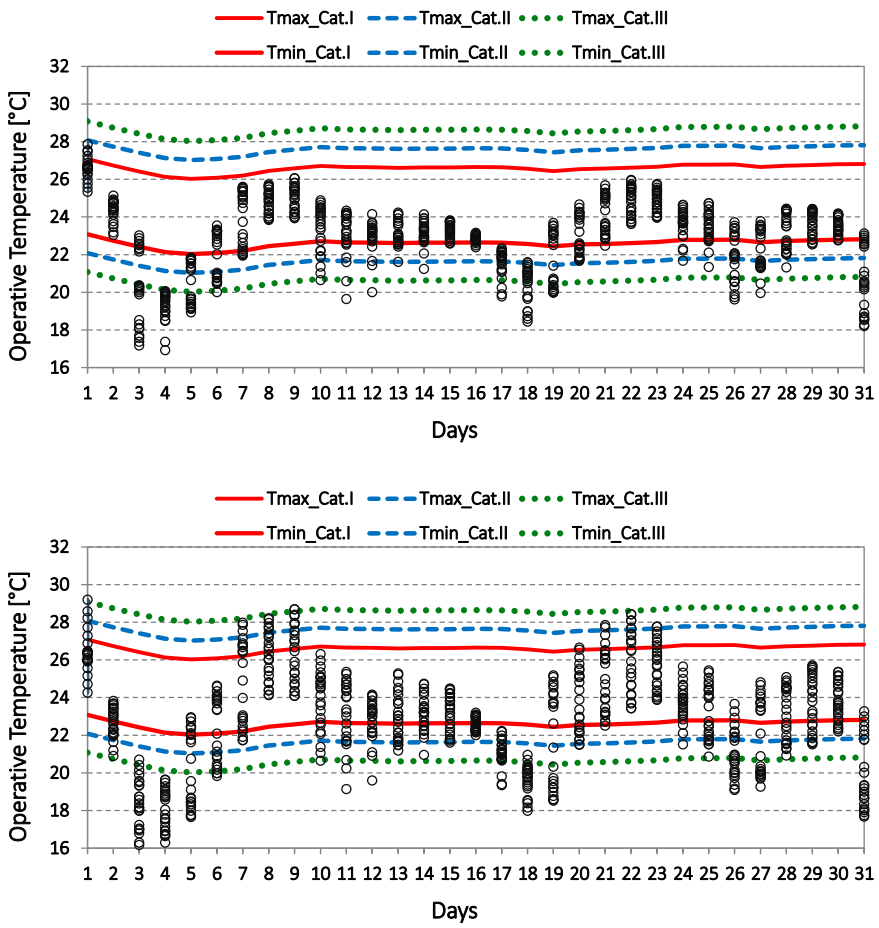

FIGURE 5.5: Operative temperature distribution over the month of July for the best thermal models of London. Top: r = 0.8. Bottom: r = 0.3 [Author]

For this cold climate, if using a cool material with r = 0.8 the percentage of time during which the operative temperature is within the most restrictive comfort zone (23°C <T_{op} <27°C) would be 40%, while just few hours would be outside the largest boundaries defined by Category III (3% of hours with too high temperatures and 15% with too low temperatures respectively).

When a roof with r = 0.3 is considered, the number of hours of overheating would raise from 3% to 6% whereas those below $T_{min\_Cat\,III}$ are reduced to about 8%.

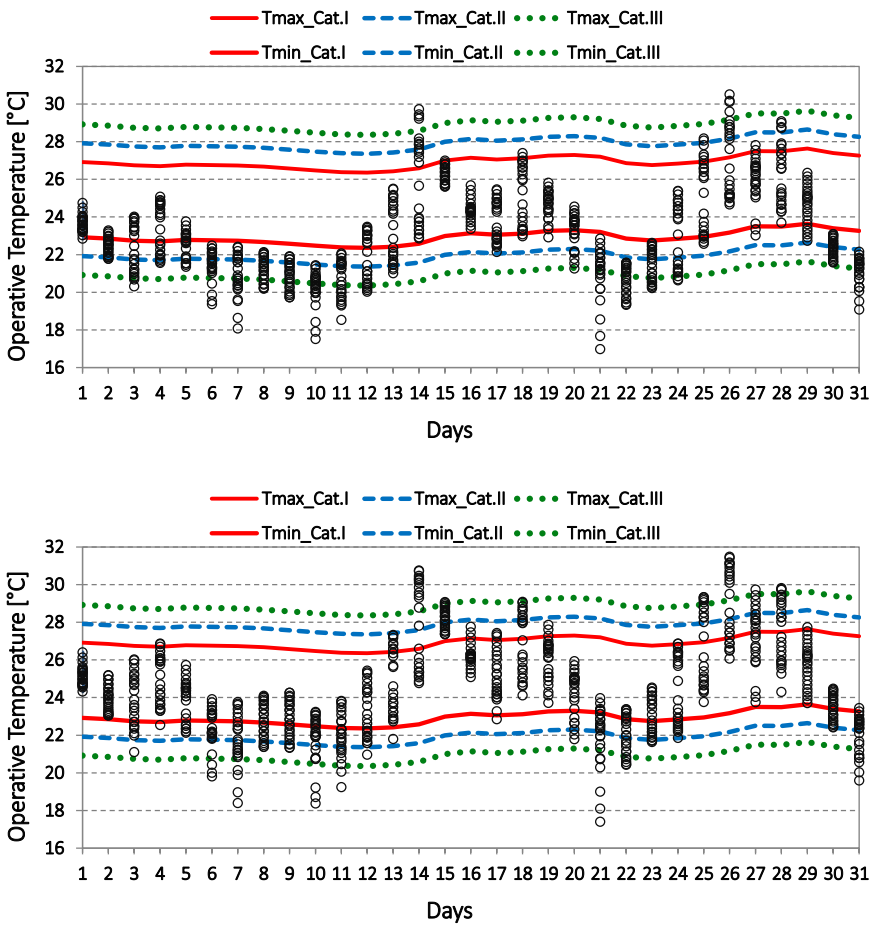

FIGURE 5.6: Operative temperature distribution over the month of July for the best thermal models of Stuttgart. Top: r = 0.8. Bottom: r = 0.3 [Author]

These findings seem to suggest that cool materials should be carefully used in mild and cold climates, such those of Lyon, London and Stuttgart, from a comfort perspective.

This is shown in Fig. 5.7 that reports, for each city, the percentage of discomfort hours (i.e. those falling outside the larger comfort band defined by Cat. III) due to too high (*out max*) or too low (*out min*) temperatures.

It is noticeable to underline that despite the use of a cool paint (r = 0.8) always split in half the number of discomfort hours due to overheating (out max) in comparison to a low-reflective roof (r = 0.3), too low temperatures (out min) may be achieved for mild and cold climates such those of Lyon, London and Stuttgart. For these cities, discomfort hours due to low temperatures are almost doubled when passing from r = 0.3 to r = 0.8.

A likely increase of discomfort hours due to low temperatures in winter will not be calculated because during the cold season the HVAC system will be fundamental for keeping temperatures within a comfortable range, also for the hot climates of Athens and Madrid.

Anyway, further analyses are requested to investigate thermal comfort, so a long-term assessment of comfort conditions will be tackled in the next section.

This task will be accomplished by calculating the ITD Index for the best comfort models in each city, by varying parameters such as solar reflectance, thermal transmittance and roof to walls ratio.

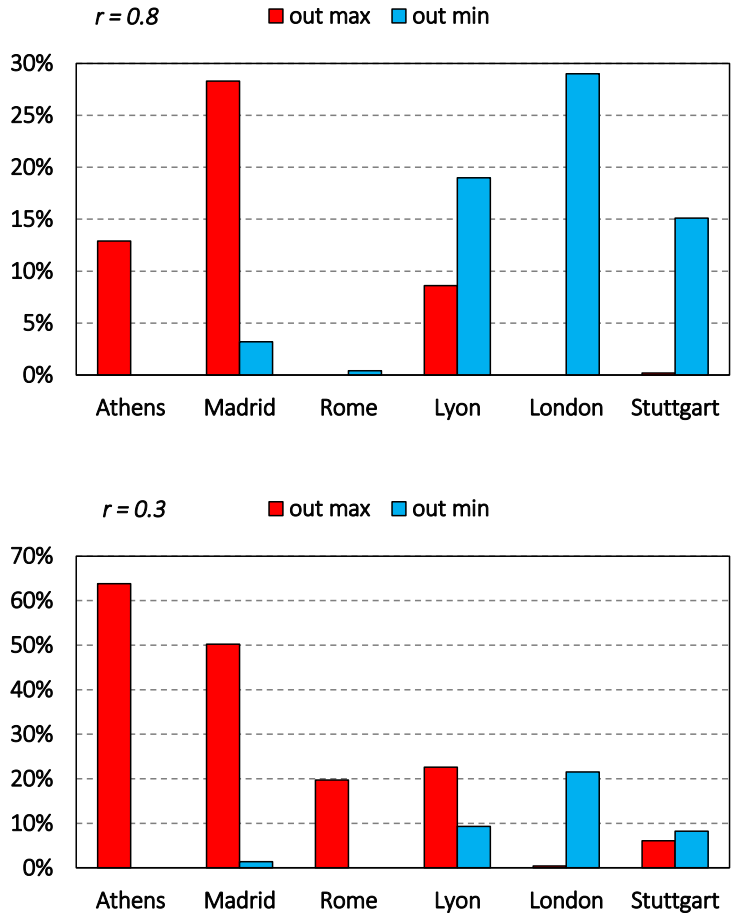

FIGURE 5.7: Percentage of discomfort hours in July for each city. Top: r = 0.8. Bottom: r = 0.3 [Author]

5.1.2 ITD Index calculation

With the aim of assessing long-term comfort conditions due to the use of cool materials, in comparison with those achievable by traditional roofing solutions, the ITD Index defined in Chapter 4 will be calculated for every city representative of different climates.

The models chosen are the *best comfort models* described in Section 4.1; these models are further analyzed by parametrically varying the roof features found to be most important to define comfort inside the building. These features, obtained from preliminary simulations, are solar reflectance *r*, thermal transmittance (by means of the age of construction) and Roofs to Walls ratio RWR. Thermal emissivity does not play the same role in determining comfort occurrence, since results are affected for less than 2%, and thus will be considered constant at the value 0.8.

This procedure leads to consider 54 models per city. For the ease of readability and the sake of comparing the results deriving from changing some parameters instead of others, each graph will report the ITD Index value (y-axis) for different combinations of solar reflectance *r* (x-axis values), RWR (line type) and age of construction (line color).

More specifically, continuous lines are used for RWR = 0.7, while dashed lines and continuous lines with circular indicators are used for RWR = 0.8 and RWR = 0.9 respectively. Light blue color is used for pre-1980 constructions, red for post-1980 constructions and green for new constructions (after 2000).

In this way, for example, a roof constructed after-1980 and with RWR = 0.9 will be identified by a red line with circular indicators.

If looking at the results of the mixed dry climate of Athens (Fig. 5.8), it is possible to appreciate how the construction period and solar reflectance are the most important parameters determining a reduction in the ITD. In fact, when passing from an old construction (pre-1980) to a newer one (both post-1980 or after 2000), an ITD reduction of about 1000 °Ch is expected for $r = 0.3$.

These reductions go diminishing if increasing *r* value: almost identical values are achieved when $r = 0.8$ irrespective of the construction period, meaning that the impact of cool materials ($r > 0.6$) is quite the same for every vintage period.

On the other hand, cool roofs are more performing when applied to poorly-insulated roofs as demonstrated by the different slopes of ITD curves confirms this statement for every construction period.

Roof to Walls Ratio plays a secondary role in reducing overheating occurrences, especially for newer buildings where the curves of different RWR are very close to each other.

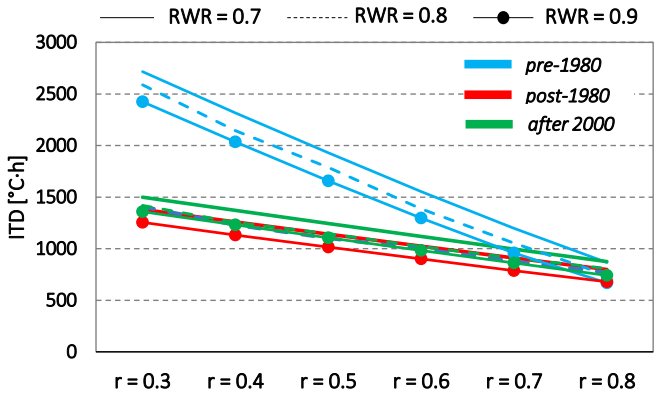

FIGURE 5.8: ITD calculation for Athens [Author]

Slightly different results are observed in Madrid (Fig. 5.9): also in this case the greatest reduction in the ITD occurs for $r = 0.8$, but for this hot dry climate is more evident that thermal insulation has a major in determining overheating. Indeed, the best performance pertain to moderate-insulated components (post-1980 constructions, red lines), while the most insulated models (new constructions, green lines) imply an increase of the ITD of about 200 °Ch when using very performing cool materials ($0.6 < r < 0.8$).

Again, no important differences due to variation in the RWR are observed for moderate or well-insulated components.

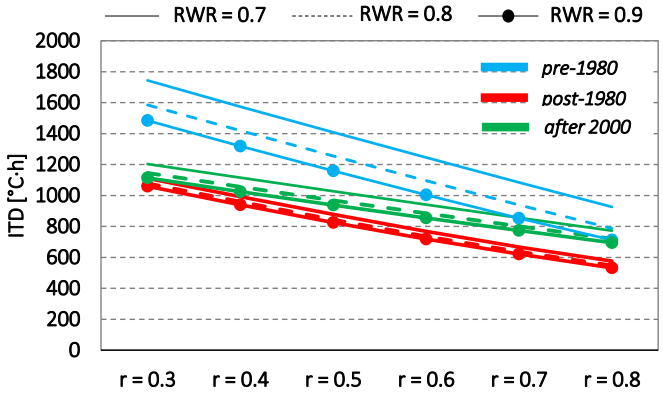

FIGURE 5.9: ITD calculation for Madrid [Author]

As for the city of Rome, Fig. 5.10 shows how for this hot humid climate the number of discomfort hours are lower if compared to Athens and Madrid. Similarly to the previous cases, the greatest reduction in the ITD is due to the use of high-reflective materials (ITD = 200 °Ch when *r* = 0.8 and new constructions are used). The influence of RWR is more evident for poorly insulated roofs (light blue lines), for which the best thermal configuration is the one that emphasizes the contribution of the roof to the building energy balance (RWR = 0.9).

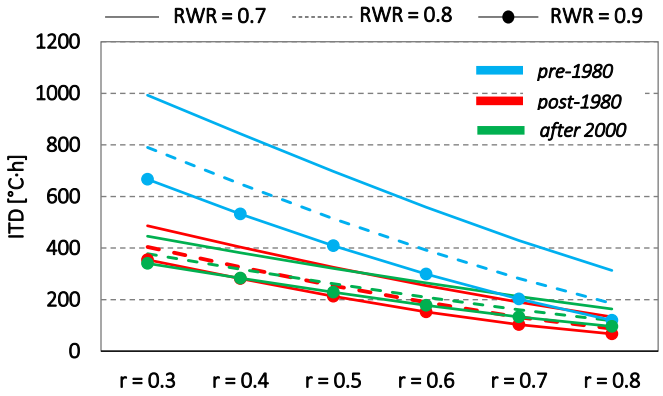

FIGURE 5.10: ITD calculation for Rome [Author]

When considering mild climate conditions like those of Lyon (Fig. 5.11), results show different trends from the previous ones. First, the influence of solar reflectance in reducing overheating is less marked than in the previous cases, as demonstrated by the lower slopes of all of the ITD curves. Secondly, RWR seems to play a more important role in improving comfort conditions, since the best performing models for each vintage period are always those with RWR = 0.9 (lines with circular indicators). Finally, *r* values greater than 0.5 would not significantly affect thermal comfort for post-1980 and new constructions models, while still having a strong impact on older buildings (for *r* = 0.8 the ITD value is almost half of the value attained when *r* = 0.5).

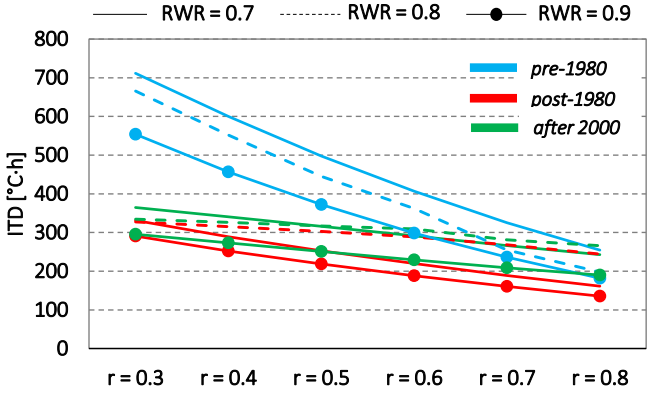

FIGURE 5.11: ITD calculation for Lyon [Author]

Lower ITD values and different trends for the ITD Index are estimated for the marine climate of London (Fig. 5.12). In this case, the curve for pre-1980 constructions and new constructions intersect at r = 0.6, meaning that for r > 0.6 new constructions perform worse than older ones, maybe because of low sun height that emphasize heat fluxes through walls and windows instead of through roofs. Therefore, the best performing models are those with RWR = 0.9.

Also for this climate, constructions that are moderately insulated (red lines) are preferable to well insulated ones (green climates) in reducing overheating.

However, the magnitude of the ITD Index is by far lower than that of the hottest climates described above.

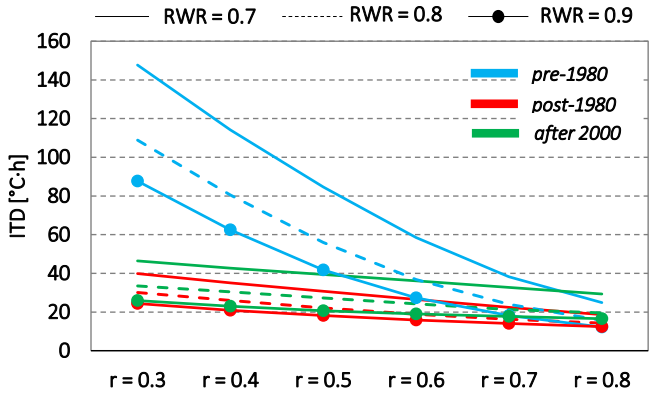

FIGURE 5.12: ITD calculation for London [Author]

Finally, Fig. 5.13 reports the results of the simulations for the cold climate of Stuttgart. Here the role played by solar reflectance in improving comfort conditions is clear for old buildings (light blue lines), while being almost negligible for newer one (green and red lines), since for these last the maximum ITD decrease is of about 30 °Ch. Also for this climate the best performing models are those with RWR = 0.9, and the worst those with RWR = 0.7, while no significant differences are shown for good insulation levels of the envelope (red and green lines). This is because of the coldest climate conditions that make less relevant summer overheating issues respect to winter cold temperatures.

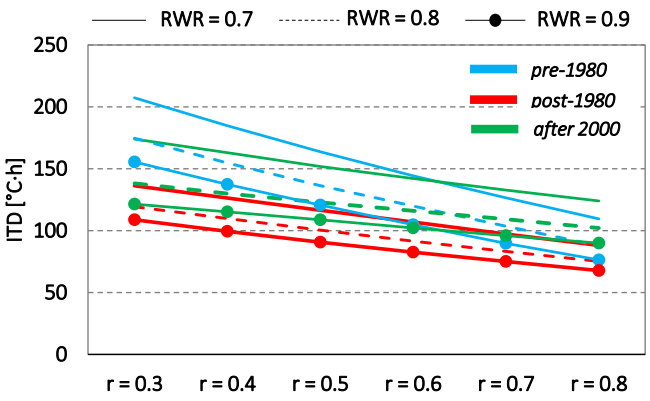

FIGURE 5.13: ITD calculation for Stuttgart [Author]

From the description of comfort conditions achievable by using cool roofs in different climates, it emerges clearly that they may represent a very performing solution for reducing overheating in scarcely insulated buildings located in moderate-to-hot climates (37°N< LAT <45°N).

Fig. 5.14 rebates this concept by summarizing the results of the ITD calculation for the best comfort models of every city. The histograms refer to RWR = 0.7 models and compare the performance of the high-reflective roof (r = 0.8, top graph) with the low-reflective one (r = 0.3, bottom graph).

As it is possible to observe, the intensity of thermal discomfort due to overheating is greatest for the hot climates of Athens and Madrid: when r = 0.3 the estimated ITD is an order of magnitude higher than that expected for the cold cities of London and Stuttgart, and the same trend is expected for high-reflective roofs (r = 0.8).

It is confirmed that from a summer comfort perspective the best models are those poorly or moderately insulated (pre-1980 and post-1980 constructions), while well-insulated constructions (after 2000) exhibit a worse behavior.

For the cold climates analyzed in this study (45°N< LAT <52°N), cool roofs still play a positive role in improving comfort conditions but the reduction in the heat fluxes entering the building through the roof could be detrimental in winter for heating.

To tackle this problem, the following section will report the results of the simulations in terms of Primary Energy needs, thus showing if heating penalties can affect summer benefits and to what extent.

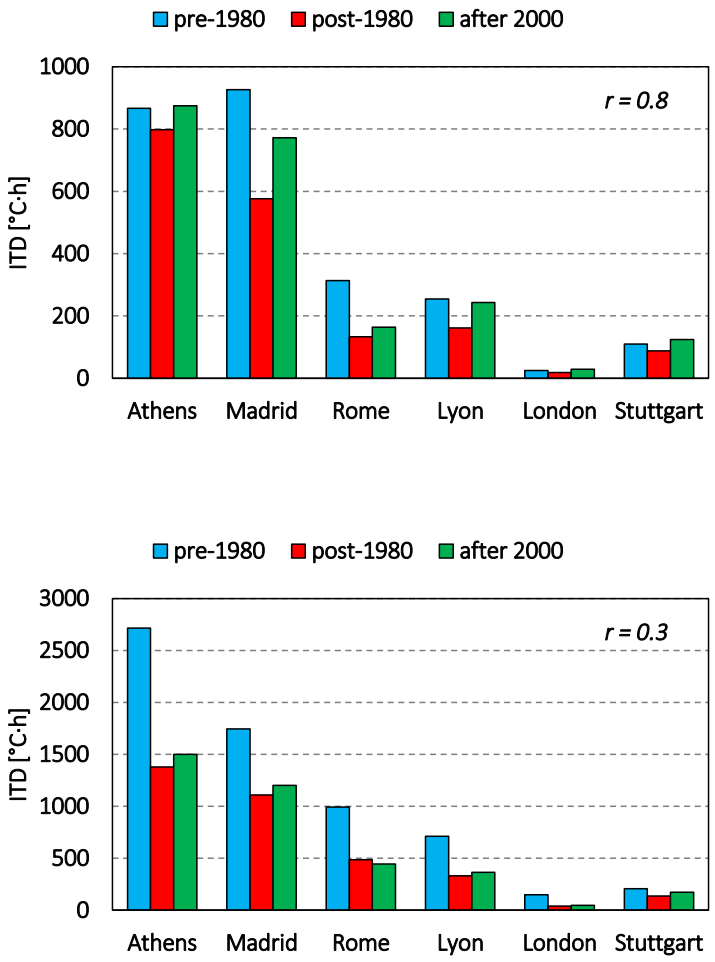

FIGURE 5.14: ITD calculation for best comfort models. Top: r = 0.8. Bottom: r = 0.3 [Author]

5.2 Energy needs and Primary Energy consumption

Energy needs simulations aim at evaluating if energy savings are obtainable when applying cool roofs to existing buildings. In fact, despite their convenience in terms of improvement of comfort conditions, the reduction in the heat fluxes transferred through the roof surface could worsen winter thermal performance, and thus raise heating needs.

The same filtering procedure described in Section 4.1 has been used for selecting the models to be analyzed in detail; this led to the definition of *best and worst energy models* for each city (32 models per city). It is important to underline that both cooling and heating energy needs are taken into account in the definition of best/worst performing models, i.e. these models are those showing best/worst performance in terms of total energy needs.

In fact, simulations results show that best heating models are always different from best cooling models: the first ones are characterized by having 0.7 < RWR < 0.8, well insulated construction

components (new constructions) and the lowest values of solar reflectance and thermal emissivity (r = 0.3 and ε = 0.8). In this way, free solar gains are maximized and stored inside the building more effectively than in the case of poor or moderately insulated components (pre-1980 and post-1980 constructions), high Roof to Walls Ratio (RWR = 0.9) and high solar reflectance and thermal emissivity values (r = 0.8 and ε = 0.9), which are all characteristics that define best cooling models.

However, it has been found that best energy models fall within the same group of best thermal models and that thermal emissivity affects building energy needs less than 3%, thus it can be set at a constant value. This allows making comparisons between thermal comfort and energy needs issues by using the same models, thus clarifying the convenience of installing cool roofs also in mild and cold climates for which heating needs may be of major concern.

In fact, it is important to preliminary notice that energy savings obtainable from the use of this passive cooling technology strongly depend on the ratio between cooling and energy needs, calculated for every model and summarized in Table 5.1 for each city.

TABLE 5.1: Cooling to heating energy needs ratios for different climates [Author]

Mixed dry	Hot dry	Hot humid	Mixed humid	Marine	Cold
Athens	Madrid	Rome	Lyon	London	Stuttgart
1.24	1	0.2	0.08	0.04	0.03

From this Table it is possible to notice how all the models analyzed for a specific city show the same cooling to heating ratio, and this value is strongly decreasing by increasing the latitude of the site. Very low values of the energy ratio, such those found for Lyon, London and Stuttgart, seem to suggest that cool roofs would not perform well in these climates.

Anyway, it is important to consider also the specific HVAC systems employed for space cooling and heating, because Primary Energy needs depend on the mechanical devices adopted.

The following discussion will focus on the same models seen in Section 4.1 (54 models per city), adopting the same representation technique and considering total Primary Energy (PE) needs - calculated according to the methodology described in Section 4.5 - of all the building thermal zones, and not just for the top floor.

The simulations thus reveal that the mixed dry climate of Athens (Fig. 5.15) always benefit from the application of cool materials to existing roofs: PE needs are reduced from 335 MWh to 334 MWh

when passing from *r* = 0.3 to *r* = 0.8 in poor-insulated buildings (pre-1980 constructions), whereas PE reductions are less pronounced for newer buildings (red and green lines), to which pertain best energy results. For these buildings, an increase in roof solar reflectance would only slightly decrease PE needs, meaning that other retrofitting strategies are needed for improving their energy performance.

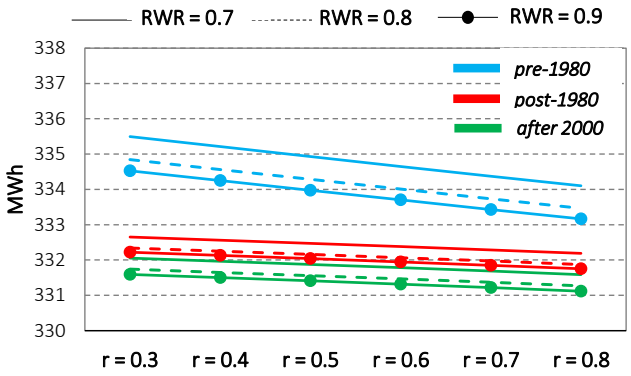

FIGURE 5.15: PE needs for Athens [Author]

The results for Madrid (Fig. 5.16) are quite similar to those of Athens, except for the higher PE needs due to more heating required in winter. Also for this climate (hot-arid) cool roofs could slightly reduce PE consumption, especially for older buildings (light blue lines) poorly insulated and with a high Roof to Walls Ratio (RWR = 0.9). Newer buildings (red and green lines) benefit too from cool materials applications, but to a lower extent.

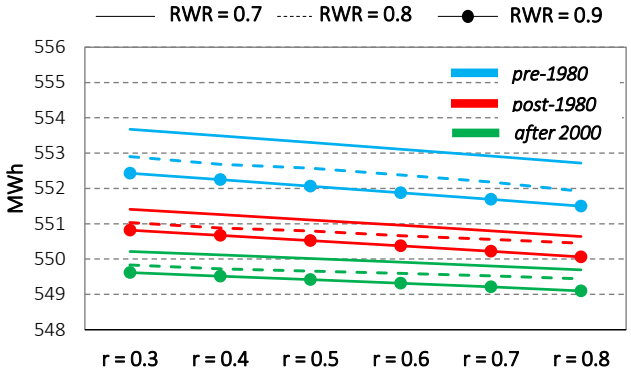

FIGURE 5.16: PE needs for Madrid [Author]

If looking at the results of the hot-humid climate of Rome (Fig. 5.17), the trends observed before for Athens and Madrid are here emphasized: very little reductions in PE needs are expected for pre-1980

and post-1980 constructions when increasing solar reflectance from 0.3 to 0.8 (about 0.2 MWh in both cases). No appreciable differences are noticed for well-insulated buildings (new constructions, green lines). Again, buildings with RWR = 0.9 perform better than buildings with RWR = 0.7 ÷ 0.8, because in these cases the weight of the roof in defining building energy balance is greater.

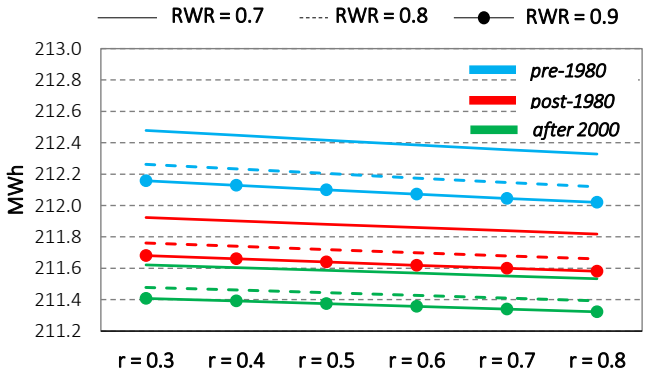

FIGURE 5.17: PE needs for Rome [Author]

The primary energy needs expected for Lyon (mixed humid climate, Fig. 5.18) and London (marine climate, Fig. 5.19) are very similar, as well as their energy trends when varying solar reflectance and insulation levels. In fact, in both cases PE consumption is slightly worsened when increasing roof solar reflectance in old buildings (light blue lines), while keeping constant in newer buildings (red and green lines) well insulated, which are the best performing.

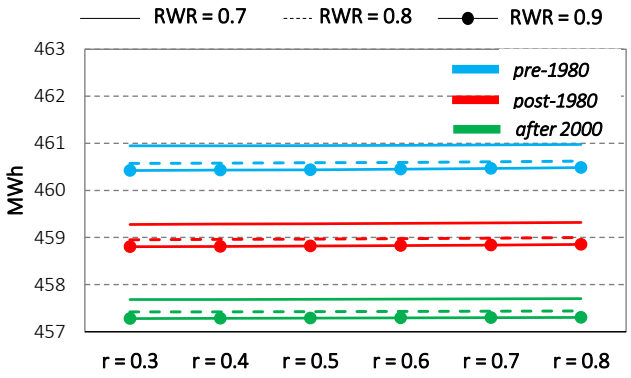

FIGURE 5.18: PE needs for Lyon [Author]

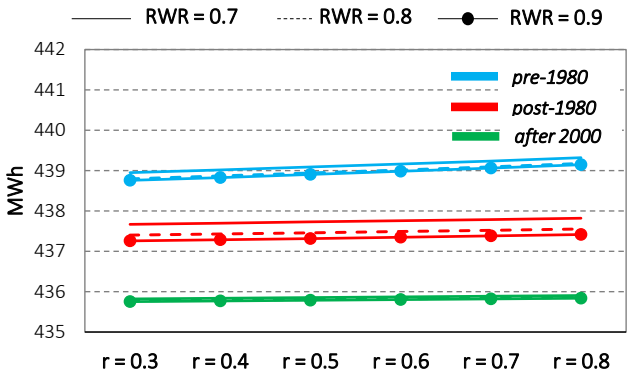

FIGURE 5.19: PE needs for London [Author]

As expected, a similar trend is observed in the cold climate of Stuttgart (Fig. 5.20), but with higher PE needs because of high heating load and very low cooling load (see also Table 5.1), thus no appreciable differences are shown in Fig. 5.18 for PE consumption when passing from low-reflective (r = 0.3) to high-reflective (r = 0.8) roofs. An almost negligible influence is given by roof extension, since changes in RWR have very little impact on poor-insulated roofs and no one on well-insulated roofs.

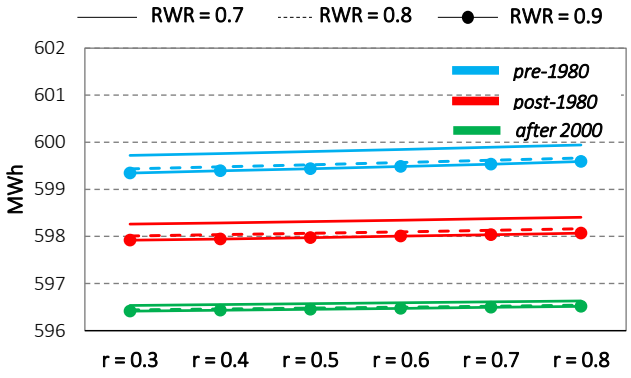

FIGURE 5.20: PE needs for Stuttgart [Author]

From the discussion of the results of each city, it clearly emerges that cool roofs could help reducing PE needs for air conditioning in hot climates (37°N< LAT <42°N) in poorly insulated buildings, while the reductions for more insulated buildings are almost negligible. This is because the role played by the roof in determining building energy balance is more evident for scarcely insulated components. Roof to Walls Ratio play a secondary role in defining the energy needs.

However, these reductions hardly achieve 2% of total PE needs when a high-reflective roof (r = 0.8) is compared to a low-reflective one (r = 0.3), and they are due to cooling savings while heating needs are only slightly worsened.

For the coldest climates (42°N< LAT <48°N) the application of cool materials to the roof would slightly increase the energy needs for older buildings (pre-1980 constructions), while not affecting those for newer ones (post-1980 and new constructions). This is likely due to lower sun height on the sky, which reduce the magnitude of heat fluxes through the roof and thus reduce its weight on building energy needs. In these cases, little heating penalties (always less than 1%) should be expected when using roofing materials with $r > 0.6$.

In conclusion, in spite of cool roofs always reduce overheating occurrence in all climates – and so enhance thermal comfort – they give a little contribution in reducing PE needs for air conditioning in hot climates, while slightly increasing energy needs in cold climates.

For these reasons, the following section will deal with an economic analysis only for the hottest climates considered in this study.

5.3 Economic analysis

The economic analysis is carried out for those models discussed in Section 5.2 for which the greatest energy savings are achievable after the application of a cool roof. More in detail, only poor-insulated buildings (pre-1980 constructions) located in hot climates are considered, since these are the only models that could give some money savings in air conditioning operation.

By changing the solar reflectance value *r*, it will be possible to appreciate to what extent this is the key parameter for the evaluation of the economic convenience of the intervention.

On the other hand, RWR does not influence the slope of the energy trend (see Figs. 5.15-5.20), so it will be retained at a fixed value in this analysis.

This effort is accomplished in terms of *discounted payback period*, which accounts for time value of both money and electricity cost by discounting the cash outflows of the intervention.

In discounted payback period, one has to calculate the present value of each cash outflow, taking the start of the first period as zero point. Moreover, one needs to set a suitable discount rate.

The annual money savings S_i stemming from annual energy savings *C* are calculated according to Eq. (5.1):

$$S_i = C \cdot 0.20 \cdot (1+\Delta)^i \tag{5.1}$$

In his equation, 0.20 is the average price of electricity [€/kWh] within EU countries as gathered from Eurostat statistics for the second half of 2014 (household consumers) and Δ is its annual increase, set to 4.5% according to the analysis of the average price trend of last 7 years.

The annual energy savings *C* are calculated with reference to a "base case" with $r = 0.3$ and are set at a constant value. In reality, they are decreasing with time because of the aging process of the cool material applied to the roof, as widely discussed in Chapter 3. However, it is possible to implicitly take into account this process by referring to a *r* value lower than the design one, especially for materials showing high solar reflectance values ($0.7 < r < 0.8$) that are those showing the highest decay in optical properties.

Finally, the cumulated money savings at year *n* are estimated by considering an increasing time value of money by means of the interest rate *p*, set to 2% to represent an average value of last 10 years fluctuations:

$$S_n = \sum_i [S_i / (1+p)^i] \tag{5.2}$$

The results of this calculation are shown in Fig. 21 for the city of Athens, by considering a unitary installation cost of cool roof ranging from 10 € m^{-2} to 20 € m^{-2} (mean values gathered after a market survey). This will result in final installation costs ranging from 10000 € to 200000 € (area enclosed by grey dotted lines), since the roof surface amounts to 1000 m^2.

If entering the graph with the installation cost (y-axis), it is possible to estimate the discounted payback time of the investment - i.e. the time after which money savings are achieved – by intercepting the lines corresponding to different solar reflectance values and thus reading the payback time on the x-axis.

What this calculation highlights is that installing a cool roof in existing office buildings does not seem a convenient investment even for the hot climate of Athens: for an investment cost of 10000 €, a payback time lower than 24 years is reached when $r > 0.6$, being about 17 years when a very performing material is used ($r = 0.8$).

For higher installation costs, payback time may easily reach values higher than 26 years, thus overtaking the nominal expected service life of the roof.

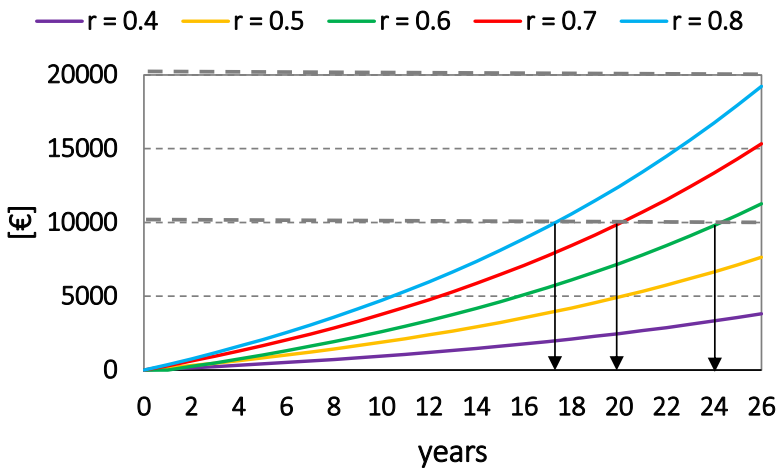

FIGURE 5.21: Payback time of cool roof installation. Athens [Author]

Worse results are expected for all the other climates because of the lower estimated energy savings, so the economic evaluation will not be repeated for them.

It is possible to conclude that, from an economic perspective, money savings due to cool roofs energy savings hardly justify the installation of cool materials, even if they show a high solar reflectance value ($r > 0.6$) and are applied to poorly insulated buildings located in hot climates (37°N< LAT <40°N). For lower r values, payback times greater than 20 years should be expected.

6. Conclusions

The aim of this thesis work is the evaluation of cool roofs application for improving thermal performance of existing office buildings located in EU countries.

Actions for improving thermal performance in this building typology raised a great interest throughout the world in the last years (IEA Task 47, CBECS survey in US, BPIE survey in EU), since they account for approximately 15% of existing buildings stock but show energy needs up to 40% higher than residential buildings.

According to the extensive BPIE survey carried out in 2011, 56% of the existing office buildings within EU countries was built before 1980, when no or very tolerant energy regulations were in force, thus they request for significative refurbishing actions.

Among them, the application of cool materials - i.e. materials able to stay cool under sun action by means of high solar reflectance and thermal emissivity values – could represent an interesting solution for reducing overheating throughout the year (given the high internal gains that are typical of the office buildings sector), thus improving thermal comfort of the occupants.

However, the energy performance stemming from their use need to be evaluated too, because likely winter penalties due to reduced heat fluxes entering the building through the roof surface could affect heating needs in a remarkable way.

To assess all these issues, this thesis carried out an extensive parametric analysis that takes into account the main building features affecting roofs energy balance, namely thermal transmittance, optical properties of the outer finishing layer (solar reflectance and thermal emissivity) and roof to walls ratio.

These parameters have been varied for a reference office-building model, defined according to the geometrical and thermal features found to be mostly representative of the EU office buildings stock.

The reference model, together with its variations (up to 648 per city), have been located in different cities representative of several climates (from the mixed arid climate of Athens to the cold climate of Stuttgart) and thermal insulation levels, with the aim of discovering the optimal outdoor conditions for cool roofs application.

The results of this analysis, conducted with the help of numerical simulations in EnergyPlus, led to analyze 3880 different thermal models; this raised the issue of selecting the results considered to be more representative to the study purposes.

After the definition of a filtering procedure, the best performing models have been selected and discussed extensively. From this discussion it emerged that cool roofs can improve comfort conditions, evaluated using both short-term and long-term analyses by using a tailored statistical indicator, for all of the climates analyzed.

More in detail, the greatest benefits are achievable for poorly insulated buildings located in hot climates when using very performing cool materials (solar reflectance values up to 0.8); no relevant differences are expected when varying roof thermal emissivity within the range 0.8-0.9, which is common for all non-metallic materials. Roof geometrical features, such as roof to walls ratio, play a secondary role in determining rooms overheating.

From an energy point of view, Primary Energy needs have been assessed considering commonly used plant solutions for space heating and cooling. The results highlight how little energy savings are achievable when using cool roofs in hot climates, while not affecting or slightly worsening those in moderate-to-cold climates.

Finally, for the best energy models an economic analysis evaluated the payback time of the investment with reference to a standard low-reflective roof, showing how up to 17 years are needed for amortizing installation costs in the best scenarios.

In conclusion, the main findings of this thesis work can be summarized as follows:

(i) Cool roofs are always good for reducing overheating and improving comfort conditions in summer, whatever is the climate;

(ii) An accurate energy needs assessment must be carried out, because of heating penalties in moderate-to-cold climates also for buildings with high internal loads such as office buildings;

(iii) For hot climates, cool roofs can be regarded as an effective and low cost technology for refurbishing existing roofs. For colder climates, refurbishing actions should focus more on thermal insulation.

APPENDIX I – thermal characteristics of the existing EU office buildings sector

			OFFICE WEIGHTED AVERAGES - WALL							OFFICE WEIGHTED AVERAGES - WINDOWS						
			uvalues W/m²/K						Calcu	uvalues W/m²/K						Calcu
Climatic region	Total floor space in EU (Mm2)	Country	Pre 1945	1945-1970	1970-1980	1980-1990	1990-2000	Post 2000	Average	Pre 1945	1945-1970	1970-1980	1980-1990	1990-2000	Post 2000	Average
Southern dry																
	21	Portugal	2.0	2.0	1.6	1.5	1.3	0.8	1.5	4.5	4.5	4.5	4.4	1.6	3.8	3.9
	84	Spain	2.5	2.2	2.2	1.8	1.7	0.9	1.9	5.8	5.8	6.1	3.3	3.3	2.8	4.5
		WEIGHTED avg	2.4	2.2	2.1	1.7	1.6	0.8	**1.8**	5.5	5.6	5.8	3.6	2.9	3.0	**4.4**
Mediterranean																
	2	Cyprus	2.1	1.9	1.5	1.5	1.5	1.5	1.7	6.2	6.2	6.2	5.9	2.5	1.6	4.8
	26	Greece	2.5	2.4	2.1	0.8	0.7		1.7	5.1	5.0	5.3	3.7	3.5		4.5
	52	Italy	1.2	1.2	0.8	0.8	0.8		0.9	5.5	5.5	4.9	4.2	3.6	3.6	4.5
	1	Malta	2.0	1.9	1.6	1.6	1.6	1.7	1.7	6.1	6.1	5.9	5.8	5.7	5.3	5.8
		WEIGHTED avg	**1.6**	**1.6**	**1.2**	**0.8**	**0.8**	**1.6**	**1.2**	**5.4**	**5.4**	**5.0**	**4.1**	**3.5**	**3.6**	**4.5**
Southern Continental																
	28	Bulgaria	1.6	1.5	1.4	1.3	1.0	0.4	1.2	3.1	3.1	3.1	3.1	2.7	1.9	2.8
	199	France	2.1	2.1	1.2	1.2	1.0	0.4	1.3	5.0	5.0	4.4	3.4	3.3	2.7	3.9
	7	Slovenia	1.4	1.4	1.4	0.9	0.9	0.6	1.1	2.4	2.4	2.1	1.6	1.6	1.6	2.0
		WEIGHTED avg	**2.0**	**2.0**	**1.2**	**1.2**	**1.0**	**0.4**	**1.3**	**4.7**	**4.7**	**4.2**	**3.3**	**3.1**	**2.5**	**3.7**
Oceanic																
	25	Belgium	1.9	1.8	1.8	1.7	1.3	0.8	1.5	4.5	4.6	4.2	3.8	3.7	2.3	3.8
	10	Ireland	1.9	1.8	1.8	0.8	0.7	0.3	1.2	4.8	4.8	4.8	3.3	2.9	2.3	3.8
	122	United Kingdom	1.8	1.7	1.3	0.7	0.5	0.4	1.1	4.9	4.9	4.9	4.6	2.7	1.8	4.0
		WEIGHTED avg	**1.8**	**1.7**	**1.4**	**0.8**	**0.6**	**0.4**	**1.1**	**4.8**	**4.9**	**4.8**	**4.4**	**2.9**	**1.9**	**4.0**
Continental																
	21	Austria	0.7	0.7	0.6	0.6	0.4	0.3	0.6	3.2	3.4	2.4	2.1	1.4	1.3	2.3
	36	Czech Republic	0.8	0.8	0.7	0.7	0.5	0.4	0.6	2.8	2.8	2.8	2.8	2.0	1.5	2.5
	360	Germany	1.5	1.5	1.2	0.9	0.4	0.4	1.0	2.9	2.9	2.9	1.9	1.6	1.3	2.3
	5	Hungary	1.4	1.2	1.2	0.7	0.7	0.5	0.9	3.0	3.0	3.0	2.7	2.7	2.2	2.8
	1	Luxembourg	1.5	1.5	1.7	0.6	0.5	0.4	1.0	4.5	3.9	3.2	2.0	1.6	1.2	2.7
	47	Netherlands	1.8	1.6	1.6	0.6	0.5	0.4	1.1	3.8	3.7	3.7	3.4	2.9	1.8	3.2
		WEIGHTED avg	**1.4**	**1.4**	**1.2**	**0.8**	**0.4**	**0.4**	**0.9**	**3.0**	**3.0**	**2.9**	**2.1**	**1.8**	**1.4**	**2.4**
Northern Continental																
	45	Denmark	1.2	1.0	0.6	0.4	0.4	0.3	0.6	2.6	2.5	2.5	1.4	1.4	1.7	2.0
	8	Lithuania	1.0	0.9	0.6	0.6	0.4	0.3	0.6	2.4	2.4	2.3	2.3	1.9	1.9	2.2
	89	Poland	1.3	1.3	1.3	0.8	0.6		1.1	4.7	3.7	2.6	2.6	2.3	2.1	3.0
	8	Romania	1.9	1.6	1.6	1.4	1.4	1.0	1.5	2.6	2.7	2.7	2.4	2.4	1.3	2.4
	7	Slovakia	1.5	1.0	1.0	0.7	1.1	0.5	1.0	3.2	3.2	2.9	2.9			3.1
		WEIGHTED avg	**1.3**	**1.2**	**1.0**	**0.7**	**0.6**	**0.4**	**0.9**	**3.8**	**3.2**	**2.6**	**2.2**	**2.0**	**1.9**	**2.6**
Nordic																
	2	Estonia	0.5	0.5	0.3	0.3	0.2	0.2	0.3	1.8	1.8	1.8	1.1	1.0	1.0	1.4
	16	Finland	0.8	0.6	0.5	0.3	0.3	0.3	0.5	2.4	2.3	2.2	2.0	1.7	1.5	2.0
	4	Latvia	1.0	1.0	1.0	1.0	0.8	0.5	0.9	2.7	2.7	2.5	2.5	2.5	1.8	2.5
	27	Sweden	0.6	0.4	0.3	0.3	0.2	0.2	0.3	3.2	3.1	3.0	2.5	2.5	0.9	2.5
		WEIGHTED avg	**0.7**	**0.5**	**0.4**	**0.4**	**0.3**	**0.2**	**0.4**	**2.8**	**2.7**	**2.6**	**2.3**	**2.2**	**1.2**	**2.3**

			OFFICE WEIGHTED AVERAGES - FLOOR							OFFICE WEIGHTED AVERAGES - ROOF						
			uvalues W/m²/K						Calcu	uvalues W/m²/K						Calcu
Climatic region	Total floor space in EU (Mm2)	Country	Pre 1945	1945-1970	1970-1980	1980-1990	1990-2000	Post 2000	Average	Pre 1945	1945-1970	1970-1980	1980-1990	1990-2000	Post 2000	Average
Southern dry																
	21	Portugal					1.9	0.8	1.4	2.5	2.8	2.8	2.7	1.5	1.2	2.2
	84	Spain	2.5	2.5	2.5	0.8	0.8	0.8	1.7	1.4	1.4	1.4	1.0	0.9	0.6	1.1
		WEIGHTED avg	2.5	2.5	2.5	0.8	1.1	0.8	**1.6**	1.6	1.7	1.7	1.4	1.0	0.8	**1.4**
Mediterranean																
	2	Cyprus										3.4	3.5	0.5	0.7	2.0
	26	Greece	0.7	0.7	0.7	0.7	0.7	0.8	0.7	3.2	3.0	2.7	0.7	0.5	0.6	1.8
	52	Italy	0.8	0.8	0.5	0.5	0.5	1.4	0.8	1.3	1.3	0.8	0.8	0.8		1.0
	1	Malta	2.6	2.6	2.4	2.0	2.1	2.3	2.3	1.7	1.7	2.0	2.0	1.7	2.1	1.9
		WEIGHTED avg	**0.8**	**0.8**	**0.6**	**0.6**	**0.6**	**1.2**	**0.8**	**1.9**	**1.9**	**1.5**	**0.9**	**0.7**	**0.6**	**1.3**
Southern Continental																
	28	Bulgaria	1.0	1.0	1.0	0.8	0.6	0.5	0.8	1.0	1.2	1.1	1.1	0.6	0.3	0.9
	199	France	1.8	1.8	1.8	1.0	0.8	0.4	1.2	1.8	1.8	1.0	0.8	0.6	0.3	1.0
	7	Slovenia	1.1	1.1	0.9	0.8	0.8	0.5	0.9	1.2	1.2	0.9	0.8	0.8	0.5	0.9
		WEIGHTED avg	**1.6**	**1.6**	**1.6**	**0.9**	**0.8**	**0.4**	**1.2**	**1.6**	**1.7**	**1.0**	**0.8**	**0.6**	**0.3**	**1.0**
Oceanic																
	25	Belgium	0.8	0.8	1.0	0.9	0.8	0.7	0.8	2.0	2.0	2.2	1.2	0.9	0.7	1.5
	10	Ireland								0.8	0.9	0.8	0.4	0.4	0.4	0.6
	122	United Kingdom	2.0	1.7	1.4	1.1	0.5	0.3	1.2	1.9	1.8	0.9	0.5	0.3	0.2	1.0
		WEIGHTED avg	**1.8**	**1.5**	**1.3**	**1.1**	**0.5**	**0.3**	**1.0**	**1.9**	**1.8**	**1.1**	**0.6**	**0.4**	**0.3**	**1.0**
Continental																
	21	Austria	1.2	1.5	1.0	0.6	0.5	0.5	0.9	1.1	0.7	0.6	0.4	0.3	0.2	
	36	Czech Republic	1.5	1.0	0.8	0.8	0.6	0.4	0.9	0.8	0.6	0.5	0.5	0.4	0.2	0.5
	360	Germany	1.2	1.2	0.9	0.4	0.4	0.4	0.7	1.0	1.0	0.8	0.5	0.3	0.3	0.6
	5	Hungary	1.0	1.0	1.0	0.8	0.8	0.5	0.9	1.4	1.4	1.0	0.7	0.7	0.3	0.9
	1	Luxembourg	1.5	1.2	0.6	0.6	0.5	0.5	0.8							
	47	Netherlands	2.0	1.7	1.5	1.0	0.9	0.5	1.3	2.1	1.7	1.2	0.7	0.5	0.5	1.1
		WEIGHTED avg	**1.3**	**1.2**	**0.9**	**0.5**	**0.5**	**0.4**	**0.8**	**1.1**	**1.0**	**0.8**	**0.5**	**0.3**	**0.3**	**0.7**
Northern Continental																
	45	Denmark	0.8	0.6	0.6	0.5	0.5	0.3	0.5	0.5	0.5	0.3	0.2	0.2	0.2	0.3
	8	Lithuania				0.4	0.3	0.3	0.3	0.7	0.7	0.7	0.7	0.3	0.2	0.5
	89	Poland	1.6	1.2	1.2	1.1	1.0	0.7	1.1	1.0	0.9	0.7	0.5	0.3		0.7
	8	Romania	1.4	1.4	1.4	1.1	1.0	1.0	1.2	1.1	1.2	1.2	1.2	1.1	0.0	1.0
	7	Slovakia	1.5	1.5	1.5	1.5	1.4	1.1	1.4	1.6	0.7	0.7	0.5	0.5	0.0	0.6
		WEIGHTED avg	**1.3**	**1.0**	**1.0**	**0.9**	**0.8**	**0.6**	**0.9**	**0.9**	**0.8**	**0.6**	**0.4**	**0.3**	**0.1**	**0.6**
Nordic																
	2	Estonia	0.4	0.4	0.4	0.3	0.2	0.2	0.3	0.4	0.4	0.4	0.2	0.2	0.2	0.3
	16	Finland	0.6	0.5	0.4	0.3	0.3	0.3	0.4	0.5	0.4	0.3	0.2	0.2	0.2	0.3
	4	Latvia	1.0	1.0	1.0	1.0	1.0	0.3	0.9	1.0	1.2	1.2	1.2	1.0	0.5	1.0
	27	Sweden	0.2	0.2	0.2	0.2	0.2	0.2	0.2	0.3	0.4	0.2	0.2	0.1	0.0	0.2
		WEIGHTED avg	**0.4**	**0.4**	**0.4**	**0.3**	**0.3**	**0.2**	**0.3**	**0.4**	**0.4**	**0.3**	**0.3**	**0.2**	**0.1**	**0.3**

APPENDIX II – energy needs for the reference office building models

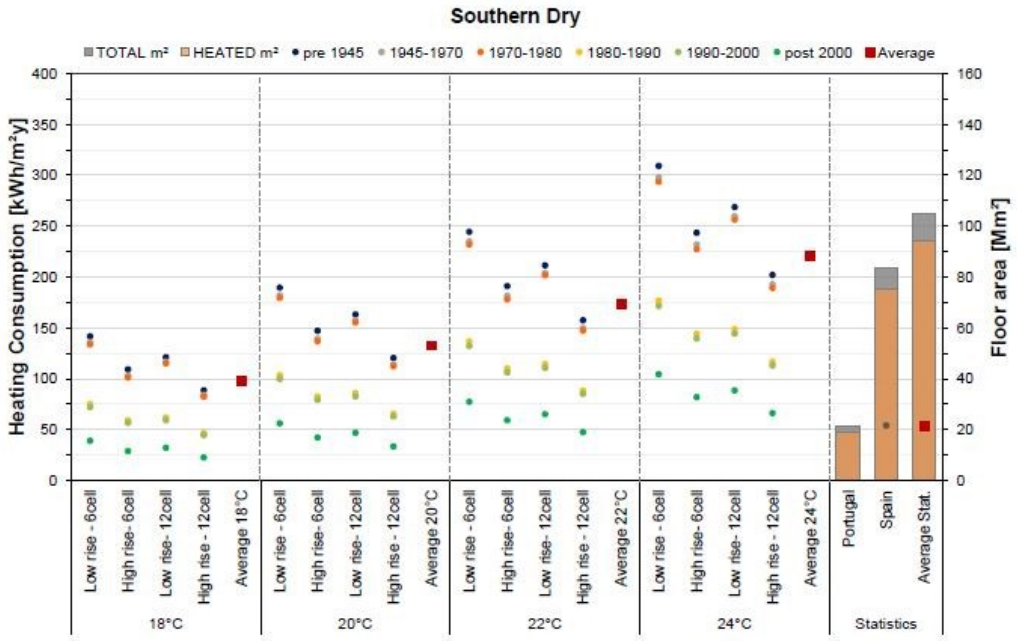

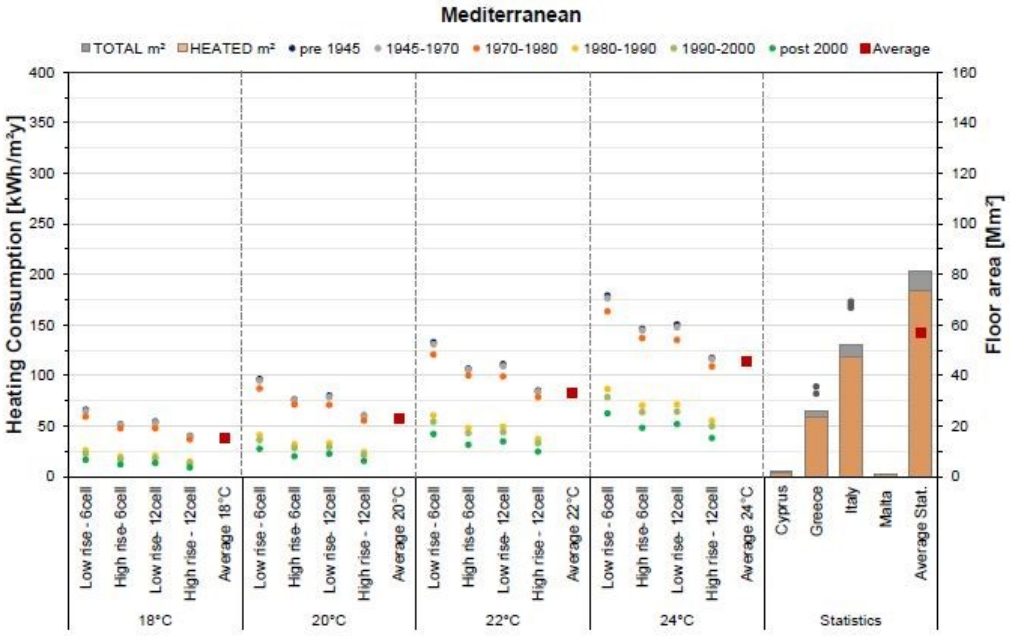

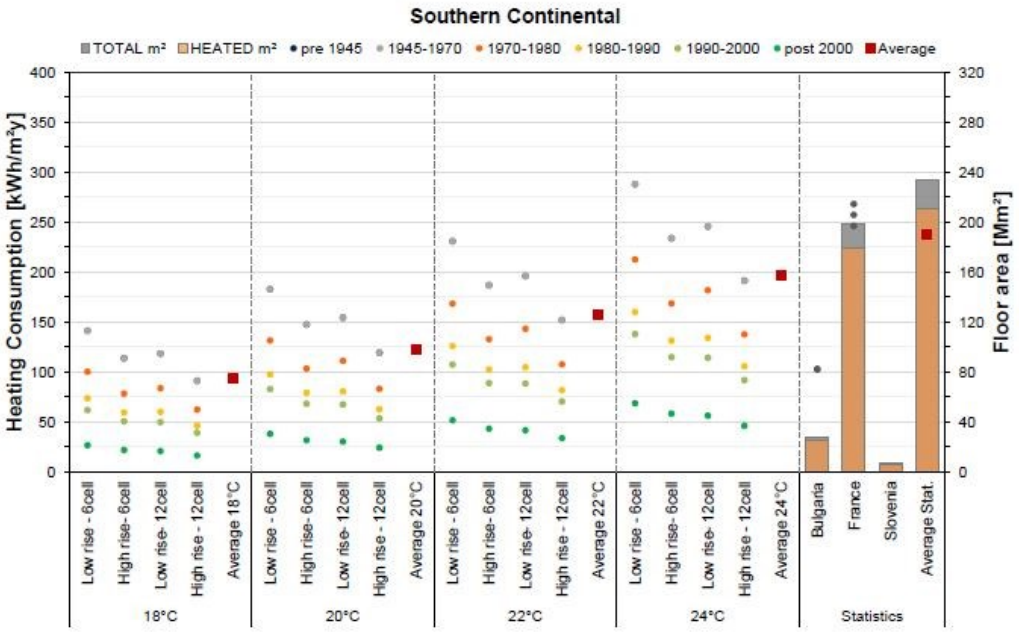
Southern Continental
TOTAL m²
HEATED m²
pre 1945
1945-1970
1970-1980
1980-1990
1990-2000
post 2000
Average
Heating Consumption [kWh/m²y]
Floor area [Mm²]
Low rise - 6cell
High rise- 6cell
Low rise- 12cell
High rise - 12cell
Average 18°C
Average 20°C
Average 22°C
Average 24°C
Bulgaria
France
Slovenia
Average Stat.
18°C
20°C
22°C
24°C
Statistics

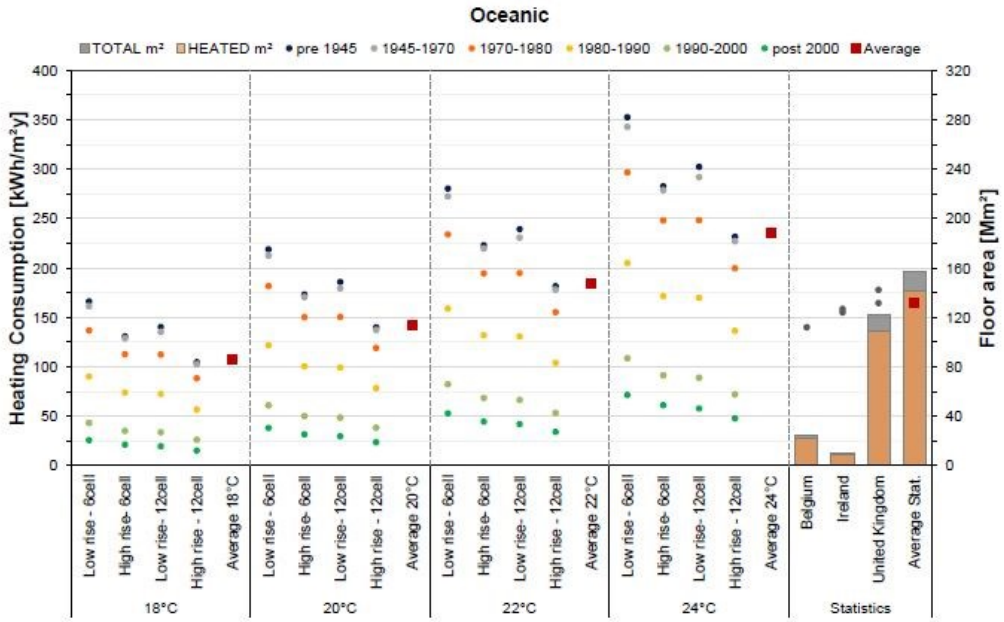
Oceanic
TOTAL m²
HEATED m²
pre 1945
1945-1970
1970-1980
1980-1990
1990-2000
post 2000
Average
Heating Consumption [kWh/m²y]
Floor area [Mm²]
Low rise - 6cell
High rise- 6cell
Low rise- 12cell
High rise - 12cell
Average 18°C
Average 20°C
Average 22°C
Average 24°C
Belgium
Ireland
United Kingdom
Average Stat.
18°C
20°C
22°C
24°C
Statistics

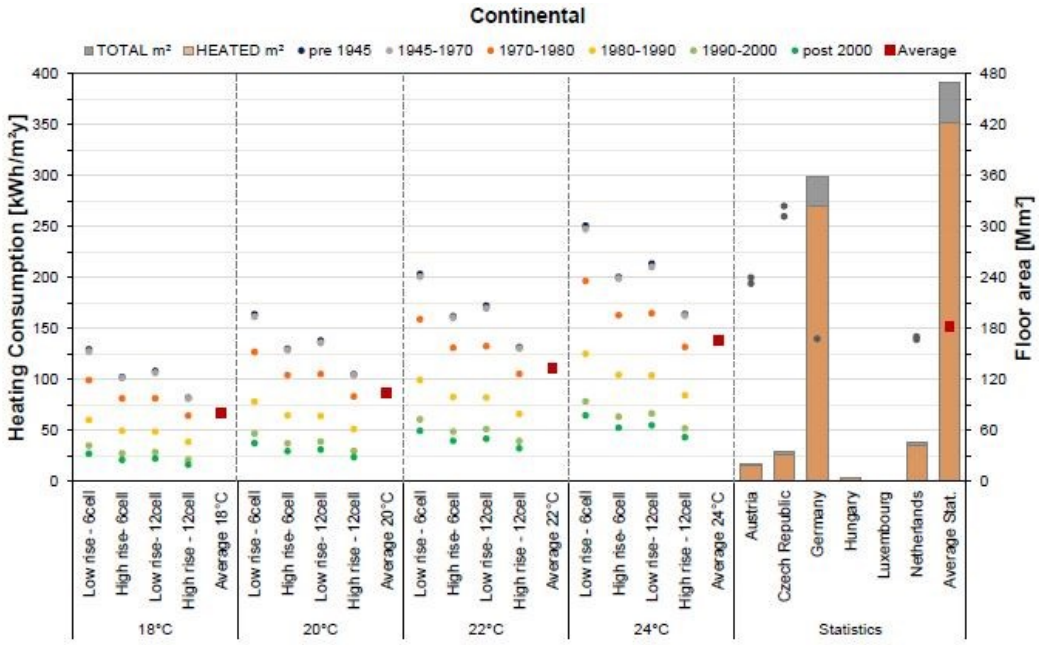
Continental
TOTAL m²
HEATED m²
pre 1945
1945-1970
1970-1980
1980-1990
1990-2000
post 2000
Average
Heating Consumption [kWh/m²y]
Floor area [Mm²]
Low rise - 6cell
High rise- 6cell
Low rise- 12cell
High rise - 12cell
Average 18°C
Average 20°C
Average 22°C
Average 24°C
18°C
20°C
22°C
24°C
Austria
Czech Republic
Germany
Hungary
Luxembourg
Netherlands
Average Stat.
Statistics

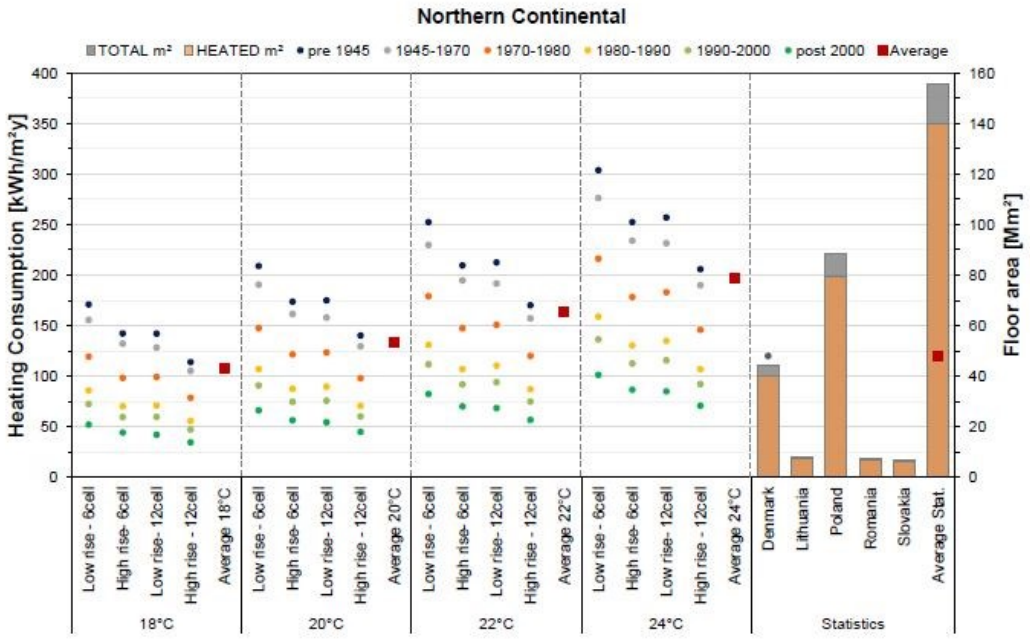
Northern Continental
TOTAL m²
HEATED m²
pre 1945
1945-1970
1970-1980
1980-1990
1990-2000
post 2000
Average
Heating Consumption [kWh/m²y]
Floor area [Mm²]
Low rise - 6cell
High rise- 6cell
Low rise- 12cell
High rise - 12cell
Average 18°C
Average 20°C
Average 22°C
Average 24°C
18°C
20°C
22°C
24°C
Denmark
Lithuania
Poland
Romania
Slovakia
Average Stat.
Statistics

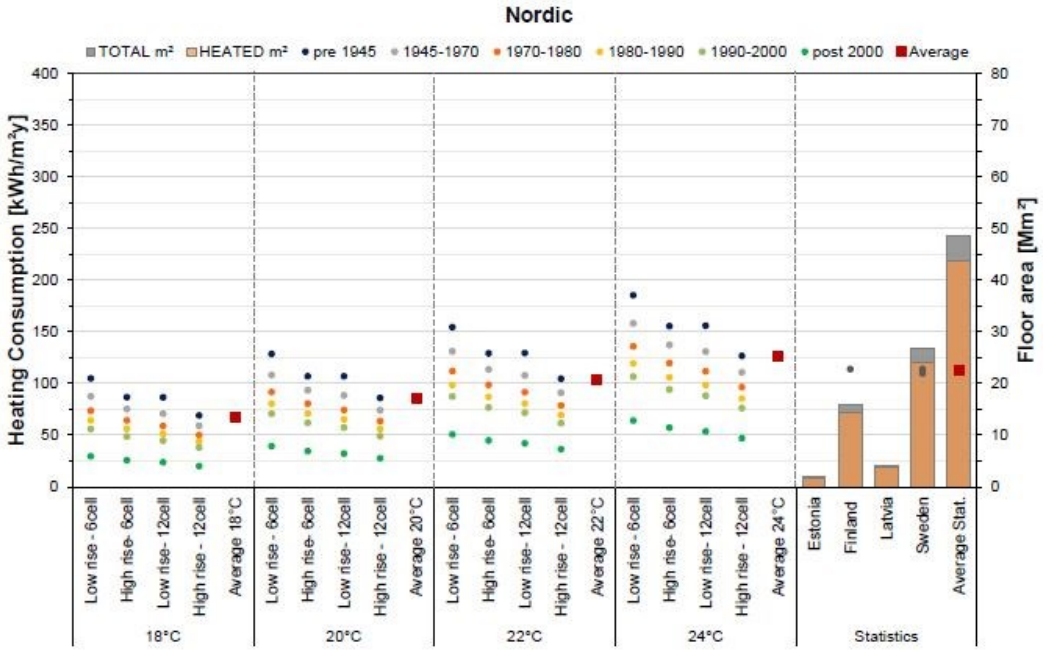
Nordic
TOTAL m²
HEATED m²
pre 1945
1945-1970
1970-1980
1980-1990
1990-2000
post 2000
Average
Heating Consumption [kWh/m²y]
Floor area [Mm²]
Low rise - 6cell
High rise- 6cell
Low rise- 12cell
High rise - 12cell
Average 18°C
Average 20°C
Average 22°C
Average 24°C
Estonia
Finland
Latvia
Sweden
Average Stat.
18°C
20°C
22°C
24°C
Statistics

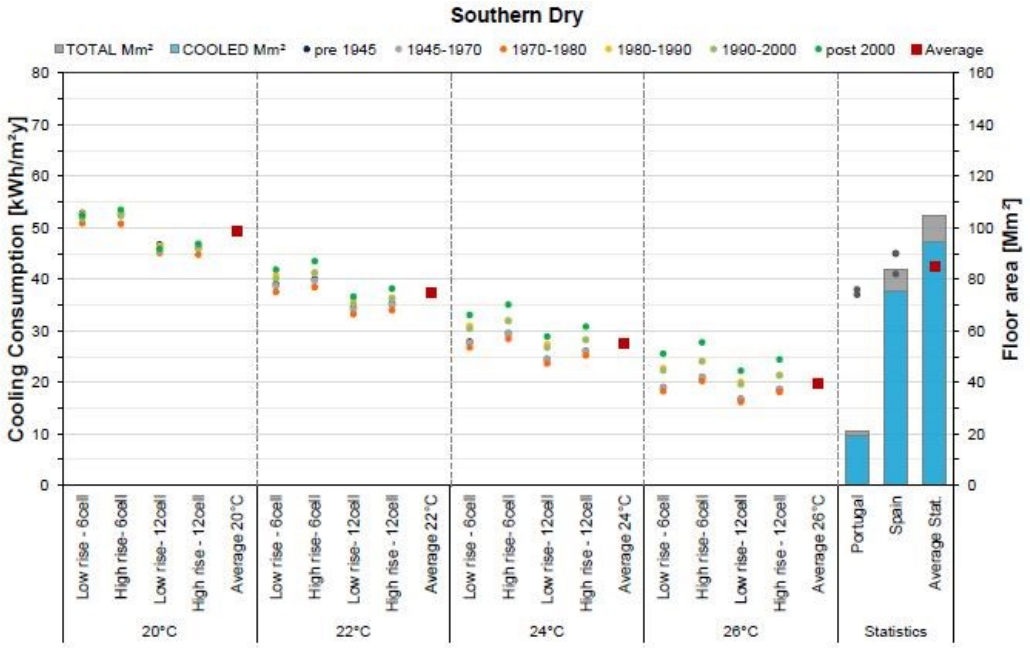
Southern Dry
TOTAL Mm²
COOLED Mm²
pre 1945
1945-1970
1970-1980
1980-1990
1990-2000
post 2000
Average
Cooling Consumption [kWh/m²y]
Floor area [Mm²]
Low rise - 6cell
High rise- 6cell
Low rise- 12cell
High rise - 12cell
Average 20°C
Average 22°C
Average 24°C
Average 26°C
Portugal
Spain
Average Stat.
20°C
22°C
24°C
26°C
Statistics

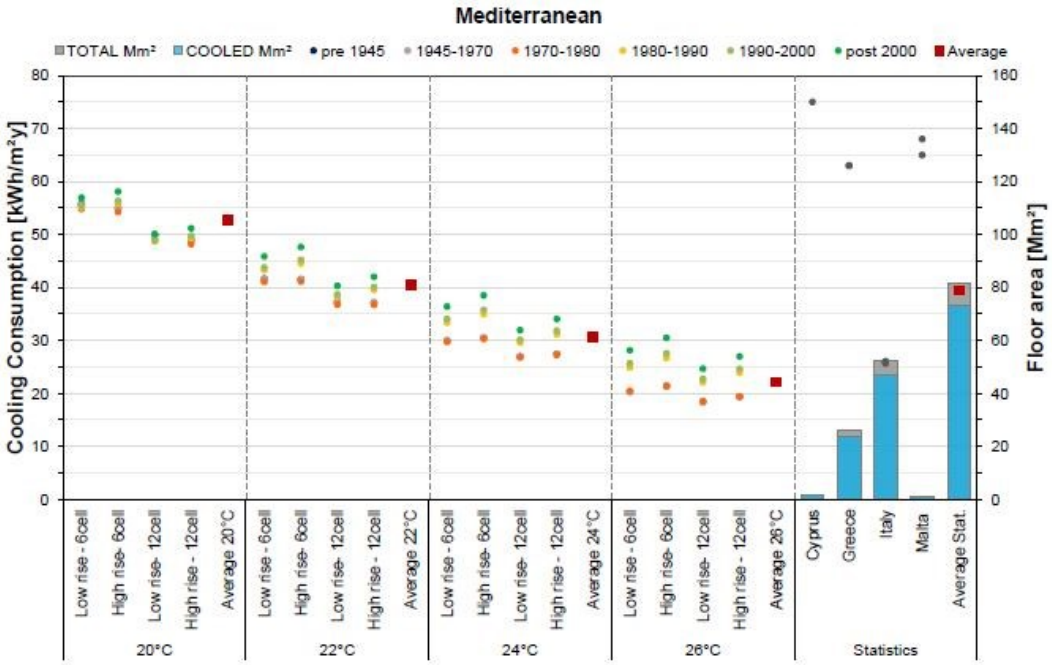
Mediterranean
TOTAL Mm²
COOLED Mm²
pre 1945
1945-1970
1970-1980
1980-1990
1990-2000
post 2000
Average
Cooling Consumption [kWh/m²y]
Floor area [Mm²]
Low rise - 6cell
High rise- 6cell
Low rise- 12cell
High rise - 12cell
Average 20°C
Average 22°C
Average 24°C
Average 26°C
Cyprus
Greece
Italy
Malta
Average Stat.
20°C
22°C
24°C
26°C
Statistics

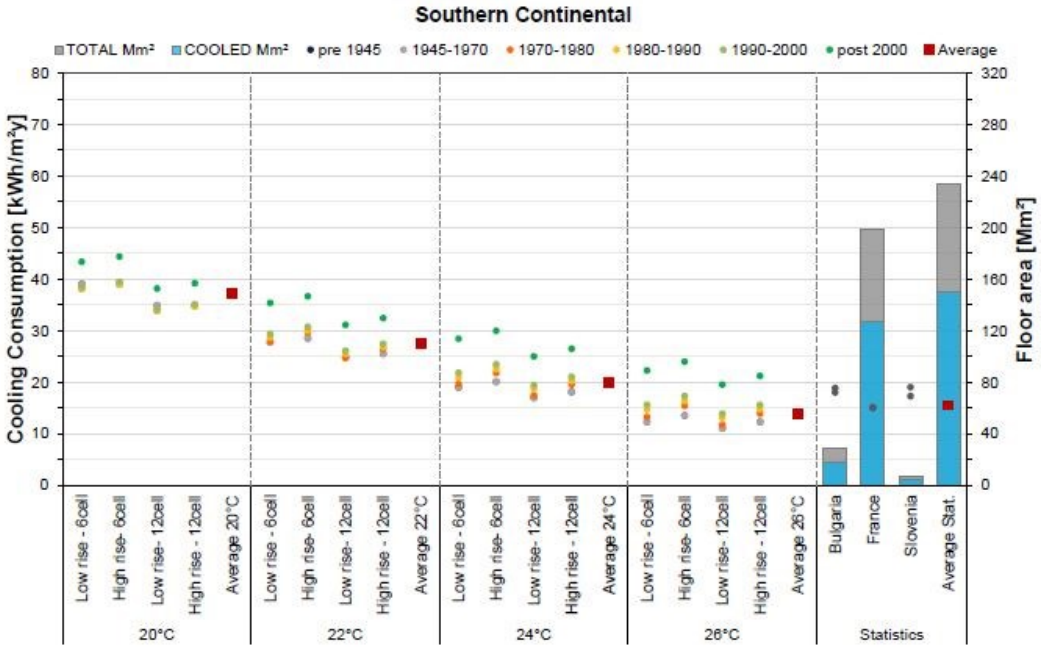
Southern Continental
TOTAL Mm²
COOLED Mm²
pre 1945
1945-1970
1970-1980
1980-1990
1990-2000
post 2000
Average
Cooling Consumption [kWh/m²y]
Floor area [Mm²]
Low rise - 6cell
High rise- 6cell
Low rise- 12cell
High rise - 12cell
Average 20°C
Average 22°C
Average 24°C
Average 26°C
Bulgaria
France
Slovenia
Average Stat.
20°C
22°C
24°C
26°C
Statistics

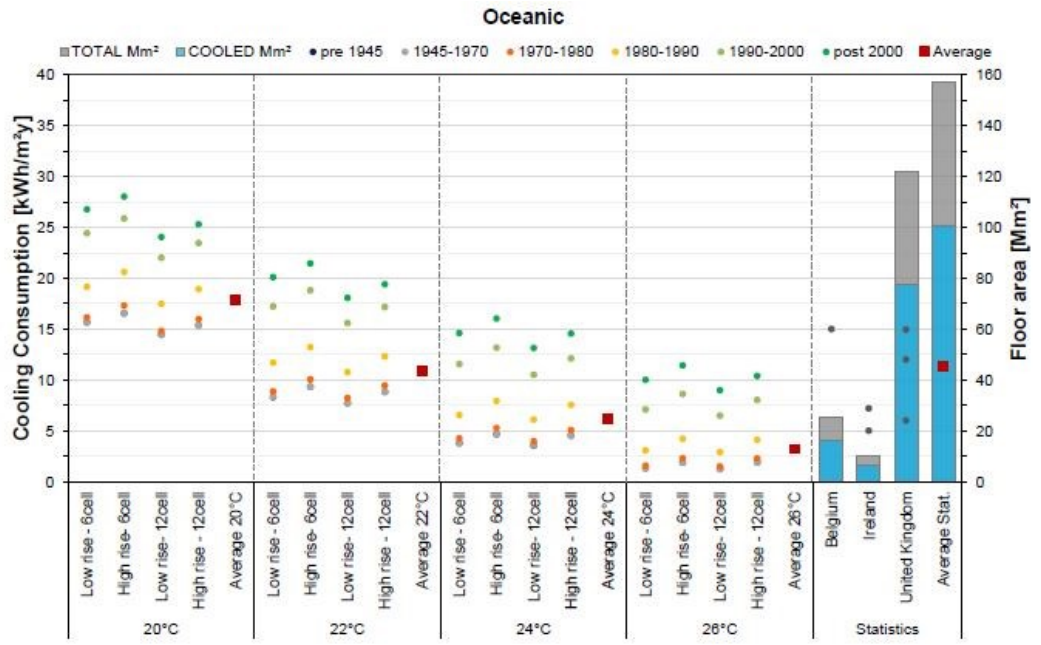
Oceanic
TOTAL Mm²
COOLED Mm²
pre 1945
1945-1970
1970-1980
1980-1990
1990-2000
post 2000
Average
Cooling Consumption [kWh/m²y]
Floor area [Mm²]
Low rise - 6cell
High rise- 6cell
Low rise- 12cell
High rise - 12cell
Average 20°C
Average 22°C
Average 24°C
Average 26°C
Belgium
Ireland
United Kingdom
Average Stat.
20°C
22°C
24°C
26°C
Statistics

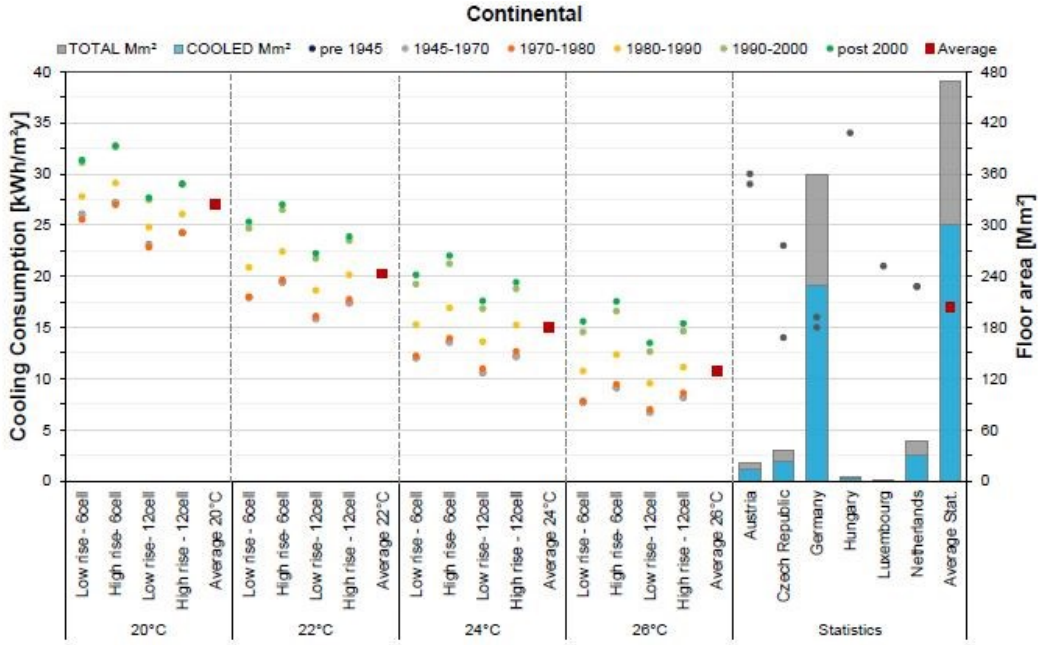
Continental
TOTAL Mm²
COOLED Mm²
pre 1945
1945-1970
1970-1980
1980-1990
1990-2000
post 2000
Average
Cooling Consumption [kWh/m²y]
Floor area [Mm²]
Low rise - 6cell
High rise- 6cell
Low rise- 12cell
High rise - 12cell
Average 20°C
Average 22°C
Average 24°C
Average 26°C
20°C
22°C
24°C
26°C
Austria
Czech Republic
Germany
Hungary
Luxembourg
Netherlands
Average Stat.
Statistics

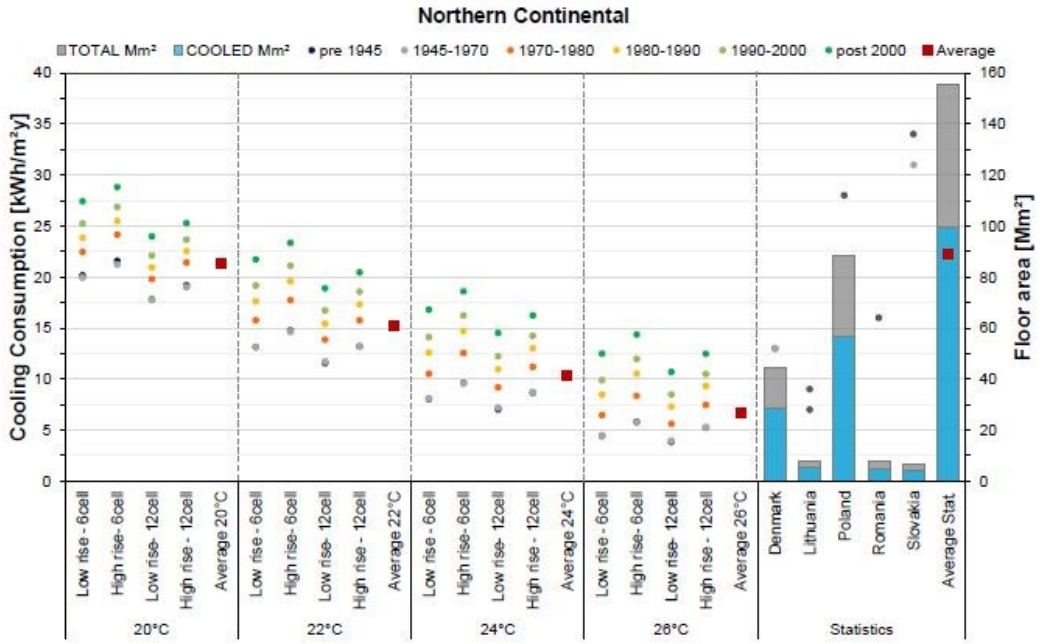
Northern Continental
TOTAL Mm²
COOLED Mm²
pre 1945
1945-1970
1970-1980
1980-1990
1990-2000
post 2000
Average
Cooling Consumption [kWh/m²y]
Floor area [Mm²]
Low rise - 6cell
High rise- 6cell
Low rise- 12cell
High rise - 12cell
Average 20°C
Average 22°C
Average 24°C
Average 26°C
20°C
22°C
24°C
26°C
Denmark
Lithuania
Poland
Romania
Slovakia
Average Stat
Statistics

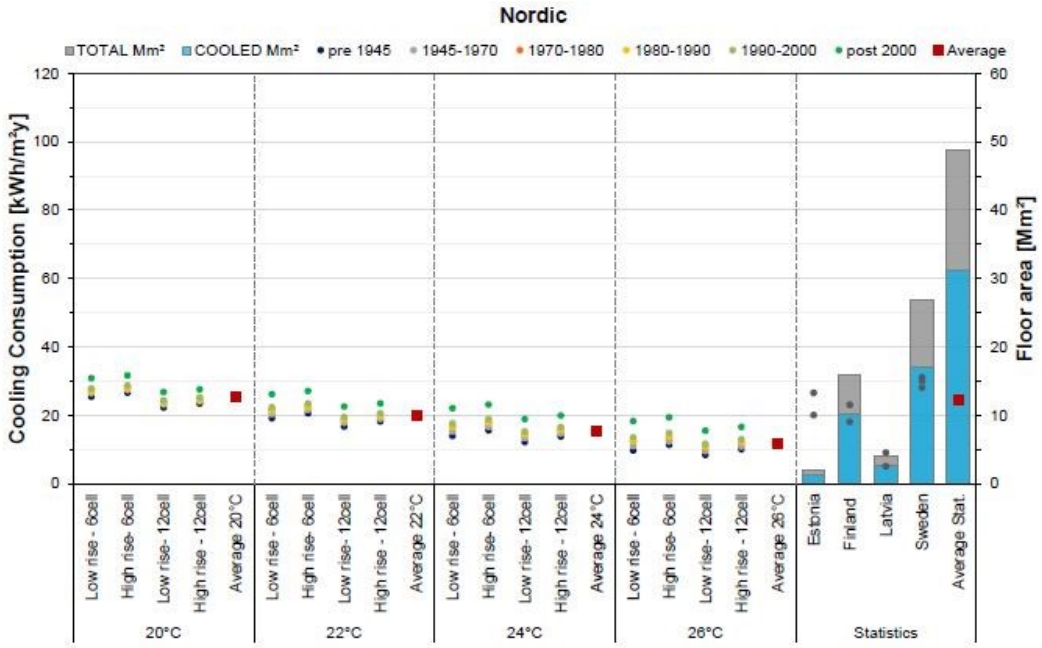
Nordic
TOTAL Mm²
COOLED Mm²
pre 1945
1945-1970
1970-1980
1980-1990
1990-2000
post 2000
Average
Cooling Consumption [kWh/m²y]
Floor area [Mm²]
Low rise - 6cell
High rise- 6cell
Low rise- 12cell
High rise - 12cell
Average 20°C
Average 22°C
Average 24°C
Average 26°C
Estonia
Finland
Latvia
Sweden
Average Stat.
20°C
22°C
24°C
26°C
Statistics